6-11-2013 12:00 AM

# The biogeochemical cycling of gold under surface and near-surface environmental conditions

Jeremiah P. Shuster, *The University of Western Ontario*

Supervisor: Dr. Gordon Southam, *The University of Western Ontario*

A thesis submitted in partial fulfillment of the requirements for the Doctor of Philosophy degree in Geology

# THE BIOGEOCHEMICAL CYCLING OF GOLD UNDER SURFACE AND NEAR-SURFACE ENVIRONMENTAL CONDITIONS

(Thesis format: Integrated Article)

by

Jeremiah Shuster

Graduate Program in Geology

A thesis submitted in partial fulfilment
of the requirements for the degree of
Doctorate of Philosophy

The School of Graduate and Postdoctoral Studies
The University of Western Ontario
London, Ontario, Canada

# Abstract

The mobility of gold at near-surface environmental conditions, e.g., supergene weathering environments, lateritic weathering systems, saline to hypersaline systems and placer gold environments, takes place as oxidised, soluble gold complexes and as reduced elemental gold. The transformation between aqueous and solid states of gold is attributed to the varying geochemical conditions that occur in dynamic environments that are catalysed in part by the biosphere. The primary focus of this research is the investigation of biogeochemical processes that contribute to the cycling of gold using laboratory models to represent various natural systems including chemolithotrophic bacteria, e.g., iron-oxidising bacteria, and heterotrophic sulphate-reducing bacteria and nitrifying bacteria. Results from these studies demonstrate that bacteria initiate the gold cycle by liberating gold through the chemical weathering of gold-bearing minerals. Through oxidative-complexation, soluble gold complexes, e.g., gold (I) thiosulphate and gold (III) chloride, could be produced; however, destabilisation of these gold complexes coupled with bioprecipitation and biomineralisation can immobilise gold thereby completing the cycle. Since the biosphere has an influence on the geochemical conditions of natural environments, the duration of the mobility of gold as soluble complexes is finite and represents a brief "snap shot" of gold's occurrence. Therefore under surface and near-surface environmental conditions gold will predominantly occur as secondary gold. Secondary gold occurs as nanometre-size to micrometre-size colloids, octahedral platelets, euhedral crystals and bacteriomorphic structures. Furthermore, when bacteria develop as a structurally cohesive biofilms, reduction and enrichment of gold can occur and produce macroscopic gold structures including foils, grains and nuggets. Therefore, bacteria can have a profound effect on the occurrence of gold in natural environments as long as nutrients necessary for microbial metabolism are sustained and gold is in the system. The direct and indirect biogenic effects on gold biogeochemistry will persist over geological time forming observed anomalous gold concentrations such as nugget formations and supergene gold enrichment. Characterising the morphology of gold grains and nuggets in association with understanding how biogeochemical conditions contribute to gold immobilisation is important for gold exploration as it has practical application in mineral vectoring.

Keywords: gold (I) thiosulphate, gold (III) chloride, gold sulphide, colloidal gold, octahedral gold platelets, iron-oxidising bacteria, sulphate-reducing bacteria, Nitrobacter sp. 263, gold grain, gold nugget, flour gold, transparent gold, gold biogeochemistry, geomicrobiology, gold

# Co-Authorship Statement

Chapter 3, entitled "The effect of iron-oxidising bacteria on the stability of gold (I) thiosulphate complex" authored by J. Shuster, A. Smith, T. Bolin, L.C.W. MacLean and G. Southam, has been prepared as a manuscript and intended for submission to *Chemical Geology*. Shuster obtained microbial samples, performed all microscopy and biogeochemical analysis, drafted the manuscript and prepared all figures. Smith assisted in microbial culturing and experimental set up. Bolin provided assistance during x-ray absorption fine structure data acquisition. MacLean performed absorption fine structure data analysis. Southam advised on all aspects of this research.

Chapter 4 constitutes a manuscript entitled, "Bacteria contribute to gold nugget structure and chemistry: evidence from in situ surface biofilms and casts", authored by J. Shuster, C.W. Johnston, N.A. Magarvey, R.A. Gordon, K. Barron, N. Banerjee, G. Southam. This manuscript has been accepted with major revision by *Geobiology* (No. GBI-087-2012, April 21, 2012). Shuster performed all the microscopy and biogeochemical analysis, drafted the manuscript and prepared all figures. Johnston and Magarvey assisted in bacterial identification. Gordon provided assistance during synchrotron-based elemental mapping. Barron obtained the gold grain samples. Banerjee and Southam provided advice on all aspects of this research.

Chapter 5, entitled "The immobilisation of gold from gold (III) chloride by a halophilic sulphate-reducing bacterial consortium", has been accepted by the *Geological Society* (No. ODEE-327R2, in press). The authors include J. Shuster, S. Marsden, L.C.W. MacLean, J. Ball, T. Bolin and G. Southam. Shuster performed all bacterial experiments, microscopy, biogeochemical analysis; drafted the manuscript and prepared all figures. Marsden assisted with bacterial experiments. MacLean performed absorption fine structure data analysis. Ball and Bolin provided assistance during x-ray absorption fine structure data acquisition. Southam advised on all aspects of this research.

*This thesis is dedicated to my father, Jerry, and in loving memory of my mother, Esther, for the countless opportunities, support and unconditional love they gave me.*

# Acknowledgments

I first met Gordon Southam when I enrolled in his third year course. At the time I didn't exactly know what the study of geomicrobiology involved; however, after the first week of classes I was hooked and decided that my undergraduate thesis project the following year had to be in geomicrobiology. Little did I know, that decision was going to pave the path of my journey into graduate school. Throughout my time working in the Southam lab, Gord was an inspiring supervisor that taught me, as I perceive it, the art of science. His mentorship has been so influential on my academic career that I am truly privileged and honoured to have had the opportunity to work under his supervision. I value his friendship and I'm very appreciative of his encouragement both in and out of the lab.

Going to the lab on daily basis and trying to make sense of results from a sometimes-maverick experiment was only a part of the excitement. The other major source of fun was working alongside the other "lablings" and "honourary lablings" throughout the years including: Ian Power, Chris Omelon, Ian Foster, Laura Donkervoort, Dusa Vukosavljevic (Dusa-moj), Andrea Fernandes (Pepper), Liane Loiselle, Jie Ren, Maija Raudsepp, Gord Campell (Scampy), Nahed Mahrous, Jenine McCutcheon (J9), Alyssa Smith (No. 1), Alex Pontefract, Louisa Preston, Kelly Summer, Matt Izawa and Jess Stromberg. Ian Power was my senior graduate mentor when I first started working in the lab. His mentorship was so influential that when Gord told me I was next in charge after Ian graduated I thought it would be impossible to fill his shoes. In reverence, I felt as though the shoes were a tad loose at times. I will always be grateful for Ian's guidance in the lab and more importantly his friendship. I admit that Ian's "drink your medicine" philosophy at 4:00 pm on Friday afternoons was the inspiration for my "lab meetings". It was through him I realised that camaraderie was part of the fabric of being a labling. I also want to thank Chris for his enlightening perspective on various aspects of scientific research. I will never forget our discussions related to *The importance of stupidity in scientific research* and *Microbiological laboratory hazards of bearded men*. It wasn't until a few months into my first year as a graduate student that I really got to know Dusa. We were independently attempting to make SRB media for the first time and were independently successful at doing it wrong. I'm almost certain we were both secretly trying to see who could get it done first as though it were a competition to prove who knew what they were doing. I remember looking across the

lab bench and declaring in frustration that I needed a “coffee break”. To my surprise, Dusa decided to join me. While sitting in the Rock Garden we contrived the idea to work together. It worked. Since that time we were inseparable and Dusa-moj will always be my best friend. To my lab princesses (Maija, Pepper, Liane, Jie, Nahed and Alex) and Scampy, I will always cherish the memorable times we had in and out of the lab whether it was: deciphering G-slam notes; trips to Argonne; cutting syringes with the sketchy drill; or figuring out a way to ignite strawberries for a birthday cake. I’m proud to have seen you come into the lab and accomplish your respective goals and I know that we will always be good friends. As the number of lablings gradually began to dwindle, I sometimes wondered how J9 single-handedly endured my antics. I suppose she really had no choice in the matter since we also shared the same office space. I enjoyed all the adventures we had together over the past two years and look forward to many more in the future (fingers crossed). She is truly a great friend. Collectively, I’d like to thank my labmates, honorary labmates and friends I’ve made within the department. There are not enough words to express my gratitude for the love and support I received from everybody outside the academic setting.

I would like to thank Liz Webb for being our acting supervisor and Neil Banerjee for his unofficial mentorship. I also owe much thanks to Dr. Susan Koval and Dr. Norman Duke for their support during my qualifying exam and more importantly their encouragement as my advisory committee members. I would also like to thank Drs. Norman Duke, Robert Linnen, Sheila Macfie and Chris Weisener for being my thesis examiners. Thanks to Todd Simpson, Tim Goldhawk, Charlie Wu and Monique Durr for their reliable assistance at the Nanofabrication Facility and the Biotron. For the collaborative work, I’d like to thank Lachlan MacLean, Sian Marsden, Robert Gordon, Trudy Bolin, Nathan Magarvey, Chad Johnston, Keith Barron and Neil Banerjee. Throughout my time as a graduate student I’ve been fortunate and thankful to receive funding from the Queen Elizabeth II Graduate Scholarship in Science and Technology, Western Graduate Research Scholarship, Robert & Ruth Lumsden Award in Science and William S. Fyfe Graduate Scholarship in Natural Resources. These generous contributions allowed me to further my research and develop as a researcher.

Lastly I would like to thank my parents (Jerry and Esther), sister (Ruth) and brother-in-law (Andre). Your love has been the support and motivation that has enabled me to accomplish my academic goals over the years.

# Table of Contents

# List of Tables

# List of Figures

# List of Appendices

# List of Abbreviations and Symbols

| | |
|---|---|
| *A.* | *Acidithiobacillus* |
| approx. | Approximately |
| ARD | Acid Rock Drainage |
| atm | Atmosphere |
| $Au_nS_m^-$ | Gold sulphide chemical formula with variable number of atoms |
| $_{(aq)}$ | Aqueous |
| BLAST | Basic Local Alignment Search Tool |
| BSE | Back Scatter Electron |
| cm | Centimetres |
| DNA | Deoxyribonucleic Acid |
| EDS | Energy Dispersive Spectrometer |
| e.g. | for example |
| Eh | Reduction potential |
| et al. | and others |
| eV | Electron volts |
| f | foreword (universal bacterial primer) |
| FEG-SEM | Field Emission Gun-Scanning Electron Microscope |
| FIB | Focused Ion Beam |
| g | Grams |
| *g* | Gravitational-force |
| Gt | Gigatonnes |
| hr. | Hours |
| ICP-AES | Inductively Coupled Plasma-Atomic Emission Spectroscopy |
| i.e. | in other words |
| kb | Kilo base pairs (nucleotides) |
| $kJ \cdot mol^{-1}$ | Kilojoules per mole |
| km | Kilometres |
| kV | Kilovolts |
| m | Metres |
| M | Molar |

| | |
|---|---|
| mg | Milligrams |
| mM | Millimolar |
| min. | Minutes |
| mL | Millilitres |
| mm | Millimetres |
| MPN | Most Probable Number |
| N | North |
| nm | Nanometres |
| PCR | Polymerase Chain Reaction |
| pH | -log[H+] |
| pL | Picolitres |
| ppm | Parts per million |
| r | reverse (universal bacterial primer) |
| rpm | Revolution per minute |
| RT | Room temperature |
| S | South |
| *S* | Svedberg unit |
| SEM | Scanning Electron Microscope |
| SEM-EDS | Scanning Electron Microscopy-Energy Dispersive Spectroscopy |
| sp. | Species (singular) |
| spp. | Species (plural) |
| SRB | Sulphur-reducing bactera |
| TEM | Transmission Electron Microscope |
| TEM-EDS | Transmission Electron Microscopy-Energy Dispersive Spectroscopy |
| t | Tonnes |
| W | West |
| (wt/vol) | Weight/ Volume |
| XAFS | X-ray absorption fine structure |
| XANES | X-ray Absorption Near-Edge Spectroscopy |
| x | by |
| × | times |
| $\mu g\ kg^{-1}$ | Micrograms per kilogram |

| | |
|---|---|
| µL | Microlitres |
| µm | Micrometres |
| $^{0}$ | Elemental |
| ° | Degrees |
| ˚C | Degrees Celsius |
| ' | Minutes |
| " | Seconds |
| % | Percent |

# Chapter 1

## 1 Introduction

Gold has been one of the most renown and sought-after natural materials since antiquity. Although generally considered as a hedge investment, it can be argued that modern applications of gold's physical properties, e.g., ductility, high conductivity and resistance to corrosion, have contributed to the persistent socioeconomic and cultural demand for this commodity. Like other precious metals, the rarity of gold in the Earth's crust creates challenges for finding economically viable source materials. A better understanding of the biogeochemistry of gold under near-surface to surface environmental conditions will possibly provide new strategies for exploration, i.e., vectoring anomalous values for undiscovered deposits, and possibly greater recovery from mining processes, e.g, biomining.

## 1.1 Gold distribution

Relative to other metals, gold is unevenly distributed throughout the Earth's crust and has an average concentration of approximately 1.5 $\mu g \cdot kg^{-1}$ (Frimmel, 2008). Gold deposits, however, are globally distributed and contain approximately $10^4$ times more concentrated gold relative to the low crustal concentration (Boyle, 1979; Frimmel, 2008). Assuming that the mass of continental crust is approximately $2.97 \times 10^{19}$ t (Frimmel, 2008), an estimated 45 Gt of gold is thought to be present in the modern continental lithosphere. To date, 183 000 t of gold has been extracted and therefore represents only a fraction of the theoretical amount of gold present (Frimmel, 2008). Although factors controlling gold distribution and deposit-level concentrations are variable and still debated, gold deposits can be associated with magmatic, hydrothermal or sedimentary origins (Boyle, 1979, 1986; Hannington, 1994; Sillitoe, 1994; Sillitoe et al., 1996; Groves et al., 2005; Bierlein et al., 2006; Pitcairn et al., 2006a,b). The geological settings in which gold deposits occur are indicative of different modes that gold were sourced, transported and concentrated. Gold deposits are categorised as either primary or secondary gold sources. Primary gold is generally associated with quartz veins and a host of metal sulphide minerals while secondary gold is associated with environments where mechanical sorting occurs, i.e., eluvial, colluvial or fluvial erosion processes (see Boyle, 1979, 1986; Mossman and Harron, 1983; Cuneen and Sillitoe, 1989;

Marsden and House, 1992; Hannington, 1994; Stillitoe et al., 1996).

## 1.2 Gold geochemistry

Gold can be dissolved as aqueous gold (I) and (III) complexes when an inorganic complexing ligand and an oxidising agent are both present in aqueous solution. Gold (I) complexes have linear stereochemistry with the gold atom having a coordination number of two. In contrast to the first oxidation state of gold, gold (III) complexes commonly have a square-planar stereochemistry with the gold atom having a coordination number of four (Puddephatt, 1978). Depending on the reaction conditions and the concentration of ligands in solution, gold (I) generally forms $AuCl_2^-$ and $Au(S_2O_3)_2^{3-}$ complexes while gold (III) forms $AuCl_4^-$ (Puddephatt, 1978; Williams-Jones et al., 2009). It is important to note that at ambient temperatures, i.e., surface to near-surface conditions, gold (I) chloride complexes are metastable and will eventually disproportionate to elemental gold and gold (III) chloride because the third oxidation state is preferred (Puddephatt, 1978; Reaction 1.1).

$$3\ AuCl \rightarrow 2\ Au^0 + AuCl_3 \qquad (1.1)$$

It should be noted that organic ligands, such as cyanide, are by-products of active microbial metabolism (Vlassopoulos and Wood, 1990) and are known to contribute to gold dissolution (Fairbrother et al., 2009). However, from a geological context, the formation of soluble gold complexes is primarily dependent on the geochemical conditions of the surrounding environment. Furthermore, gold mobility as soluble gold complexes within surface and near-surface hydrological regimes will depend on the type and the availability of ligands present (Puddephatt, 1978; Mann, 1984; Webster, 1985; Benedetti and Boulegue, 1991). Therefore, under oxidising conditions where an abundance of metal sulphides exist in association with gold, gold (I) thiosulphate complexes could conceivably be formed during biooxidation of these materials. In this environment, oxidised sulphur compounds would likely be more prominent as a complexing ligand than chloride (Mann, 1984; Webster, 1986; Benedetti and Boulegue, 1991; Reaction 1.2). Under saline to hypersaline environmental conditions the occurrence of gold (I) thiosulphate would be unlikely since chloride would be the dominant ion present (Mann, 1984). Gold (I and III) chloride complexes are generally stable under acidic conditions when a solution contains high chloride content and a strong oxidizing agent; however, the gold (III) chloride complex is most likely to occur under ambient

conditions (Mann, 1984; Reaction 1.3). Furthermore, it should be noted that the oxidation of elemental gold to form soluble gold (I) and gold (III) complexes depends on the other chemical factors, i.e., pH, Eh and the concentration and type of complexing ligands (Puddephatt, 1978). Surface and near-surface hydrologic regimes are dynamic systems that are influenced by the physical and chemical conditions of the environment in which they occur. For example, the formation and transport of soluble gold complexes in ground waters located proximal to mesothermal gold deposits are affected by different ground water salinity gradients. In these environments, the convective mixing of varying brines can affect the distributions and stability of gold complexes (Carey et al., 2003; Williams-Jones et al., 2009). Therefore, the ionic state of gold in any given surficial environment must be considered to be dynamic as the formation of various soluble gold complexes can occur such as gold (I) thiosulphate and gold (III) chloride.

$$2\ Au^0 + 2\ S_4O_6^{2-} + 2\ H_2O + Fe^{2+} \rightarrow 2\ Au(S_2O_3)_2^{3-} + 4\ H^+ + FeO_2 \quad (1.2)$$

$$Au^0 + 4\ Cl^- + 0.5\ O_2 \rightarrow AuCl_4^- + 3\ OH^- \quad (1.3)$$

## 1.3 Gold biogeochemistry

Bacteria are ubiquitous in nature and are considered a “simple” example of life that is capable of carrying out metabolic processes. However, as a group, they have existed and evolved for billions of years, which has given them the opportunity to adapt to a wide range of environmental conditions (Rothschild and Mancinelli, 2001). Metabolically active bacteria are capable of altering the geochemical conditions of their surrounding environment ranging from micrometre to global scales (see Beveridge, 1981; MacLean et al., 2007; Wanger et al., 2006; Southam and Saunders, 2005).

Goldschmidt (1937) was the first to suggest the significance of biogeochemical processes that enabled the selective concentration of metals from the surrounding environment. Further contributions to this idea by Lowenstam (1981) identified the role of bacteria as nucleation sites for mineral formations. Similarly Beveridge (1981) highlighted the importance of bacterial cell envelopes, i.e., gram-positive and gram-negative cell walls, in determining the cell morphology and in providing an interface between the internal cellular environment and the surrounding external milieu (Beveridge and Fyfe, 1985; Schultze-Lam et al., 1996; Southam, 2001). The outer surface of gram-negative cell walls possesses

lipopolysaccharides that contain carboxylate and phosphoryl groups. Gram-positive bacteria contain metal-reactive ionic groups at their cell water interface in association with the peptidoglycan layer that also incorporates teichoic and teichuronic acids. The net negative charge of bacterial cell surfaces is responsible for metal binding (Daughney et al., 1998; Beveridge and Fyfe, 1985; Southam and Saunders, 2005). This passive mineral precipitation acts as a mode by which mineral precipitates are nucleated and mediated by biological systems. Collectively, the functional groups found on both gram-negative and gram-positive bacteria are also capable of ionisation and metal binding (Beveridge and Fyfe, 1985; Daughney et al., 1998; Karthikeyan and Beveridge, 2002; Southam and Saunders, 2005; Lengke et al., 2006; Fairbrother et al., 2012 Kenny et al., 2012; Song et al., 2012). Therefore, bacterial envelopes can function as kinetic factors by donating electrons that contribute to the reduction of soluble gold complexes forming elemental gold. Furthermore, Karthikeyan and Beveridge (2002) also suggested that cells from biofilms lyse due to toxicity effects of increased metal concentrations thereby releasing intracellular material. This increased amount of "organic debris" can then act as additional substrates on which a greater quantity of metal ions can be reduced and eventually precipitate relative to non-lysed bacterial cells (Karthikeyan and Beveridge, 2002).

A microbe-driven biogeochemical cycle for gold has been proposed (Reith et al., 2006). In this biogeochemical cycle, the dissolution and precipitation of gold in surface to near-surface environments are often directly linked to the transformation of iron and sulphur compounds (Southam and Saunders, 2005). Bacteria can actively oxidise metals or use metals as terminal electron acceptors. In both modes, bacteria interact with a metal stressed environment in which the metals are used in dissimilatory metabolic reactions (Bonneville et al., 2003; Chatellier et al., 2001; Roden and Urratia, 2002; Southam, 2001). Biomineralisation has the potential to continue to occur in any environment as long as metabolic growth is maintained, reproducing biomass that is lost to biomineralisation (Southam and Saunders, 2005).

## 1.4 Study objectives

Since microorganisms contribute to the biogeochemical conditions of surrounding environments and mediate the precipitation of secondary gold, they should have both a direct

and indirect role in the mobility of gold. The main objective of these studies was to understand the biogeochemical cycling of gold under surface and near-surface environmental conditions with particular emphasis on the immobilisation of gold through the reduction of soluble gold (I) thiosulphate or gold (III) chloride complexes leading to secondary gold enrichment. In this context, five laboratory studies representing different natural systems were conducted.

Chapter 2 focuses on the biological-induced weathering of gold-bearing metal sulphide minerals to demonstrate that acidophilic iron-oxidising bacteria "liberate" primary gold. Through this process the biogeochemical cycling of gold is initiated as gold can be mobilised as particles or as dissolved soluble complexes. The interaction between soluble gold (I) thiosulphate with acidophilic iron-oxidising bacteria and associated biogeochemical conditions, attributed to their active metabolism, is examined in Chapter 3. In addition, the same experiments are performed using soluble gold (III) chloride (Appendix A). A suite of gold grains is extensively characterised in Chapter 4 in association with a series of laboratory experiments involving the reaction of a pure bacterial culture, obtained from a gold grain surface, with gold (III) chloride. These combined studies address how bacteria contribute to the structure and chemistry of gold grains. Chapter 5 focuses on the interaction of gold (III) chloride with halophilic sulphur-reducing bacteria and how varying salinity, i.e., excess chloride ions, could potentially inhibit secondary gold biomineralisation. Investigations in Chapter 6 demonstrate the completion of gold biogeochemical cycling under surface and near-surface environmental conditions and the *in vitro* bioaccumulation of secondary gold into gold nuggets. Finally, in Chapter 7 I discuss the combined contributions of these experiments to the study of gold biogeochemistry. Understanding gold biogeochemical cycling under surface and near-surface environmental conditions is important because it provides the basis for developing innovative and sustainable modes of mineral exploration and recovery.

## 1.5 References

Benedetti, M., Boulegue, J., 1991. Mechanism of gold transfer and deposition in a supergene environment. Geochimica et Cosmochimica Acta, 55, 1539-1547.

Beveridge, T.J., 1981. The interaction of metals in aqueous solution with bacterial cell walls from *Bacillus subtilis*. Ann Arbor Scientific Publishing. Michigan, USA.

Beveridge, T.J., Fyfe, W.S., 1985. Metal fixation by bacterial cell walls. Canadian Journal of Earth Science, 22, 1893-1898.

Bierlein, F.P., Groves, D.I., Goldfarb, R.J., Dube, B., 2006. Lithospheric controls on the formation of provinces hosting giant orogenic gold deposits. Mineralium Deposita, 40, 874-886.

Bonneville, S. Behredns, T., Van Cappellen, P., Hyacinthe, C., Roling, W.F.M., 2003. Reduction of Fe (III) colloids by *Shewanella putrefaciens*: A kinetic model. Geochemica et Cosmochimica Acta, 70, 5842-5854.

Boyle, R.W., 1979. The geochemistry of gold and its deposits. Geological Survey of Canada Bulletin, 280, 584.

Boyle, R.W., 1986. Gold deposits in turbidite sequences: Their geology, geochemistry and history of theories of their origin, in Keppie, J.D., Boyle, R.W., Haynes, S.J., eds., Turbidite-hosted Gold Deposits Special Paper Geological Association of Canada, 32, 1-13.

Carey, M.L., McPhail, D.C., Taufen, P.M., 2003. Groundwater flow in playa lake environments: Impact on gold and pathfinder element distributions in groudwaters surrounding mesothermal gold deposits, St. Ives area, Eastern Goldfields, Western Australia. Geochemistry-Exploration, Environment, Analysis, 3, 57-71.

Chatellier, X., Fortin, D., West, M., Leppard, G., Ferris, F., 2001. Effect of the presence of bacterial surfaces during the synthesis of Fe oxides by oxidation of ferrous ions. European Journal of Mineralogy, 13, 705-714.

Cuneen, R., Sillitoe, R.H., 1989. Paleozoic hot spring sinter in the Drummond Bassin, Queensland, Australia. Economic Geology, 84, 135-142.

Daughney, C.J., Fein, J.B., Yee, N., 1998. A comparison of the thermodynamics of metal adsorption onto two common bacteria. Chemical Geology, 144, 161-176.

Fairbrother, L., Brugger, J., Shapter, J., Laird, J.S. Southam, G., Reith, F., 2012. Supergene gold transformation: Biogenic secondary and nano-particulate gold from arid Australia. Chemical Geology, 321, 17-31.

Frimmel, H.E., 2008. Earth's continental gold endowment. Earth and Planetary Science Letters, 286, 45-55.

Goldschmidt, V.M., 1937. The principles of distribution of chemical elements in minerals and rocks. Journal of the Chemical Society, 1, 655-673.

Groves, D.I., Condie, K.C., Goldfarb, R.J., Hronsky, J.M.A., Vielreicher, R.M., 2005. Secular changes in global tectonic processes and their influence on the temporal distribution of gold-bearing mineral deposits. Economic Geology, 100, 203-224.

Hannington, M.D., 1994. Shallow marine hydrothermal systems in modern arc settings. Geological Association of Canada Newletters-The Gangue, 43, 6-8.

Karthikeyan, S. and Beveridge, T.J., 2002. *Pseudomonas aeruginosa* biofilms react with and precipitate toxic soluble gold. Environmental Microbiology, 4, 667-675.

Kenny, J.P.L., Song, Z., Bunker, B.A., Fein, J.B., 2012. An experimental study of Au removal from solution by non-metabolising bacterial cells and their exudates. Geochimica et Cosmochimica Acta, 87, 51-60.

Lengke, M.F., Fleet, M.E., Wanger, G., Ravel, B., Southam, G., 2006. Precipitation of gold by reactions of aqueous gold (III) chloride with cyanobacteria at 25-80 degrees Celsius: Studied by X-ray absorption spectroscopy. Canadian Journal of Chemistry, 85, 651-659.

Lowenstam, H., 1981. Minerals formed by organisms. Science, 211, 1126-1131.

MacLean, L.C.W., Pray, T.J., Onstott, T.C., Brodie, E.L., Hazen, T.C., Southam, G., 2007. Mineralogical, chemical and biological characterisation of an anaerobic biofilm collected from a borehole in a deep gold mine in South Africa. Geomicrobiology Journal, 24, 491-504.

Mann, A.W., 1984. Mobility of gold and silver in lateritic weathering profiles; some observations from Western Australia. Economic Geology and the Bulletin of the Society of Economic Geologist, 79, 38-49.

Marsden, J., House, I.H., 1992. The chemistry of gold extraction. Ellis Horwood Publishing. New York. 13-58.

Mossman, D.J., Harron, G.A., 1983. Origin and distribution of gold in Huronian Supergroup, Canada-the Case for Witwatersrand-type paleoplacers. Journal of Precambrian Geology, 20, 543-583.

Pitcairn, I.K., Teagle, D.A.H., Craw, D., Olivo, G.R., Kerrich, R., Brewer, T.S., 2006a. Sources of metals in orogenic gold deposits: insights from the Otago and Alpine Schists, New Zealand. Economic Geology, 101, 1525-1546.

Pitcairn, I.K., Warwick, P.E., Milton, J.A., Teagle, D.A.H., 2006b. A method for ultra-low level analysis of gold in rocks. Analytical Chemistry, 78, 1280-1285.

Puddephatt, R., 1978. The Chemistry of Gold. Elsevier Publishing Company. New York. 31-87.

Reith, F., Rogers, S.L., Falconer, D., Craw, D. and Southam, G., 2006. Biomineralisation of gold: Biofilms on bacterioform gold. Science, 313, 233-236.

Roden, E.E., Urratia, M.M., 2002. Influence of biogenic Fe (II) on bacterial crystalline Fe (III) oxide reduction. Geomicrobiology Journal, 19, 209-251.

Rothschild, L.J., Mancinelli, R.L., 2001. Life in extreme environments. Nature, 409, 1092-1101.

Schultze-Lam, S., Fortin, D., Davis, B.S., Beveridge, T.J., 1996. Mineralisation of bacterial surfaces. Chemical Geology, 132, 171-181.

Sillitoe, R.H., 1994. Erosion and collapse of volcanoes: Causes of telescoping in intrusion-centered ore deposits. Geology, 22, 945-948.

Sillitoe, R.H., Hannington, M.D., Thompson, J.F.H., 1996. High sulphidation deposits in the volcanogenic massive sulphide environment. Economic Geology, 91, 204-212.

Song, Z., Kenney, J.P.L., Fein, J.B., Bunker, B.A., 2012. An x-ray fine structure study of Au adsorbed onto the non-metabolising cells of two soil bacterial species. Geochimica et Cosmochimica Acta, 86, 103-117.

Southam, G., 2001, Quantification of sulphur and phosphorus within secondary gold rims on Yukon placer gold. Geology, 26, 339-342.

Southam, G. and Saunders, J.A., 2005. The geomicrobiology of ore deposits. Economic Geology, 100, 1067-1984.

Vlassopoulos, D. and Wood, S.A., 1990. Gold speciation in natural waters: 1. Solubility and hydrolysis reactions of gold in aqueous solution. *Geochimica et Cosmochimica Acta*, 54, 3-12.

Wanger, G., Southam, G., Onstott, T.C., 2006. Structural and chemical characterisation of a natural fracture surface from 2.8 kilometres below land surface: Biofilms in the deep subsurface. Geomicrobiology Journal, 23, 443-452.

Webster, J.G, 1985. Thiosulphate in surficial geothermal waters, North Island, New Zealand. Applied Geochemistry, 2, 5-6.

Williams-Jones, A.E., Bowell, R., Migdisov, A.A., 2009. Gold in solution. Elements, 5, 281-287.

# Chapter 2

## 2 Microbial weathering of gold-bearing sulphide ore

Many studies have demonstrated that the oxidation of sulphide minerals, e.g., pyrite, chalcopyrite, and arsenopyrite, in aqueous conditions generally involves either chemical or electrochemically catalysed reactions (see Steger and Desjardin, 1978; Lowson, 1982; Nicholson et al., 1988; Buckley and Walker, 1988; Nesbitt et al., 1995; Nordstrom and Southam, 1997; Nesbitt and Muir, 1998; Rimstidt and Vaughan, 2003; Chandra and Gerson, 2010). The oxidation of metal sulphides has geochemical significance since it can lead to the formation and release of sulphuric acid into the environment and, in the case of arsenopyrite, arsenic and arsenous acids (Nesbitt et al., 1995). In near-surface weathering environments, significant dissolution of (iron) sulphide minerals has been attributed to the metabolic activity of lithoautotrophic, iron-oxidising bacteria (Singer and Stumm, 1970). The importance of the biosphere in catalysing metal sulphide oxidation and dissolution has been shown in a wide range of environments (see Ohmura et al., 1993; Bhatti et al., 1993; Nordstrom and Southam, 1997; Fowler and Crundwell, 1999; Edwards et al., 2000a,b; Rodriquez et al., 2003a,b,c; Jones et al., 2003; Mielke et al., 2003; Chan et al., 2009; Thurston et al., 2010; Africa et al., 2012). In every one of these systems, the oxidation of ferrous iron is the rate-determining step promoting the abiotic oxidation of metal sulphide minerals (Singer and Stumm, 1970). Under laboratory conditions, iron-oxidising bacteria have been shown to oxidise soluble ferrous iron up to six orders of magnitude faster relative to abiotic iron oxidation (Lacey and Lawson, 1970; Tyagi et al., 1993). However, in natural environments ferrous iron oxidation rates are likely to occur somewhere between abiotic rates and this maximal rate since metabolic growth of iron-oxidising bacteria are influenced by other environmental factors, i.e., temperature, essential nutrients for growth, hydrological activity and pH (Nordstrom and Southam, 1997). Arredondo et al. (1994) demonstrated that leaching of chalcopyrite occurred by direct attachment of bacteria to mineral surfaces. However, Jones et al. (2003) demonstrated that direct bacterial attachment to metal sulphide mineral surfaces was not necessary to promote the dissolution of arsenopyrite.

Gold from primary sources is generally associated with a wide range of metal sulphide minerals (Boyle, 1979). The ore associated with the Capillitas mine, located in the Province of Catamarco, Argentina is characterised as a sequence of highly-sulphidised epithermal veins, i.e. the San Salvador vein. These veins contain metal sulphide minerals including chalcopyrite, pyrite, pyrrhotite, galena, enargite and arsenopyrite. Gold generally occurs as tens of micrometre-size, irregular grains associated with these sulphide minerals within a quartz matrix (Marquez-Zavalia and Craig, 2004). Millimetre- and centimetre-size cavities are also common features within the veins. The surficial oxidation and supergene enrichment horizons of the Capillitas mine are 50 m and 150 m thick, respectively (Marquez-Zavalia and Craig, 2004). Understanding the oxidation of gold-bearing, highly-sulphidised, epithermal ore deposits, such as the Capillitas mine, is important from a geochemical exploration perspective because weathering can lead to the redistribution of gold within near-surface environments (Cooke and Simmons, 2000). Southam and Saunders (2005) highlighted how bacteria influence the geochemistry of ore deposits at near-surface conditions. Studies have demonstrated that the transport of metals in solution was a consequence of bacterial contributions to the dissolution of sulphide minerals. However, bacteria also mediate the formation of secondary mineral precipitates through the oxidation or reduction of soluble metals (Nordstrom and Southam, 1997; Rawlings, 2002; Johnson and Hallberg, 2003). Through the oxidation of metal sulphide minerals, rock permeability and porosity is increased which contributes to low temperature transport of metals (Enders et al., 2005). Studies by Rainbow et al. (2006) demonstrated that microbes do in fact contribute to the supergene oxidation of highly-sulphidised, epithermal gold-silver deposits.

The effect of iron-oxidising bacteria on a highly-sulphidised, gold-bearing, polymetallic sulphide ore is an important question because these organisms contribute to metal sulphide mineral dissolution that could lead to supergene weathering in near-surface environments. Therefore, in this study, biotic and abiotic systems representing aqueous weathering environments were constructed to characterise bacterial colonisation and the physical and chemical weathering effects attributed to iron-oxidising bacteria on a gold-bearing polymetallic sulphide ore.

# 2.1 Materials and Methods

## 2.1.1 Bacterial enrichment and enumeration

Submersed cobbles in Rio Tinto, Spain (Fig. 2.1a) (37° 35' 33.27" N, 6° 33 1.84" W) contained mineralised biofilms approximately 3 cm thick (Fig. 2,1a). See Fernandez-Remolar et al. (2005) for elemental composition and mineralogy of cobbles and coatings. This biofilm was sampled along with river water. The pH of the river water was 2.9 (measured using Electron Microscopy Sciences colourpHast Indicator Strips 0.0-4.0). The unconsolidated (yellow-orange, fine-grained, iron oxide) biofilm was dispersed within the sampled river water using a vortex before culturing. Primary bacterial enrichments were prepared by inoculating 0.5 mL of the dispersed consortium into Fisherbrand® 13 × 100 mm borosilicate glass test tubes containing 4 mL of modified media defined by Silverman and Lundgren (1959) with 0.5 mL of 33.3 g/100 mL ferrous sulphate heptahydrate. The pH of the growth medium and the iron supplement were adjusted to pH 2.3 using 2 M sulphuric acid (Denver Instrument Basic pH/Eh Meter calibrated to pH 2 and 4 reference standards using potassium biphthalate buffer at room temperature). Precision of pH measurements was ±0.03 pH units. The test tubes were covered with sterile, plastic push caps to prevent contamination and were incubated for three weeks under aerobic conditions at room temperature (RT, approx. 22˚C). Replicate bacterial enrichments were used for electron microscopy (see section 2.1.3), aqueous geochemical analysis and to count viable cells using the Most Probable Number (MPN) statistical method described by Cochran (1950).

## 2.1.2 Gold-bearing metal sulphide sample preparation

A gold-bearing metal sulphide ore was obtained from the San Salvador vein from the Capillitas mine, Argentina (Marquez-Zavalia and Craig, 2004; 27° 27' S, 66° 30' W). The sample was cut into two pieces each approximately 3 mm in thickness. One side of each piece was polished to expose a “fresh” mineral surface using a 500 nm aluminium silicate paste (Fig. 2.1b).

### 2.1.3 Bacterial enrichment and gold-bearing metal sulphide characterisation

Bacterial cells from the fluid phase of a three week bacterial enrichment was obtained (see section 2.1.4) and fixed with $2\%_{(aq)}$ glutaraldehyde for 24 hours, dehydrated in sequential $25\%_{(aq)}$, $50\%_{(aq)}$, $75\%_{(aq)}$ and 3 × 100% ethanol series and dried using a Tousimis Research Corporation Samdri-PVT-3B critical point drier. The sample was then placed on an aluminium stub with a 12 mm carbon adhesive tab. All samples were coated with a 5 nm osmium deposition using a Denton Vacuum Desk II sputter coater to reduce charging effects during sample characterisation. Bacteria from the enrichment and gold-bearing sulphide samples were characterised using a LEO Ziess 1540XB Field Emission Gun-Scanning Electron Microscope (FEG-SEM) equipped with an Oxford Instruments' INCAx-sight Energy Dispersive Spectrometer (EDS). The FEG-SEM, operating at an accelerating voltage of 3 or 10 kV, was used for surface imaging and qualitative elemental composition, respectively.

### 2.1.4 Bacterial weathering system assemblage

Three 5 mL bacterial enrichments, incubated for 3 weeks, were homogenised using a vortex to help "liberate" loosely bound "individual" cells from the iron oxyhydroxide minerals that precipitate on the interior surface of the borosilicate glass test tube (Fig. 2.1a, inset). The majority of the iron oxyhydroxide precipitates, dislodged from the walls of the test tubes, were allowed to settle to the bottom of the tubes for 1 min. to ensure that a 10 mL bacterial suspension possessed a limited amount of iron oxyhydroxide (confirmed using light microscopy). The bacterial weathering system was constructed in a sterile, 125 mL volume Erlenmeyer flask by adding the 10 mL fluid phase "inoculum" to 90 mL of basal medium defined by Silvermann and Lungdren (1959) with no addition of ferrous sulphate heptahydrate.

The polished gold-bearing metal sulphide ore samples were sonicated three times for 5 min. each to remove the osmium coating from imaging (see section 2.1.3), sterilised using 100% ethanol and rinsed with filter-sterilised, deionised water and attached to sterile polyethylene twine. One gold-bearing metal sulphide was suspended in the bacterial weathering system

(see section 2.1.2). The purpose of suspending the sample was to ensure that bacteria in solution were attaching and not settling onto mineral surfaces. The other gold-bearing metal sulphide sample was suspended in a separate, sterile, 125 mL Erlenmeyer flask containing the same basal medium without the addition of bacteria, representing an abiotic control. Both systems were covered with sterile aluminium foil to prevent contamination and reduce evaporation. The first laboratory model represents the biogeochemical conditions encountered in near-surface environments in which sulphide-bearing rocks are weathered via biogeochemical processes. The abiotic control system was used to evaluate the catalytic effect of having bacteria in the reaction systems and to determine whether or not the acidic conditions could be responsible for the dissolution of sulphide minerals. Both reaction systems were incubated for 60 days at RT. The pH was re-measured after the incubation period using a Denver Instrument Basic pH/ Eh Meter as described in section 2.1.1.

### 2.1.5 Gold-bearing metal sulphide re-characterisation

After 60 days incubation, the surfaces of bacterial and abiotic control gold-bearing metal sulphide ores were re-characterised along with an iron oxyhydroxide precipitate that developed at the bottom of the flask in the bacterial weathering system. Scanning Electron Microscopy (SEM) conditions and sample preparation were the same as the methods described for the characterisation of the bacterial cells and gold-bearing metal sulphide prior to bacterial exposure (see section 2.1.3).

### 2.1.6 Aqueous geochemical analysis

Duplicate 5 mL aliquots were sampled from both systems and were filtered using a 0.1 µm pore-size filter to remove any solid material. These solutions represented the initial aqueous geochemical conditions of the bacterial weathering system and the abiotic control at the start of the experiment. After 60 days, additional duplicate 5 mL aliquots were sampled and represented the geochemical conditions at the end of the experiment. All samples were acidified to pH 1 using concentrated (71%) nitric acid and analysed for soluble silver, arsenic, gold, copper, iron, mercury, molybdenum, nickel, lead and zinc using Perkin-Elmer Optima 3300-DV Inductively Coupled Plasma-Atomic Emission Spectroscopy (ICP-AES). High Purity™ Standards, purchased from Delta Scientific, were used for ICP-AES analysis.

## 2.2 Results

### 2.1.1 Bacterial enumeration and characterisation

The MPN count of the iron-oxidising bacterial enrichments was $2.4 \times 10^4$ bacteria/mL. Evidence of active iron-oxidising bacterial metabolism from the enrichment was indicated by the increased acidity, i.e., pH = 2.1, and the formation of a red-orange, iron oxyhydroxide precipitate that coated the inside surface of the borosilicate test tubes (Fig. 2.1a, inset). SEM characterisation indicated that the bacterial enrichment contained predominantly rod-shaped bacteria and a lesser amount of spirilla occurring on the surface of nanometre-size, acicular precipitates composed of iron and oxygen that formed micrometre-scale sheets (Fig. 2.1c, d).

### 2.1.2 Gold-bearing metal sulphide characterisation

Prior to exposure in the bacterial weathering system, SEM analysis demonstrated that the gold-bearing metal sulphide contained natural crevices that occurred within and along metal sulphide mineral boundaries within a quartz matrix. Backscatter SEM micrographs and EDS spectra indicated that sulphide minerals contained a range of elements including arsenic, copper, iron, manganese, lead and tin and were consistent with previous studies identifying metal sulphide minerals (see section 2; Marquez-Zavalia et al., 1999; Marquez-Zavalia and Craig, 2004; de Brodtkorb, 2009). Gold and silver occurred along sulphide mineral boundaries as irregular, tens of micrometre-size "grains" (Fig. 1e-h).

After 60 days of exposure in the bacterial weathering system, an abundance of bacteria were observed on articulated surfaces of metal sulphide minerals and extensive biofilms were also observed within crevices (Fig. 2.2a). A coating composed of iron, phosphorus and oxygen occurred as a laminate structure that coated the polished surface of the ore. Bacteria were directly attached to this iron phosphate coating (Fig. 2.2b-d). Although rod-shaped bacteria were the dominant morphotype, a greater proportion of spirilla relative to the inoculum were observed. More importantly, both types of cells had extracellular, secondary mineral precipitation. These nanometre-size precipitates were composed of iron and sulphur (Fig. 2.2e, f). SEM analysis indicated that a micrometre-size, discoidal mineral precipitate composed of iron, sulphur and oxygen formed on the surface of metal sulphides and the iron

phosphate coating (Fig. 2.3a, b). The once polished metal sulphide surfaces now appeared weathered. The discoidal precipitate occurred on the surface of weathered minerals along with bacteria (Fig. 2.3c). A fragment of metal sulphide mineral was also found at the bottom of the flask along with the discoidal precipitates. This demonstrates that weathering may have occurred along grain boundaries, releasing mineral fragments from the polish rock surface. The metal sulphide at the bottom of the flask had a rough surface texture similar to the weathered mineral surfaces observed on the suspended sample. However, bacteria attachment was not observed but bacterial-size impressions were present (Fig. 2.3d-f).

### 2.1.3 Geochemical analysis

Detailed results from ICP-AES analysis are found in Table 2.1. Prior to the addition of the gold-bearing metal sulphide sample, the fluid phase of the bacterial weathering system contained iron and sulphur from the bacterial inoculum. After 60 days, the fluid phase of the bacterial weathering system contained trace metal concentrations including silver, arsenic, copper, iron, lead, sulphur and zinc. Interestingly, the iron concentration had decreased while sulphur slightly increased relative to the initial respective concentrations. In the abiotic control system copper, iron, lead, and zinc were present but concentrations were less than those of the bacterial weathering system. The pH of the biological weathering system dropped from pH 2.3 to pH 2.1 while the abiotic system remained the same.

## 2.2 Discussion

Iron-oxidising bacteria are capable of oxidising both iron and sulphur (Fowler and Crundwell, 1999) and are commonly found in near-surface weathering environments. The presence of iron-oxidising bacteria has a profound effect by catalysing the dissolution of metal sulphides (see Erhlich, 1964; Singer and Stumm, 1970; Hedrich et al., 2011). The contribution of the biosphere in acidic, oxidised environments is important for the physical and chemical weathering of metal sulphides because it potentially leads to the liberation and mobility of soluble gold complexes or solid gold particles. The bacterial weathering system, used in this study, represented an amplified natural system containing a high water:rock ratio such as an oxidised zone of a gold-bearing, sulphide ore body exposed to near-surface conditions.

Sasaki et al. (1995) and Sasaki and Konno (2002) demonstrated that jarosite-group minerals form as a by-product of actively metabolising iron-oxidising bacteria, i.e., *Acidithiobacillus ferrooxidans*. Since sodium and potassium were limited constituents in the media defined by Silvermann and Lundgren (1959), it is likely that the nanometre-size, acicular iron oxyhyroxide precipitate formed in the bacterial enrichments were likely hydroniumjarosite (Fig. 2.1d, inset).

Since the gold-bearing metal sulphide ore was suspended in solution, the iron-oxidising bacteria must have attached onto the sample from the fluid-phase rather than settling onto the surface due to gravitational forces. More importantly, the preferential attachment of enriched iron-oxidising bacterial consortia onto metal sulphide mineral grains instead of quartz surfaces was consistent with many previous studies (Ohmura et al., 1993; Sand et al., 1995; Escobar et al., 1996; Edwards et al., 2000a,b; Sampson et al., 2000; Kinzler et al., 2003; Mielke et al., 2003; Rodriquez et al., 2003a,b,c; Sand and Gehrke, 2006; Africa et al., 2012). Evidence of extensive biofilm development including extracellular polymeric substances (Fig. 2.2a) within creviced regions suggests that active bacterial growth occurred on the metal sulphide components of the sample. Evidence of bacterial metabolism was also demonstrated by the formation of secondary minerals occurring on extracellular surfaces. These nanometre-size, secondary minerals containing iron and sulphur were consistent with previous studies demonstrating extracellular iron mineralisation (Fortin et al., 1996). Evangelou (1994) proposed that phosphate coatings could act as a "protective barrier" to reduce polymetallic sulphide oxidation. Conversely, Jones et al. (2003) demonstrated that bacterial-catalysed oxidation of arsenopyrite can occur in a phosphate-rich culture medium even when an abiotic, iron phosphate precipitate coated arsenopyrite mineral surfaces (Reaction 2.1). The laminated structure of the iron phosphate precipitate observed in this study was consistent with observations by Jones et al. (2003). Both studies demonstrated the continuous biogeochemical weathering of metal sulphides under acidic and oxidised conditions despite the presence of this coating. Although it is intuitive that some soluble iron would have come from the inoculum, the formation of the secondary iron phosphate and iron oxyhydroxide mineral coatings presumably resulted from microbial activity. The discoidal precipitate is interpreted as potassium jarosite based on the chemical identification from the

EDS spectra and its morphology (see Grishin et al., 1988; Herbert, 1997; Sasaki and Konno, 2002; Henao and Godoy, 2010). Sasaki and Konno (2002) highlighted that the mode and rate of iron oxidation were critical for the formation of different crystal morphologies of jarosite-group minerals; therefore, bacteria and the presence of associated organics, i.e. extracellular polymeric substances, could play an important role in jarosite formation (Chan et al., 2009; Sasaki et al., 1995; Sasaki and Konno, 2002). The jarosite overlaying the iron phosphate patina indicated that the iron phosphate formed first and was less soluble than jarosite. It is interesting to note the two morphological differences between jarosite that formed in the enriched iron-oxidising bacterial consortia relative to the bacterial weathering system. Both systems contained the same basal medium but different sources of energy, i.e., soluble ferrous sulphate heptahydrate and solid iron sulphide minerals. Based on the abiotic control, the active metabolism of iron-oxidising bacteria caused the widespread dissolution and release of the metal sulphide minerals (and their associated gold grains) from the polished rock surface.

$$Fe^{3+} + PO_4^{3-} \rightarrow FePO_4 \qquad (2.1)$$

The dissolution of iron sulphide minerals would lead to an increased concentration of soluble iron and sulphate in solution. However, the decreased iron concentration and slightly increased sulphur concentrations in the bacterial weathering system are underestimates of the amount of iron sulphides that "dissolved" due to the growth of iron-oxidising bacteria. The decreased iron and sulphur concentrations are attributed to the precipitation of iron phosphate and jarosite (which also contains sulphur; Reaction 2.2). While these sulphide mineral coatings appeared to occur as a physical barrier between bacteria and sulphide mineral surfaces, these precipitates possess high surface area and appear to have enabled or promoted increased attachment of bacteria (Fig. 2.3c). The weathered texture of the suspended metal sulphide sample and the fragment found at the bottom of the flask suggests that abiotic processes, e.g., ferric iron leaching, were also contributing to sulphide mineral dissolution. Furthermore, results from ICP-AES analysis confirmed that Ag, As, Cu, Pb and Zn occurred in the fluid phase of the bacterial weathering system (see Table 2.1). The initial iron concentration was proportional to the amount of iron from the inoculum. Copper, iron, lead and zinc were found in solution in the abiotic control and could be attributed to the acidic conditions of the fluid phase. However, these metal concentrations were not as high as in the

bacterial weathering system. This indicates that active microbial metabolism was responsible for the increased dissolution of polymetallic sulphide minerals. Although soluble gold concentrations were not detected in the fluid phase of the bacterial weathering system, low levels of soluble silver were present. As bacteria contributed to the oxidation and dissolution of polymetallic sulphide minerals, thiosulphate leaching of silver from gold grains "embedded" within sulphide minerals intuitively occurred (Reaction 2.3). It is possible that leaching and dissolution of gold could have also occurred in a similar manner (Aylmore and Muir, 2001). However, gold concentrations could have been below the 0.01 ppm detection limit of ICP-AES analysis. Furthermore, gold was not observed in association with the weathering pits on the ore surface suggesting that it was released along with the metal sulphides. Unfortunately, the fine grained, i.e., tens of micrometre-sized, gold grains were not found at the bottom of the flask along with the weathered sulphide material and iron oxides.

$$3\ Fe^{3+} + 2\ SO_4^{2-} + K^+ + 6\ H_2O \rightarrow KFe_3(OH)_6(SO_4)_2 + 6\ H^+ \qquad (2.2)$$

$$Ag_2S + 4\ S_2O_3^{2-} + 2\ SO_3^{2-} + 6H^+ \rightarrow 2\ Ag(S_2O_3)_2^{3-} + 3\ S + 3\ H_2O \qquad (2.3)$$

The results presented here have important implications for understanding gold mobility under surface and near-surface biogeochemical conditions and for the development of industrialised biomining practices. Bioleaching is the biotechnological application of living processes to recover precious and base metals from primary sources including ore and mineral concentrates. As an efficient alternative method for gold extraction, it reduces the harmful effect associated with the use of fossil fuels in conventional extraction methods (Mannion, 1992; Rawlings and Johnson, 2007; Johnston et al., 2013). The effects of microbes on copper enrichment at ore deposits and from mine tailings have been studied (Southam and Saunders, 2005; Merson, 1992) and gold enrichment by *Pedomicrobium* in placer deposits has also been highlighted (Mann, 1992). Therefore, in the case of gold-bearing metal sulphides, the same principle of gold "liberation" using iron-oxidising bacteria can be applied. Using arsenopyrite as a model of a gold-bearing metal sulphide, bacterial-catalysed oxidation of iron sulphide minerals can promote gold mobility as suspended particles in solution or as soluble complexes if gold is completely dissolved (Reaction 2.4 and 2.5). The continuous exposure of highly-sulphidised, gold-bearing ore to iron-oxidising bacteria under

acidic and oxidised weathering conditions will affect primary gold emplacement by favouring gold distribution and enrichment in surrounding supergene horizons.

$$2\ FeAsS\text{-}Au^0 + 7\ O_2 + 2\ H_2O + H_2SO_4 \rightarrow Fe(SO_4)_3 + 2H_3AsO_4 + Au^0 \qquad (2.4)$$

$$2\ Au^0 + 2\ S_4O_6^{2-} + 2\ H_2O + Fe^{2+} \rightarrow 2\ Au(S_2O_3)_2^{3-} + 4\ H^+ + FeO_2 \qquad (2.5)$$

## 2.3 Conclusion

The bacterial weathering experiment demonstrated that attachment and growth of a consortium of acidophilic, iron-oxidising bacteria contributed to both the chemical and physical weathering of a gold-bearing, polymetallic sulphide ore. Evidence of microbial growth and active metabolism was demonstrated by the development of extensive biofilm formation and the precipitation of micrometre-size iron oxides (discoidal jarosite) and extracellular precipitation of nanometre-scale iron oxides on some bacterial surfaces. Bacterial attachment was heterogeneously distributed as cells preferentially attached to metal sulphide mineral surfaces rather than to polished quartz. The precipitation of the iron phosphate patina did not inhibit the biooxidation of sulphide minerals. Bacterial-catalysed dissolution of gold-bearing, polymetallic sulphides was demonstrated by the presence of soluble silver, arsenic, copper, lead and zinc in the fluid phase of the bacterial weathering system after the 60 day reaction. The solubilisation of silver (and presumably trace gold) signifies that biogeochemical leaching, e.g., thiosulphate complexation, was active under these weathering conditions. The contribution of metabolically active bacteria to the biogeochemical weathering of gold-bearing metal sulphide ore led to the “release” of embedded gold grains, i.e., the dispersion of gold particles. Over geological time, this weathering and redistribution of gold would contribute to placer or supergene gold enrichment.

**Table 2.1.** Chemical analysis of soluble metals from the bacterial weathering system and the abiotic control system.

| Chemical Analysis of Soluble Metals | | | | | |
|---|---|---|---|---|---|
| | | Bacterial Weathering System | | Abiotic Control | |
| Element | Detection Limit (ppm) | T = 0 days (ppm) | T = 60 days (ppm) | T = 0 days (ppm) | T = 60 days (ppm) |
| Ag | 0.01 | bdl | 0.05 | bdl | bdl |
| As | 0.03 | bdl | 4.51 | bdl | bdl |
| Au | 0.01 | bdl | bdl | bdl | bdl |
| Cu | 0.01 | bdl | 45.3 | bdl | 7.27 |
| Fe | 0.05 | $3.94 \times 10^3$ | $3.52 \times 10^3$ | bdl | 0.92 |
| Hg | 0.03 | bdl | bdl | bdl | bdl |
| Mo | 0.01 | bdl | bdl | bdl | bdl |
| Ni | 0.01 | bdl | 0.03 | bdl | bdl |
| Pb | 0.02 | bdl | 1.59 | bdl | 0.04 |
| S | 0.02 | $2.20\times 10^3$ | $3.35 \times 10^3$ | $8.90 \times 10^2$ | $8.97 \times 10^2$ |
| Zn | 0.01 | bdl | 1.77 | bdl | 0.82 |

bdl = below detection limit

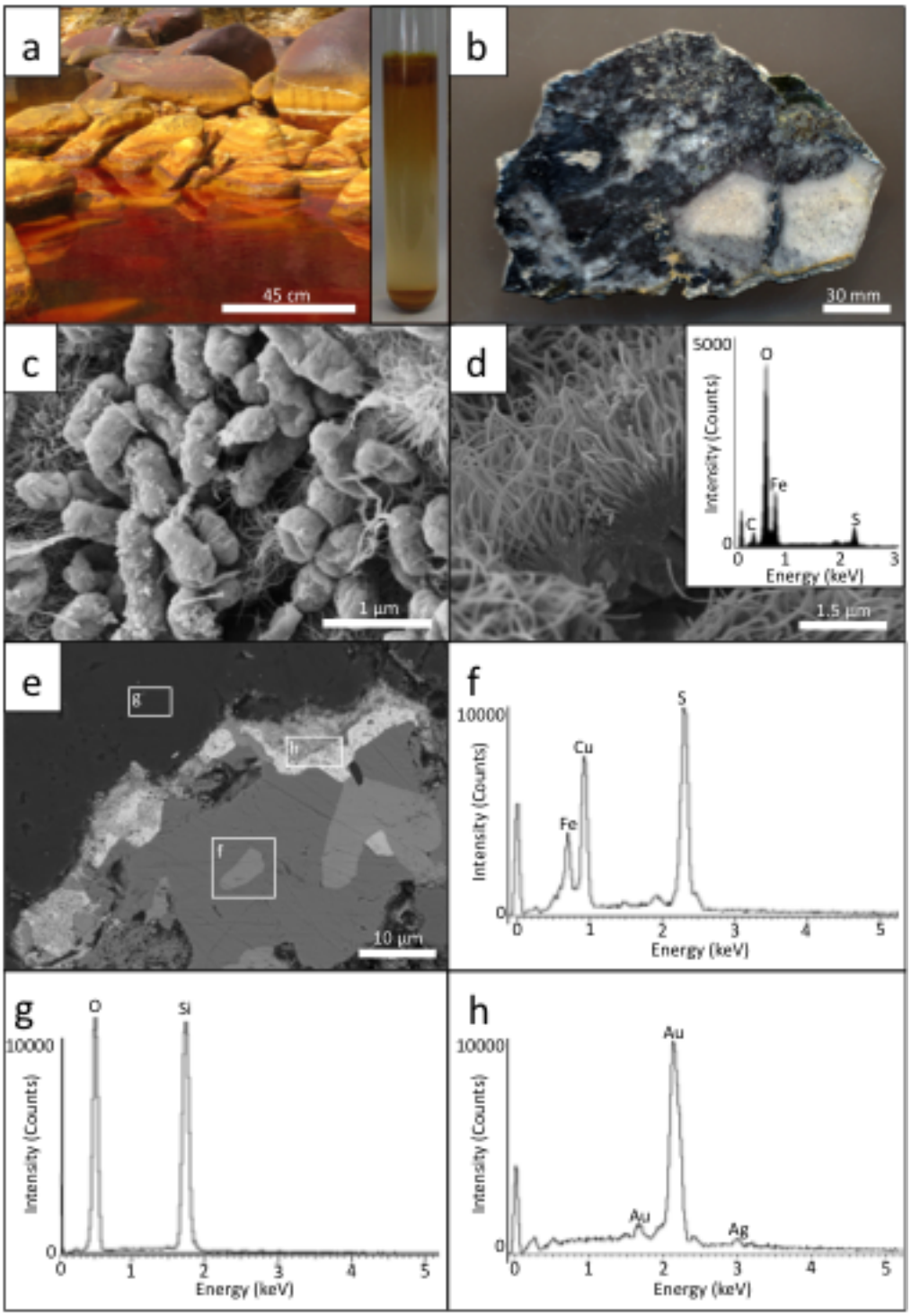


**Figure 2.1. SEM-EDS characterisation of iron-oxidising bacteria and a gold-bearing, polymetallic sulphide ore.** A photograph of Rio Tinto and the coating on submersed cobbles (a) that served as the source material for iron-oxidising bacterial enrichments (inset). A representative image of the polished gold-bearing, metal sulphide ore (b). A high-resolution SEM micrograph of bacterial enrichment after 3 weeks (c) and the associated acicular, iron oxide precipitate (d). A backscatter SEM micrograph of the metal sulphide ore with micrometre-size crevices. (e) EDS analysis determined that mineral grains were composed of iron, copper and sulphur (f) within a matrix composed of silica and oxygen (g) and gold and silver occurred at the perimeter of grain boundaries (h).

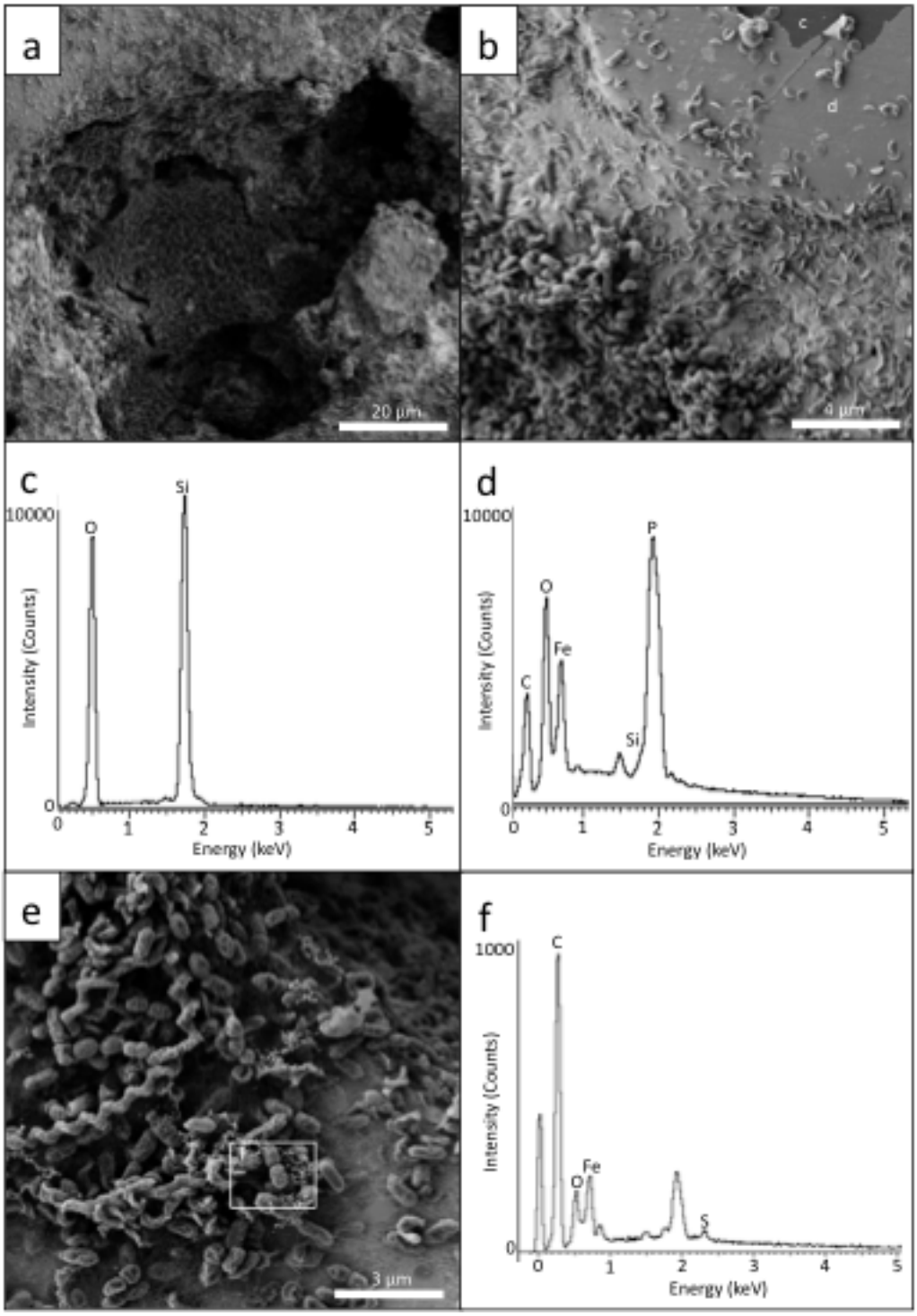


**Figure 2.2. SEM-EDS characterisation of the biogeochemically weathered gold-bearing, polymetallic sulphide ore.** A series of SEM micrographs demonstrating the attachment of bacteria onto the sulphide ore after 60 days of exposure. Extensive development of biofilm formation occurred within creviced regions (a). The surface of the sample (b, c) also contained a "patina" coating comprised of iron and phosphate (d) to which bacteria were attached. Some bacteria demonstrated nanometre-size secondary minerals composed of Fe, S and O (e, f). The unlabelled peak corresponds to the Os coating.

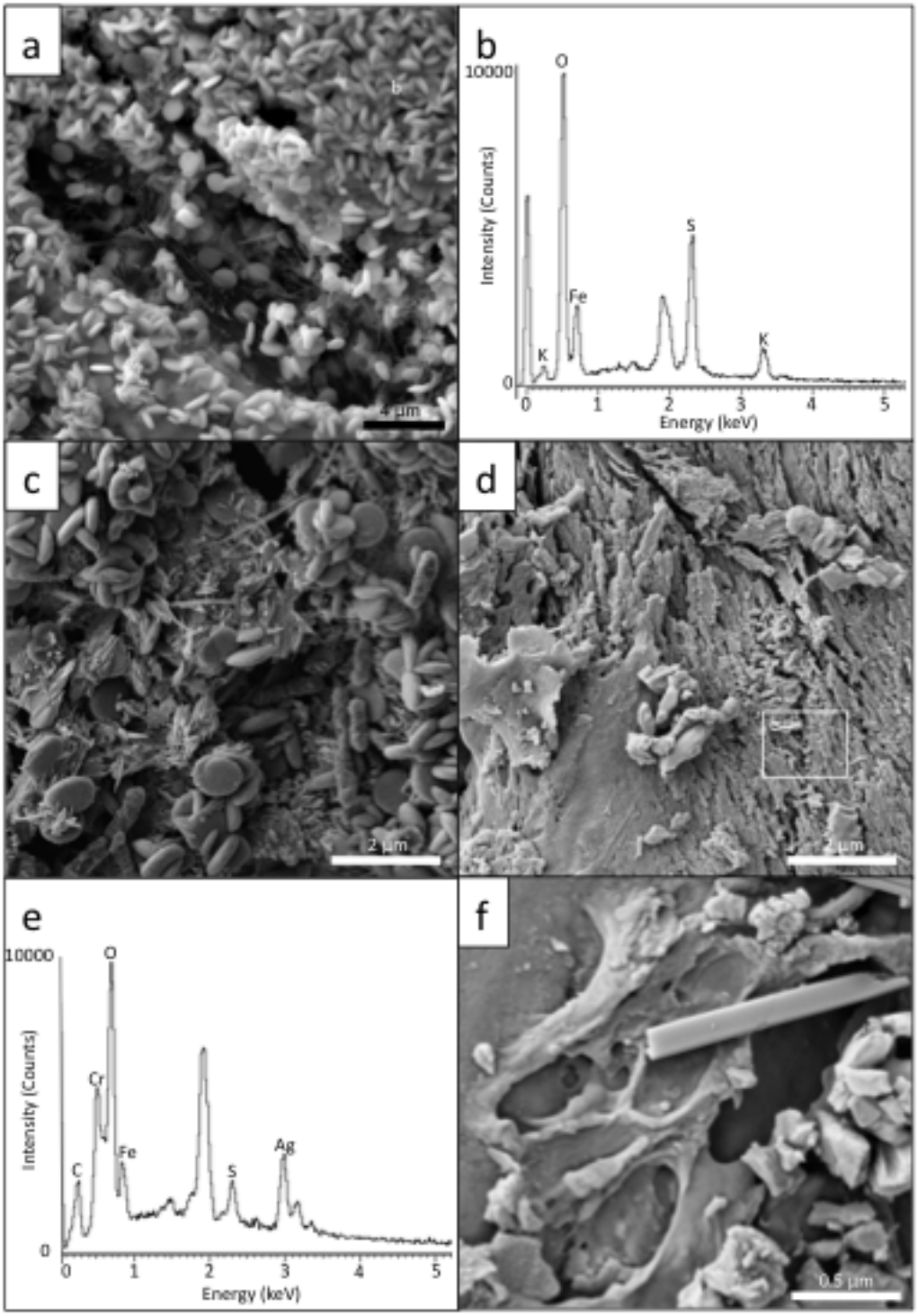


**Figure 2.3. SEM-EDS characterisation of bacterial-catalyzed mineral dissolution and precipitation.** A high-resolution SEM micrograph of the discoidal precipitate composed of Fe, P, S, K and O occurring on the iron phosphate precipitate and within creviced regions along with organic material (a, b). The surface of the sulphide ore appeared weathered and overlain by jarosite and bacteria (c). The metal sulphide mineral collected at the bottom of the flask contained similar weather surface textures (d). The sample contained metals such Cr, Fe and Ag (e). High-resolution SEM micrographs indicated that the surface also contained bacterial-size impressions within exopolymer material, suggesting that the bacteria had "abandoned" the surface (f). The unlabelled peak corresponds to the Os coating.

## 2.4 References


Africa, C.J., van Hille, R.P., Harrison, S.T., 2012. Attachment of *Acidithiobacillus ferrooxidans* and *Leptospirillum ferriphilum* cultured under varying conditions to pyrite, chalcopyrite, low-grade ore and quartz in a packed column reactor. Applied Microbiology Biotechnology, 97, 1317-1324.

Arrendondo, R., Garcia, A., Jerez, C.A., 1994. Partial removal of lipopolysaccharide from *Thiobacillus ferrooxidans* affects its adhesion to solids. Applied Environmental Microbiology, 60, 2846-2851.

Alymore, M.G., Muir, D.M., 2001. Thiosulphate leaching of gold: a review. Minerals Engineering, 14, 135-174.

Bhatti, T.M., Bigham, J.M., Carlson, L., Tuovinen, O.H., 1993. Mineral products of pyrrhotite oxidation by *Thiobacillus ferrooxidans*. Applied and Evironmental Microbiology, 59, 1984-1990.

Buckley, A.N., Walker, G.W., 1988. The surface composition of arsenopyrite exposed to oxidising environments. Applied Surface Science, 35, 227-240.

Chan, C.S., Fakra, S.C., Edwards, D.C., Emerson, D., Banfield, J.F., 2009. Iron oxyhydroxide mineralisation on microbial extracellular polysaccharides. Geochimica et Cosmochimica Acta, 73, 3807-3818.

Chandra, A.P., Gerson, A.R., 2010. The mechanisms of pyrite oxidation and leaching: a fundamental perspective. Surface Science Reports, 65, 293-315.

Cochran, W.G., 1950. Estimation of bacterial densities by means of the "Most Probable Number". Biometrics. 6, 105-116.

Cooke, D.R., Simmons, S.F., 2000. Characteristics and genesis of epithermal gold deposits. Society of Economic Geology Reviews, 13, 221-244.

de Brodtkorb, M.K., 2009. Precious metal tellurides and other Te-bearing minerals in different paragenesis of Argentina. A Review. Revista de la Asociacion Geologica Argentina, 64, 365-372.

Edwards, K.J., Bond, P.L., Banfield, J.F., 2000a. Characteristics of attachment and growth of *Thiobacillus caldus* on sulphide minerals: A chemotactic reponse to sulphur minerals? Environmental Microbiology, 2, 324-332.

Edwards, K.J., Bond, P.L., Druschel, G.K., McGuire, M.M., Hamers, R.J., Banfield, J.F., 2000b. Geochemical and biological aspects of sulphide mineral dissolution: lessons from iron Mountain, California. Chemical Geology, 169, 383-397.

Enders, M.S., Knickerbocker, C., Titley, S.R., Southam, G., 2005. The role of bacteria in the supergene environment of the Morenci porphyry copper deposit, Greenlee County, Arizona. Economic Geology, 101, 59-70.

Erhlich, H.L., 1964. Bacterial oxidation of arsenopyrite and enargite. Economic Geology, 59, 1306-1312.

Escobar, B., Jedlicki, E., Wierts, J., Vargas, T., 1996. A method for evaluating the proportion of free and attached bacteria in the bioleaching of chalcopyrite with Thiobacillus ferrooxidans. Hydrometallurgy, 40, 1-10.

Evangelou, V.P., 1994. Potentail microencapsulation of pyrite by artificially inducement of FePO4 coatings. In Proceedings of the International Land Reclamation and Mine Drainage Conference and Third international Conference on the Abatement of Acidic Drainage, Vol. 2: Mine Drainage. Bureau of Mines Special Publications SP06B-94, 96-103. United States Department of the Interior, Washington, DC.

Fortin, D., Davis, B., Beveridge, T.J., 1996. Role of Thiobacillus and sulfate-reducing bacteria in iron biocycling in oxic and acidic mine tailings. FEMS Microbiology Ecology, 21, 11-24.

Fowler, T.A., Crundwell, F.K., 1999. Leaching of zinc sulphide by Thiobacillus ferrooxidans: Bacterial oxidation of the sulphur product layer increases the rate of zinc sulphide dissolution at high concentrations of ferrous ions. Applied and Environmental Microbiology, 65, 5285-5292.

Grishin, S.I., Bigham, J.M., Tuovinen, O.H., 1988. Characterisation of jarosite formed upon bacterial oxidation of ferrous sulfate in a packed-bed reactor. Applied and Environmental Microbiology, 54, 3101-3106.

Hedrich, S., Schlomann, M., Johnson, D.B., 2011. The iron-oxidising proteobacteria. Microbiology, 157, 1551-1564.

Henao, D.M.O., Godoy, M.A.M., 2010. Jarosite pseudomoph formation from arsenopyrite oxidation using Acidithiobacuillus ferrooxidans. Hydrometallurgy, 104, 162-168.

Herbert, R.B., 1997. Properties of goethite and jarosite precipitated from acidic groundwater, Dalarna, Sweden. Clays and Clay Minerals, 45, 261-273.

Johnson, D.H., Hallberg, K.B., 2003. The microbiology of acidic mine waters. Research in Microbiology, 154, 466-473.

Johnston, D.B., Grail, B.M., Hallberg, K.B., 2013. A new direction for biomining: Extraction of metals by reductive dissolution of oxidised ores. Minerals, 3, 49-58.

Jones, R.A., Koval, S.F., Nesbitt, H.W., 2003. Surface alteration of arsenopyrite (FeAsS) by Thiobacillus ferroocidans. Geochimica et Cosmochimica Acta, 67, 955-965.

Kinzler, K., Gerhrke, T., Telegdi, J., Sand, W., 2003. Bioleaching-a result of interfacial processes caused by extracellular polymeric substances (EPS). Hydrometallurgy, 71, 82-88.

Lacey, D.T., Lawson, F., 1970. Kinetics of the liquid-phase oxidation of acid ferrous sulphate by the bacterium Thiobacillus ferrooxidans. Biotechnology and Bioengineering, 12, 29-50.

Lowson, R.T., 1982. Aqueous oxidation of pyrite by molecular oxygen. Chemical Reviews, 82, 462-497.

Márquez-Zavalía, M.F., Craig, J.R., 2004. Tellurium and precious-metal ore minerals at Mina Capillitas, Northwestern Argentina, Neues Jahrbuch für Mineralogie, Monatshefte, 4, 176-192.

Marquez-Zavalia, M.F., Craig, J.R., Solberg, T.N., 1999. Duranusite, product of realgar alteration, Mina Capillitas, Argentina. The Canadian Mineralogist, 37, 1255-1259.

Mann, S., 1992. Bacteria and the Midas touch. Nature, 357, 358-359.

Mannion, A.M., 1992. Sustainable development and biotechnology. Environmental Conservation, 19, 297-306.

Merson, J., 1992. Mining with Microbes. New Scientist, 133, 17-19.

Mielke, R.E., Pace, D.L., Porter, T., Southam, G., 2003. A critical stage in the formation of acid mine drainage: Colonization of pyrite by Acidithiobacillus ferrooxidans under pH-neutral conditions. Geobiology, 1, 81-90.

Nicholson, R.V., Gillham, R.W., Reardon, E.J., 1988. Pyrite oxidation in carbonate-buffered solution: 1. Experimental kinetics. Geochimica et Cosmochimica Acta, 52, 1077-1085.

Nesbitt, H.W., Muir, I.J., 1998. Oxidation states and speciation of secondary products on pyrite and arsenopyrite reacted with mine waste waters and air. Mineralogy and Petrology, 62, 123-144.

Nesbitt, H.W., Muir, I.J., Pratt, A.R., 1995. Oxidation of arsenopyrite by air and air-saturated, distilled water, and implications for mechanism of oxidation. Geochimica et Cosmochimica Acta, 59, 1773-1786.

Nordstrom, D.K., Southam, G., 1997. Geomicrobiology of sulphide mineral oxidation. Reviews in Mineralogy and Geochemistry, 35, 361-390.

Ohmura, N., Kitamura, K., Saiki, H., 1993. Selective adhesion of Thiobacillus ferrooxidans to pyrite. Applied and Environmental Microbiology, 59, 4044-4050.

Rainbow, A., Kyser, T.K., Clark, A.H., 2006. Isotopic evidence for microbial activity during supergene oxidation of a high-sulphidation epithermal gold-silver deposit. Geology, 34, 269-272.

Rawlings, D.E., 2002. Heavy metal mining using microbes. Annual Review of Microbiology, 56, 65-91.

Rawlings, D.E., Johnson, D.B., 2007. The microbiology of biomining: Development and optimisation of mineral-oxidising microbial consortia. Microbiology, 153, 315-324.

Rimstidt, D., Vaughan, D.J., 2003. Pyrite oxidation: a state-of-the-art assessment of the reaction mechanism. Geochimica et Cosmochimica Acta, 67, 873-880.

Rodriquez, Y., Ballaster, A., Blazquez M.L., Gonzalez, F., Munoz, J.A., 2003a. Study of bacterial attachment during the bioleaching of pyrite, chalcopyrite and sphalerite. Geomicrobiology Journal, 20, 131-141.

Rodriquez ,Y., Ballaster A., Blazquez M.L., Gonzalez, F., Munoz, J.A., 2003b. New information on the pyrite bioleaching mechanism at low and high temperature. Hydrometallurgy, 71, 37-46.

Rodriquez, Y., Ballaster, A., Blazquez, M.L., Gonzalez, F., Munoz, J.A., 2003c. New information on the chalcopyrite bioleaching mechanism at low and high temperature. Hydrometallurgy, 71, 47-56.

Sampson, M.I., Phillips, C.V., Blake, R.C. II, 2000. Influence of the attachment of acidophilic bacteria during the oxidation of mineral sulphides. Mineral Engineering, 13, 373-389.

Sand, W., Gerke, T., Hallmann, R., Schippers, A., 1995. Sulphur chemistry, biofilm, and the (in)direct attach mechanism-A critical evaluation of bacterial leaching. Applied Microbiology Biotechnology, 43, 961-966.

Sand, W., Gehrke, T., 2006. Extracellular polymeric substances mediate bioleaching/biocorrosion via interfacial processes involving iron (III) ions and acidophilic bacteria. Research in Microbiology, 157, 49-56.

Sasaki, K., Konno, H., 2002. Morphology of jarosite-group compounds precipitated from biologically and chemically oxidized Fe ions. Canadian Mineralogist, 38, 45-56.

Sasaki, K., Tsunekawa, M., Konno, H., 1995. Characterisation of argentojarosite formed from biologically oxidized Fe3+ ions. Canadian Mineralogist, 33, 1311-1319.

Silvermann, M.P., Lundgren, D.G., 1959. Studies on the chemoautotrophic iron bacterium Ferrobacillus ferrooxidans. An improved medium and a harvesting procedure for securing high cell yields. Journal of Bacteriology, 77, 642-647.

Singer, P.C., Stumm, W., 1970. Acidic mine drainage: the rate determining step. Science, 167, 1121-1123.

Southam, G., Saunders, J.A., 2005. The geomicrobiology of ore deposits. Economic Geology, 100, 1067-1084.

Steger, H.F., Desjardin, L.E., 1978. Oxidation of sulphide minerals, 4. Pyrite, chalcopyrite and pyrhotite. Chemical Geology, 23, 225-237.

Thurston, R.S., Mandernack, K.W., Shanks, W.C., 2010. Laboratory chalcopyrite oxidation by Acidithiobacillus ferrooxidans: oxygen and sulphur isotope fractionation. Chemical Geology, 269, 252-261.

Tyagi, R.D., Blais, J.F., Auclair, J.C., 1993. Bacterial leaching of metals from sewage sludge by indigenous iron-oxidising bacteria. Environmental Pollution, 82, 9-12.

# Chapter 3

## 3 The effect of iron-oxidising bacteria on the stability of gold (I) thiosulphate complex

Both natural and anthropogenic weathering of massive sulphide deposits leads to near-surface environments characterised by increased acidity and soluble ferric iron and sulphate concentrations due to oxidation of sulphide-bearing minerals (Blowes and Jambor, 1990; Nordstrom and Southam, 1997; Nordstrom and Alpers, 1999; Lopez-Archilla et al., 2001; Levings et al., 2005; Ferreira da Silva et al., 2006; Alvarez-Valero et al., 2008; Fernandez-Remolar et al., 2008). These environments, broadly referred to as acid rock drainage (ARD) systems, are influenced by surrounding geology, topography, climate and water table levels since all factors promote abiotic, e.g. physical and chemical, weathering (Webster and Mann, 1984; Dold and Fontbote, 2001; Nordstrom, 2009; Reaction 3.1). However, Singer and Stumm (1970) indicated that increased acidity and soluble ferric iron concentrations are attributed in a large part to microbial metabolic activity. Acidophilic and acidotolerant chemolithoautotrophic bacteria are ubiquitous in ARD weathering environments where sulphide-bearing minerals provide ideal substrates for bacterial growth (Gonzalez-Toril et al., 1999; Ferris et al., 2004). Iron-oxidising bacteria such as *Acidithiobacillus ferrooxidans* solubilise iron sulphide minerals via metabolic ferrous iron oxidation and ultimately generate increased acidity, ferric iron and sulphate concentrations in solution relative to abiotic weathering (Singer and Stumm, 1970; Reactions 3.2, 3.3 and 3.4).

$$FeS_2 + 3\ H_2O + 6\ Fe^{3+} \rightarrow S_2O_3^{2-} + 7\ Fe^{2+} + 6\ H^+ \quad (3.1)$$

$$4\ FeS_2 + 14\ H_2O + 15\ O_2 \rightarrow 4\ Fe(OH)_3 + 8\ SO_4^{2-} + 16\ H^+ \quad (3.2)$$

$$4\ Fe^{2+} + O_2 + 4\ H^+ \rightarrow 4\ Fe^{3+} + 2\ H_2O \quad (3.3)$$

$$FeS_2 + 14\ Fe^{3+} + 8\ H_2O \rightarrow 15\ Fe^{2+} + 2\ SO_4^{2-} + 16\ H^+ \quad (3.4)$$

The occurrence of gold in near-surface weathering environments is considered to be dynamic (Wilson, 1984; Webster and Mann, 1984). Massive sulphide ore deposits that contain gold, e.g., the Iberian Pyrite Belt of southern Spain and Portugal (Huston and Large, 1989; Hutchinson, 1990; Large, 1990; Huston et al., 1992; Leistel et al., 1998) also possess soluble gold concentrations in their natural waters. Furthermore, enriched secondary gold dispersion halos have also been observed “downstream” in supergene environments (Spurr and Garrey,

1908; Bowles, 1981; McHuge, 1984, 1988; Freyssinet et al., 1989; Boyle, 1979; Colin et al., 1997; Hough et al., 2008). Sulphur-bearing ligand ions, such as thiosulphate, are formed during the oxidative weathering of iron sulphides and are thought to be an important gold complexing agent in these systems (Puddephatt, 1978; Plyusnin et al., 1981; Mann, 1984; Webster, 1985; Renders and Seward, 1989; Bendetti and Boulegue, 1991; Bowell, 1992; Reaction 3.5). It is important to note that sulphur-oxidising bacteria can also contribute to the formation of thiosulphate ions (Lakin et al., 1974). In these environments, thiosulphate ions are common ligands contributing to soluble gold mobility as stable complexes under acidic, oxidising conditions when excess sulphur is present. These complexes are transported within surficial hydrological systems (Webster 1985; Bowell; 1992; Reaction 3.6). The formation of gold complexes with other oxidised sulphur ligands such as sulphite ($SO_3^{2-}$), sulphate ($SO_4^{2-}$) and tetrathionate ($S_4O_6^{2-}$) has not been observed in natural environments and are therefore considered meta-stable, transitory ligands (Bowell et al., 1992; Aylmore and Muir, 2001).

$$4\ S + 3\ O_2 + H_2O \rightarrow S_4O_6^{2-} \qquad (3.5)$$

$$2\ Au^0 + 2\ S_4O_6^{2-} + 2\ H_2O + Fe^{2+} \rightarrow 2\ Au(S_2O_3)_2^{3-} + 4\ H^+ + FeO_2 \qquad (3.6)$$

Many field and experimental studies on gold mobility and dispersion have focused on gold co-precipitation and adsorption with ferric iron-bearing solutions and minerals leading to supergene enrichment (Andrade et al., 1991; Machensky et al., 1991; Schoonen et al., 1992; Greffie et al., 1996; Uchida et al., 2002). However, Freise (1931) was the first to suggest that organic substances could act as reducing agents for soluble gold complexes and result in the formation of secondary gold. Goldschmidt (1937) contributed to this idea by suggesting that observed metal concentrations within natural environments could be attributed to bacterially catalysed geochemical processes. Since these early works more recent studies (see Southam and Beveridge, 1994, 1996; Lengke et al., 2006a,b, 2007; Reith and McPhail, 2006; Reith et al., 2006, 2007; Kenney et al., 2012; Song et al., 2012, Fairbrother et al., 2012) have focused specifically on the biogeochemical cycling of gold in near-surface environments. These studies demonstrated the effects of various bacteria on the immobility of soluble aurous and auric complexes through both passive and active gold biomineralisation.

An unanswered question, however, is the “fate” of soluble gold complexes in oxidised, weathering environments where high iron concentrations and acidic conditions are sustained

by active metabolism of chemolithoautotrophic bacteria. Therefore, the purpose of this study was to examine the stability of gold (I) thiosulphate when exposed to acidophilic, iron-oxidising bacteria and the associated geochemical conditions induced by this physiological group.

## 3.1 Materials and Methods

### 3.1.1 Sample acquisition and bacterial enrichments

Reduced water levels in Rio River, Spain (37° 35' 33.27" N, 6° 33' 1.84" W) exposed cobbles with dark, brown-red coatings (Fig. 3.1). For detailed mineralogy and composition of coatings see Fernandez-Remolar et al. (2005). Cobbles submersed in the water had biofilms attached to the surface. The loose biofilm coating was approximately 3 cm thick and composed of an iron-oxidising bacterial consortium with yellow-orange, fine-grained, iron oxyhydroxide. The iron-oxidising bacterial consortium, along with river water, was sampled and pH was measured using Electron Microscopy colourpHast Indicator Strips 0.0-4.0.

The microbial sample collected from Rio Tinto was homogenised using a vortex and a bacterial count estimate was determined using 5 μL aliquots and a Petroff-Hausser counting chamber. Enrichments of iron-oxidising bacteria were obtained by inoculating 0.5 mL of the consortia in 4 mL of modified media defined by Silverman and Lundgren (1959) with 0.5 mL of 33.3 g/ 100 mL ferrous sulphate heptahydrate ($FeSO_4 \cdot 7H_2O$) and pH adjusted to 2.3 using 2 M sulphuric acid. This modified medium, without a bacterial inoculum, will be referred to as "fresh media" for simplicity. Enrichments were incubated at room temperature (RT, approx. 22˚C) for three weeks in Fisherbrand® 13 × 100 mm borosilicate glass test tubes with plastic push caps to maintain sterile and aerobic culture conditions. A second bacterial count was performed after three weeks of incubation using the Most Probable Number (MPN) statistical method described by Cochran (1950). Rinsed iron oxyhydroxide precipitate (see section 3.1.3) was air-dried at RT for 24 hours and weighed. The pH and eH of bacterial enrichments were also measured using a Denver Instrument Basic pH/eH Meter with an electrode calibrated to pH 2 and 4 reference standards using potassium biphthalate buffer and ZoBell's solution (Nordstrom, 1977) at RT, respectively. Uncertainties of pH measurements were ±0.03 pH units and Eh measurements were ±0.05 V.

### 3.1.2 Gold stock solutions

Sodium gold (I) thiosulphate of 99.9% purity was purchased from Alfa Aesar and dissolved in distilled, deionised water to make a calculated 40 mM gold stock solution. The pH of the gold stock solution was also measured. The gold stock was filter-sterilised using a 0.1 μm pore-size filter and used to make four ten-fold serial dilutions each with a final concentration of 0.02, 0.2, 2, or 20 mM gold. It is important to note that the 0.002 mM gold stock was analogous to gold concentrations found in natural environments (McHugh, 1988). The purpose of higher gold concentrations was to enable greater detection using scanning and transmission electron microscopy and synchrotron-based analysis of experimental systems.

### 3.1.3 Experimental systems

Iron-oxidising bacterial enrichments are comprised of soluble ferric iron, iron oxyhydroxide precipitates and organics, i.e., bacteria; these components all have the potential to react with gold (I) thiosulphate. Bacterial enrichments and each separate component were exposed to gold stocks creating four different experimental systems to examine the direct and indirect effects of iron-oxidising bacteria on gold (I) thiosulphate stability. Each separate experimental system was mixed using a vortex and wrapped in aluminium foil to prevent photocatalytic effects once gold stocks were added. All experiment systems were performed in triplicate. Filtering the experimental systems with a 0.1 μm pore-size filter removed solid material and stopped the exposure reaction. Solid filtrates were analysed using Scanning Electron Microscopy (SEM) and Transmission Electron Microscopy (TEM). Filtered solutions were analysed for un-reacted, soluble gold using Perkin-Elmer Optima 3300-DV Inductively Coupled Plasma-Atomic Emission Spectroscopy (ICP-AES). The amount of gold immobilised from solution calculated by subtracting the measured residual gold in solution from the initial input added to each experimental-system. The pH and Eh of all experimental systems were measured in the same manner described for bacterial enrichments (3.1.1).

*Bacterial culture enrichment-gold system:* Gold stocks were added to bacterial enrichments to produce final 0.002, 0.02, 0.2, 2 or 20 mM gold concentrations. The culture enrichment-gold systems were allowed to react for 1, 2, 4, 8 and 24 hours.

*Spent media-gold system:* Iron-oxidising bacteria produce a high concentration of ferric iron in solution as a by-product of their active metabolism via ferrous iron oxidation (Singer and Stumm, 1970). Bacterial enrichments were filtered to remove solid components, i.e., iron oxyhydroxide precipitates and bacteria, leaving only the fluid phase containing soluble ferric iron. Hereafter, the filtered fluid phase of bacterial enrichments will be called "spent media" for simplicity. A 40 mM gold stock was added to spent media forming a spent media-gold system with a final concentration of 20 mM gold. This system was allowed to react for 24 hours.

*Fresh media-gold system:* Spent media may also contain residual, non-metabolised ferrous iron even after three weeks of incubation. Therefore, a 40 mM gold stock was added to fresh media to obtain an overall concentration of 20 mM gold. This fresh media-gold system was complimentary to the spent media-gold system because its purpose was to determine whether or not residual, non-metabolised ferrous sulphate would react with gold (I) thiosulphate after 24 hours of exposure.

*Iron oxyhydroxide-gold system:* Active metabolism of iron-oxidising bacteria also produces an abundance of solid ferric iron oxyhydroxide precipitates as a by-product (Singer and Stumm, 1970). Spent media, along with any bacteria occurring in the fluid phase, of bacterial enrichments were discarded leaving iron oxyhydroxide precipitates attached to the inner surface of the borosilicate glass tubes. Sterile, distilled, deionised water was added so that the iron oxyhydroxide precipitates could be removed from the glass surface by vortex. The iron oxyhydroxide precipitates were then filtered and re-suspended in sterile, distilled deionised water to rinse off any spent media. The rinsed iron oxyhydroxide precipitates were then centrifuged for 1 min. at 12,000 *g* forming a pellet and the supernatant was discarded. The rinse procedure was performed three times. After the final rinse and the supernatant was discarded, 20 mM gold stock was added to the pellet forming an iron oxyhydroxide-gold system and the system was allowed to react for 24 hours.

*Bacterial-gold system:* The iron oxyhydroxide minerals were removed from the inner glass surface by vortex to liberate any bacteria from the mineral surface. Once the iron oxyhydroxide minerals settled to the bottom of the tube, spent media were removed from two bacterial enrichments and centrifuged for 1 min. at 12,000 *g* to obtain a pellet containing a high concentration of iron-oxidising bacterial cells. The pellet was suspended in 1 mL of

sterile, distilled, deionised water with vortex to obtain an estimated bacterial count of approximately $2.35 \times 10^5$ bacteria/mL using a Petroff-Hauser counting chamber. This bacterial suspension was re-centrifuged to form a pellet and the supernatant was discarded. The pellet was then rinsed three times and the supernatant was discarded in the same manner and purpose described for the iron oxide precipitates. After the final rinse procedure, 20 mM gold stock was added to the pellet forming a bacterial-gold system that was allowed to react for 24 hours.

*Chemical control:* Each gold stock was also used as a chemical control. The purpose of these chemical controls was to determine whether or not reduction of gold (I) thiosulphate could occur abiotically over 24 hours.

### 3.1.4 Scanning electron microscopy-energy dispersive spectroscopy

Filtrate samples were obtained from a bacterial enrichment and from culture enrichment-gold systems and spent media-gold systems exposed to 20 mM gold for 24 hours. These filtrates were prepared for Scanning Electron Microscopy-Energy Dispersive Spectroscopy (SEM-EDS). The filtrates were: fixed for 2 hours with $2\%_{(aq)}$ glutaraldehyde, dehydrated in sequential $25\%_{(aq)}$, $50\%_{(aq)}$, $75\%_{(aq)}$ and $3 \times 100\%$ ethanol series, dried using a Tousimis Research Corporation Samdri-PVT-3B critical point drier, and mounted onto aluminium stubs with 12 mm carbon adhesive tabs. A Denton Vacuum Desk II sputter coater was used to coat the filtrates with a 3 nm thick osmium deposition to reduce charging during SEM-EDS analysis. A LEO Ziess 1540XB Field Emission Gun-Scanning Electron Microscope (FEG-SEM) equipped with an Oxford Instruments' INCAx-sight Energy Dispersive Spectrometer (EDS) operating at 3 kV or 10 kV accelerating voltage was used for imaging and semi-quantitative elemental analysis, respectively.

### 3.1.5 Transmission electron microscopy-energy dispersive spectroscopy

Separate pellets of iron oxyhydroxide precipitate and bacteria were used as a comparison for filtrates from iron oxide- and bacteria-gold systems exposed to 20 mM gold for 24 hours. All four samples were prepared for Transmission Electron Microscopy-Energy Dispersive Spectroscopy (TEM-EDS). Samples were fixed for 2 hours in $2\%_{(aq)}$ glutaraldehyde, enrobed in $2\%_{(wt/vol)}$ noble agar, dehydrated in a $25\%_{(aq)}$, $50\%_{(aq)}$, $75\%_{(aq)}$ and $3 \times 100\%$ acetone series

and embedded in Epon plastic. The embedded samples were cut to 70 nm ultrathin sections using a Reichert-Jung Ultracut E ultramicrotome and collected on formvar-carbon coated, 200-square mesh copper grids. The sections were examined using a Phillips CM-10 Transmission Electron Microscope (TEM) operating at 80 kV. Semi-quantitative elemental analysis was determined using a Philips 420 TEM equipped with EDS Genesis x-ray microanalysis system operating at the same voltage.

### 3.1.6 X-ray absorption near-edge spectroscopy

Culture enrichment-, spent media- and iron oxyhydroxide-gold systems exposed to 20 mM gold for 1 hour were studied using X-ray Absorption Near-Edge Spectroscopy (XANES) to differentiate possible intermediate gold oxidation states. The oxidation states of gold were determined using analyses performed at beamline 9-BM, Advanced Photon Source, Argonne National Laboratory, Illinois, U.S.A. Each experimental-gold system was centrifuged and rinsed with deoxygenated, deionised water in the same manner described for preparation of iron oxide- and bacterial-gold systems. The rinsed experimental systems formed wet pastes that were separately sealed in an acid-resistant, Teflon fluid cell (3.5 cm × 1 cm × 0.5 cm) with Kapton film. Five to seven scans of each fluid cell were collected in fluorescence mode using a Canberra solid-state germanium, multi-elemental detector and were averaged. All spectral scans were monitored for induced radiation effects during data acquisition although none were detected. The Si (III) monochromator was calibrated to the gold III edge (11919 eV) using the first peak of the first derivative XANES spectrum of a metallic gold foil standard. Energy scales for each fluid cell, containing an experimental system, were referenced to the gold foil spectrum.

Gold (I) thiosulphate, gold (I) thiomalate, gold (I) sulphide and metallic gold foil each with 99.9% purity were purchased from Alfa Aesar and used as reference standards. Gold (I) thiosulphate and gold (I) thiomalate were dissolved in distilled, deionised water forming separate 20 mM gold solutions, while a fine monolayer of gold (I) sulphide was placed on Kapton tape. The XANES spectra of gold standards were measured in transmission mode using an ionisation chamber filled with nitrogen gas at 1 atm and were also measured simultaneously with the experimental systems. The different standards represented potential

gold complexes that could form during gold (I) thiosulphate destabilisation when exposed to iron-oxidising bacterial enrichments and each separate constituent.

### 3.1.7 X-ray absorption near-edge spectroscopy analysis

Athena 8.054 (Ravel and Newville, 2005) was used to processes the XANES data. A linear regression was fitted to the pre-edge, i.e., -150 to -75 eV relative energy, and post-edge, i.e., 150 and 300 eV, regions of the XANES spectra in order to subtract the pre-edge baseline and to apply XANES normalisation.

## 3.2 Results

### 3.2.1 Bacterial enrichment

The bacterial count of the consortia was approximately $7 \times 10^3$ bacteria/mL. The MPN count of iron-oxidising bacterial enrichments was $2.4 \times 10^4$ bacteria/mL after three weeks of incubation indicating positive growth. Iron-oxidising bacteria are comparable in size to *Escherichia coli*, a model bacterium (Neidhardt et al., 1990). Based on bacterial concentration in the enrichment and approximate weight of one cell, the bacterial enrichments contained approximately $1.2 \times 10^{-7}$ g of cells. Evidence of active iron-oxidising bacterial metabolism from the enrichment was indicated by the increase in acidity (Table 3.1) and formation of a red-orange, iron oxide precipitate that coated the inside surface of the borosilicate test tubes (Fig. 3.1, inset). The average dry weight of iron oxide precipitate from each bacterial enrichment was 0.0189 ±0.0004 g.

### 3.2.2 Chemical analysis

Chemical analyses of soluble constituents, i.e., fresh media, bacterial enrichments, spent media and gold stocks, prior to experimental use and each experimental system are recorded in Table 3.1. The reduction of gold (I) thiosulphate was observed in the culture enrichment-gold systems as the fluid phase gradually changed from red-orange to clear and the iron oxyhydroxide precipitates turned slightly brown. ICP-AES analysis indicated that greater than 90% of gold in the culture enrichment-gold systems was removed from solution within the first hour of exposure and increased with time. More importantly, the culture enrichment-gold systems exposed to 20 mM gold for 24 hours removed more gold in

comparison to iron oxide- and bacterial-systems added together. Spent media-gold systems, however, removed approximately the same amount of gold as the "intact" culture enrichment-gold system. A rapid removal of gold was observed in this experimental system as an opaque, black precipitate that formed in suspension. The precipitate settled to the bottom of the borosilicate glass tube within minutes leaving the solution completely transparent. Fresh media-gold system and the chemical controls had no observed colour change and ICP-AES analysis indicated that gold concentrations remained the same after 24 hours. The pH and eH increased over time in all experimental-gold systems.

### 3.2.3 Scanning electron microscopy-energy dispersive spectroscopy

The bacterial enrichment contained nanometre-size, acicular iron oxyhydroxide precipitate forming micrometre-size sheet and spherical structures with rod-shaped bacteria occurring on the surface (Fig. 3.2a). Filtrates from culture enrichment-gold systems contained the same iron oxyhydroxide morphology with bacteria. However, soluble gold was immobilised as 100 nm gold sulphide colloids forming clusters on the surface of acicular, iron oxyhydroxide precipitates (Fig. 3.2b). Filtrates from spent media-gold systems demonstrated that soluble gold was immobilised as spherical precipitates ranging from 200 nm to 2 μm in diameter and were also composed of gold and sulphur (Fig. 3.3). Aggregation of these spherical precipitates explains the observed colour change of iron oxyhydroxides and opaque, black precipitate that formed in suspension in each respective experimental system.

### 3.2.4 Transmission electron microscopy-energy dispersive spectroscopy

High-resolution TEM-EDS analysis demonstrated that iron oxyhydroxide precipitate also occurred as clustered spheres 100 nm in size and were composed of radial acicular minerals (Fig. 3.4a). When exposed to 20 mM gold for 24 hours, the iron oxyhydroxide-gold system formed 2 nm colloids composed of gold and sulphur (see section 3.2.5). It is important to note that the filamentous appearance of iron oxyhydroxide diminished as the precipitation of gold sulphide colloids replaced the acicular minerals (Fig. 3.4b). Bacteria obtained from the fluid phase of enriched cultures contained no evidence of iron mineralisation (Fig. 3.5a). However, bacteria from bacterial-gold systems demonstrated extensive extracellular gold mineralisation. Immobilisation of gold from solution occurred as colloidal gold sulphide

approximately 2 nm in diameter (Fig. 3.5b). Remains of the cell wall were not observed although the extensively gold-mineralised bacteria appeared frayed (Fig. 3.5c).

### 3.2.5 X-ray absorption near-edge structure (XANES)

The XANES spectra of the four relevant gold compounds are illustrated in Figure 3.6. Unlike characteristic peaks of the elemental gold standard, gold sulphide and gold thiosulphate standards have broad spectral features occurring after the Au L-111 absorption edge (11919 eV). The XANES spectra generated from the culture enrichment-, spent media- and iron oxide-gold systems exposed to 20 mM gold for 1 hour confirmed the precipitation of gold sulphide from the reduction of gold (I) thiosulphate (Fig. 3.6).

## 3.3 Discussion

In acid rock drainage environments, thiosulphate would be the dominant ligand responsible for the solubility of gold in which transport is facilitated by mixing or possibly driven by convection of different hydrological regimes (Boulegue, 1981; Mann, 1984; Webster, 1985). Understanding the mobility of gold (I) thiosulphate in these environments is important because iron-oxidising bacteria contribute to the geochemical conditions.

Previous studies have demonstrated that active metabolism of iron-oxidising bacteria such as *A. ferrooxidans* forms jarosite-group minerals that are stable under oxidised, highly acidic, iron- and sulphur-rich conditions (Sasaki et al., 1995; Sasaki and Konno, 2000; Brown, 1971). In this study, iron oxide precipitate from bacterial enrichments was likely hydroniumjarosite ($(H_3O)Fe(SO_4)_2(OH)_6$) since potassium and sodium, cations for other potential end members, were limited in the media defined by Silvermann and Lundgren (1959). The formation of iron oxyhydroxide precipitate as hydroniumjarosite is also consistent with the mineralogy of biofilm coatings described by Fernandez-Remolar et al. (2005). The fluid phase of bacterial enrichments contained the greater concentration of ferric iron since iron oxyhydroxide precipitate, i.e., hydroniumjarosite, constituted approximately 8.5% of oxidised ferrous iron from the fresh media (see section 3.2.1). Although this percentage appears small, the dry weight of iron oxyhydroxide precipitate is much greater than the weight of cells from the enrichment. The difference in weight of iron oxyhydroxide precipitate to bacteria demonstrates the extent in which iron-oxidising bacteria can

biologically mediate a large amount of solid ferric iron. This also supports the notion that cells can be “trapped” or mineralised within the iron oxide (Konhauser, 1998; Ferris et al., 1988, 2004; Preston et al., 2011). The change in Eh after growth of bacterial enrichments indicated that iron-oxidising bacteria are capable of changing the redox potential of their surrounding aqueous environment. Under acidic and oxidised conditions, the reduction of solid ferric iron, i.e. iron oxyhydroxide precipitate, is slow in comparison to soluble ferric iron, i.e., spent media, (Brown, 1971).

Bacterial enrichments represented biogeochemical conditions of ARD environments and entire enrichment-gold systems were accelerated laboratory models of natural systems demonstrating the direct and indirect effect of iron-oxidising bacteria on the stability of gold (I) thiosulphate (Fig. 3.2). Thiosulphate can remain stable in aqueous solution across a range of pH when complexed with certain metals such as gold; however, the gold complex is no longer stable under acidic conditions when ferric iron is present (Alymore and Muir, 2001). Gold (I) thiosulphate stability was demonstrated by both the fresh media-gold systems and the chemical controls that retained the same gold concentration over 24 hours (Table 3.1). The instability was demonstrated by the immobilisation of gold in culture enrichment-, spent media- and iron oxide-gold systems exposed to 20 mM gold for 24 hours. The presence of ferric iron was important because it reduced to ferrous iron as it oxidised the thiosulphate ligand leading to the initial destabilisation of the gold (I) thiosulphate complex and "liberating” gold (Reaction 3.7). The rapid formation and agglomeration of precipitate observed in the spent media-gold system (Fig. 3.3) suggests that the reduction of soluble ferric iron was faster in comparison to solid ferric iron from the iron oxyhydroxide-gold system (Fig. 3.4). Furthermore, soluble ferric iron was primarily responsible for the oxidation of the thiosulphate ligand that destabilised the gold (I) thiosulphate complex. Note that the amount of gold immobilised in the spent media-gold systems was approximately equal to the amount immobilised in culture enrichment-gold systems.

$$8Fe^{3+} + Au(S_2O_3)_2^{3-} + 5\ H_2O \rightarrow 8Fe^{2+} + Au^{+} + S_2O_3^{2-} + 2SO_4^{2-} + 10H^{+} \qquad (3.7)$$

Once the gold complex was destabilised, further oxidation of thiosulphate continued and led to subsequent reduction of gold as gold sulphide (Reaction 3.8 and 3.9). Formation of gold sulphide colloids and colloidal clusters (Fig. 3.2-3.4) were consistent with studies by Morris

et al. (2002) who demonstrated that colloidal gold sulphide begins by rapid nucleation of $Au_nS_m^-$ and varying colloidal sizes can occur depending on the presence of excess sulphur. Gold (I) sulphur compounds are important intermediate soluble gold complexes during bacterial reduction of gold chloride (Lengke et al., 2006a). However XANES analysis of the experimental-gold systems in this study indicated that a gold thio-organic compound, e.g., thiomalate, did not form or was perhaps a highly unstable transient species. Immobilisation of gold (I) thiosulphate occurred as precipitated gold sulphide.

$$S_2O_3^{2-} + H_2O + H^+ \rightarrow H_2SO_4 + HS^- \quad (3.8)$$

$$2Au^+ + HS^- \rightarrow + Au_2S + H^+ \quad (3.9)$$

Some gold could have been reduced to elemental gold via oxidation of previously reduced iron (Reaction 3.10) suggesting that gold (I) thiosulphate destabilisation and subsequent gold reduction could be a regenerative process. Furthermore, organic material derived from iron-oxidising bacteria also acted as a potential gold-reducing agent (Reaction 3.11). Previous studies by Lengke and Southam (2007) demonstrated reduction of gold (I) thiosulphate and the precipitation of colloidal gold along cellular membranes of *Acidithiobacillus thiooxidans* highlighted the importance of thiosulphate ligand oxidation via bacterial metabolic activity. In this study, extensive extracellular mineralisation of iron-oxidising bacteria in bacterial-gold systems indicated that nanometre-size gold colloids formed by "stripping" electrons from organic material (Reaction 3.11). This subsequently led to cell wall disruption leaving no evidence of the semi-permeable membrane or other relic cell structures (Fig. 3.5). The chemical reaction of gold (I) thiosulphate destabilisation by ferric iron and reduction by hydrogen sulphide ($HS^-$) and organics ($CHO_2^-$) explain both the quantitative and qualitative observations of soluble gold removed from each experimental system.

$$Au^+ + Fe^{2+} \rightarrow Au^0 + Fe^{3+} \quad (3.10)$$

$$Au^+ + CHO_2^- \rightarrow Au^0 + CHO_2 \quad (3.11)$$

## 3.4 Conclusion

In this study, iron-oxidising bacteria had an indirect effect on the stability of gold (I) thiosulphate by increasing ferric iron concentrations via ferrous iron oxidation. Upon the destabilisation of the gold complex, each system produced colloidal gold sulphide of varying

sizes based upon the dominant reducing agent present, i.e., ferric iron, hydrogen sulphide, organics. These experimental systems were laboratory models demonstrating the accelerated biogeochemical cycling of gold within near-surface weathering environments dominated by acidic and oxidised conditions. Therefore, it can be concluded that the residence time of gold mobility as a soluble gold (I) thiosulphate complex in an acidic, oxidised weathering environment is finite. These conditions, influenced by active bacterial metabolism, promote gold reduction and the potential for mobility as colloidal gold sulphide. From a geochemical perspective, the destabilisation, reduction and biomineralisation of gold (I) thiosulphate would occur concurrently with the continued oxidation and weathering of the host metal sulphides. As a result, this biogeochemical cycling of gold could lead to supergene gold enrichment.

**Table 3.1.** Chemical analysis of constituents and experimental-gold systems.

| **Chemical Analysis Constituents (prior to experimental use)** | | |
|---|---|---|
| Constituents | pH | eH (V) |
| Growth media | 2.30 | 0.65 |
| Bacterial enrichment[b] | 2.24 | 0.73 |
| 20 M gold stock | 5.22 | -- |

| **Chemical Analysis of Gold Immobilised from Solution in Experimental-Gold Systems** | | | | | | | | | | | | | | | |
|---|---|---|---|---|---|---|---|---|---|---|---|---|---|---|---|
| **Time (hours)** | **0.0019 mM Au[a]** | **pH** | **Eh (V)** | **0.022 mM Au[a]** | **pH** | **Eh (V)** | **0.21 mM Au[a]** | **pH** | **Eh (V)** | **2.05 mM Au[a]** | **pH** | **Eh (V)** | **20.3 mM Au[a]** | **pH** | **Eh (V)** |
| Entire enrichment - gold system | | | | | | | | | | | | | | | |
| 1 | 0.0016 | 2.24 | 0.62 | 0.018 | 2.24 | 0.62 | 0.19 | 2.25 | 0.62 | 2.01 | 2.23 | 0.61 | 19.87 | 2.23 | 0.55 |
| 2 | 0.0016 | 2.24 | 0.62 | 0.018 | 2.24 | 0.61 | 0.20 | 2.25 | 0.60 | 2.03 | 2.25 | 0.59 | 20.07 | 2.25 | 0.55 |
| 4 | 0.0016 | 2.23 | 0.61 | 0.019 | 2.25 | 0.60 | 0.20 | 2.27 | 0.58 | 2.03 | 2.25 | 0.56 | 20.15 | 2.26 | 0.55 |
| 8 | 0.0017 | 2.25 | 0.61 | 0.019 | 2.28 | 0.60 | 0.20 | 2.27 | 0.58 | 2.03 | 2.26 | 0.56 | 20.19 | 2.28 | 0.51 |
| 24 | 0.0018 | 2.24 | 0.61 | 0.019 | 2.28 | 0.59 | 0.20 | 2.29 | 0.58 | 2.03 | 2.26 | 0.53 | 20.28 | 2.28 | 0.51 |
| Spent media - gold system | | | | | | | | | | | | | | | |
| 24 | | | | | | | | | | | | | 20.21 | 2.28[b] | -- |
| Fresh media - gold system | | | | | | | | | | | | | | | |
| 24 | | | | | | | | | | | | | 0 | 2.30 | -- |
| Iron oxide - gold system | | | | | | | | | | | | | | | |
| 24 | | | | | | | | | | | | | 6.25 | 1.32 | -- |
| Bacterial - gold system | | | | | | | | | | | | | | | |
| 24 hrs | | | | | | | | | | | | | 0.89 | 1.30 | -- |

[a] Concentrations of gold added to experimental systems and chemical controls
[b] The pH measurements of spent media were the same as the bacterial enrichments


**Figure 3.1. Photograph of Rio Tinto, Spain.** Photograph of boulder-size rock coated in a range of hydrated (orange-yellow) to dehydrated (red) iron oxhydroxide in Rio Tinto, Spain. The hydrated iron oxide submersed in the water (circle) was sampled material for iron-oxidizing bacterial enrichments (see inset).

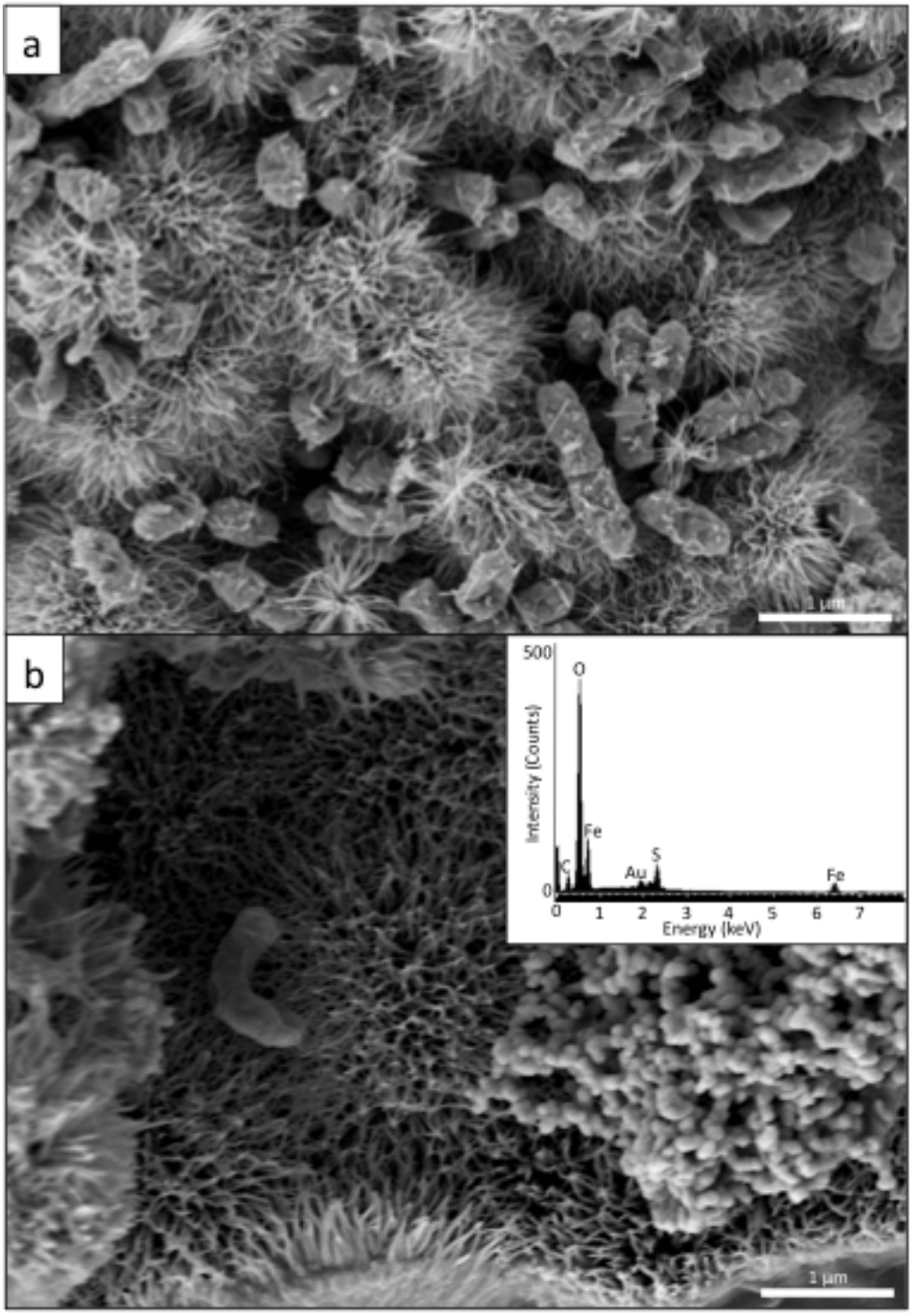


**Figure 3.2. SEM-EDS characterisation of an entire enrichment-gold system.** High-resolution SEM micrograph of an entire enrichment-gold system exposed to 20 mM gold for 24 hours. Individual rod-shaped bacterial cells and clusters of 100 nm size gold sulphide colloids occurred on the surface of sheet-like acicular iron oxide.

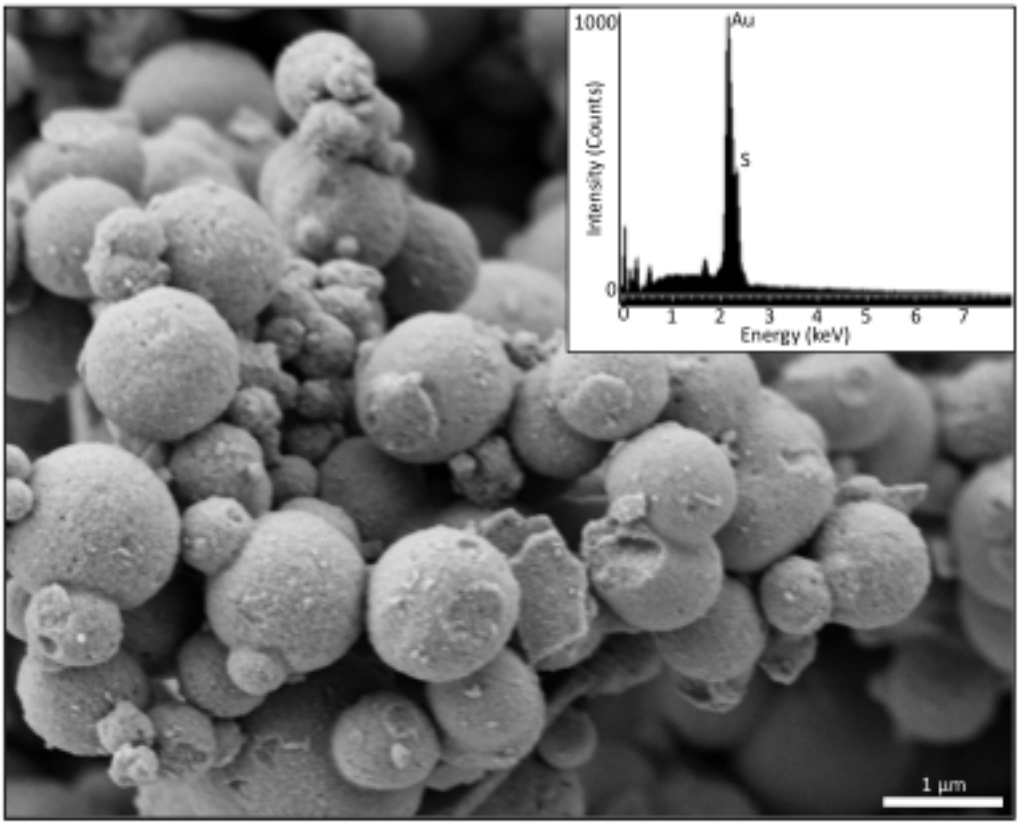


**Figure 3.3. SEM-EDS characterisation of precipitate from a spent media-gold system.** High-resolution SEM micrograph of a spent media-gold system exposed to 20 M gold for 24 hours. The black precipitate formed clusters of gold sulphide colloids ranging from 200 nm to 2 µm in diameter.

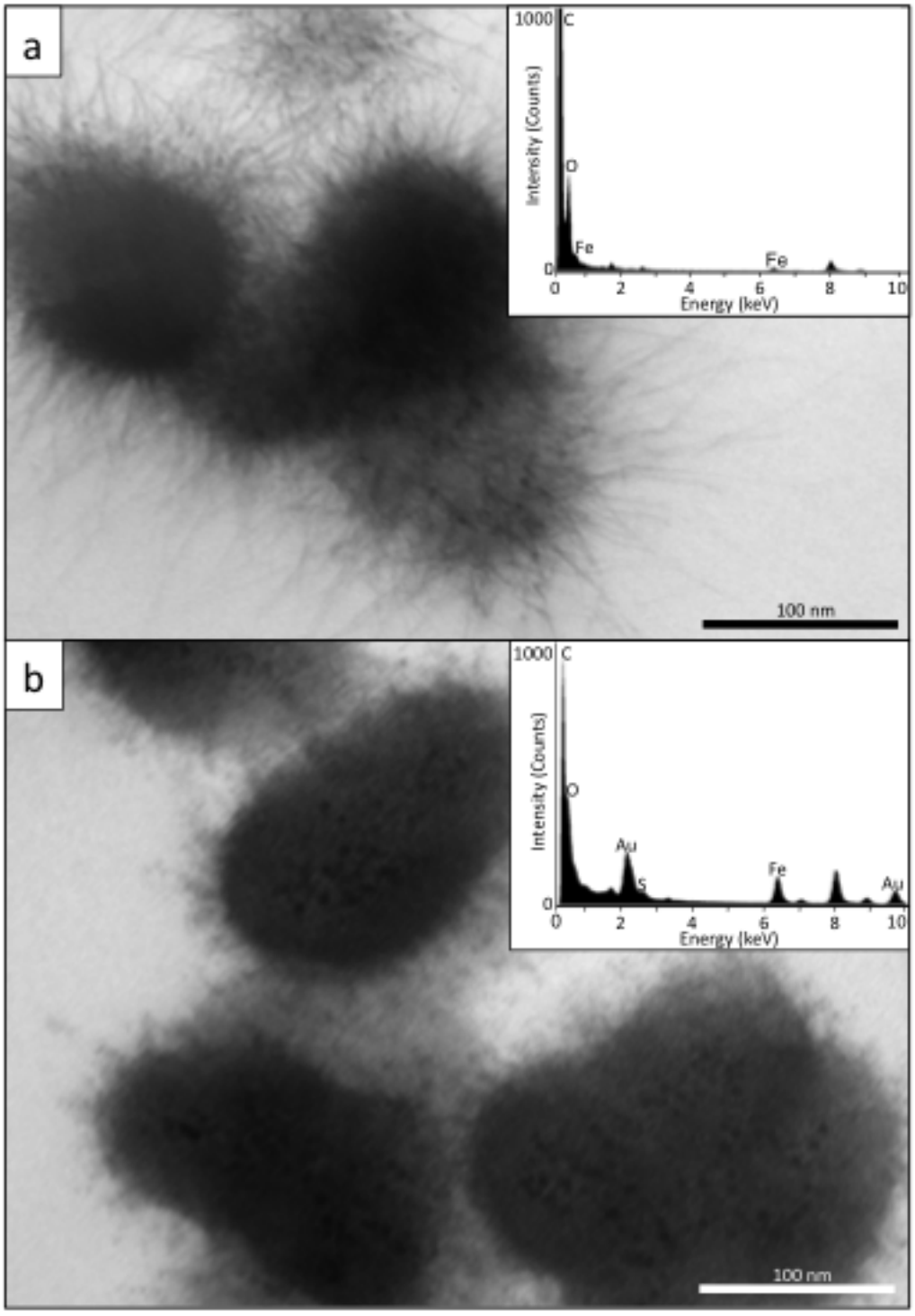


**Figure 3.4. TEM-EDS of acicular iron oxide minerals and colloidal gold sulphide.** A high-resolution TEM micrographs of the iron oxide precipitate demonstrated that acicular iron oxide minerals formed radial structures approximately 100 nm in diameter (a). An iron oxide-gold system exposed to 20 M gold for 24 hours demonstrated that replacement of acicular iron "filaments" with 10 nm size gold sulphide colloids (b). Note the C peak is attributed to the coating on the copper grid or Epon plastic.

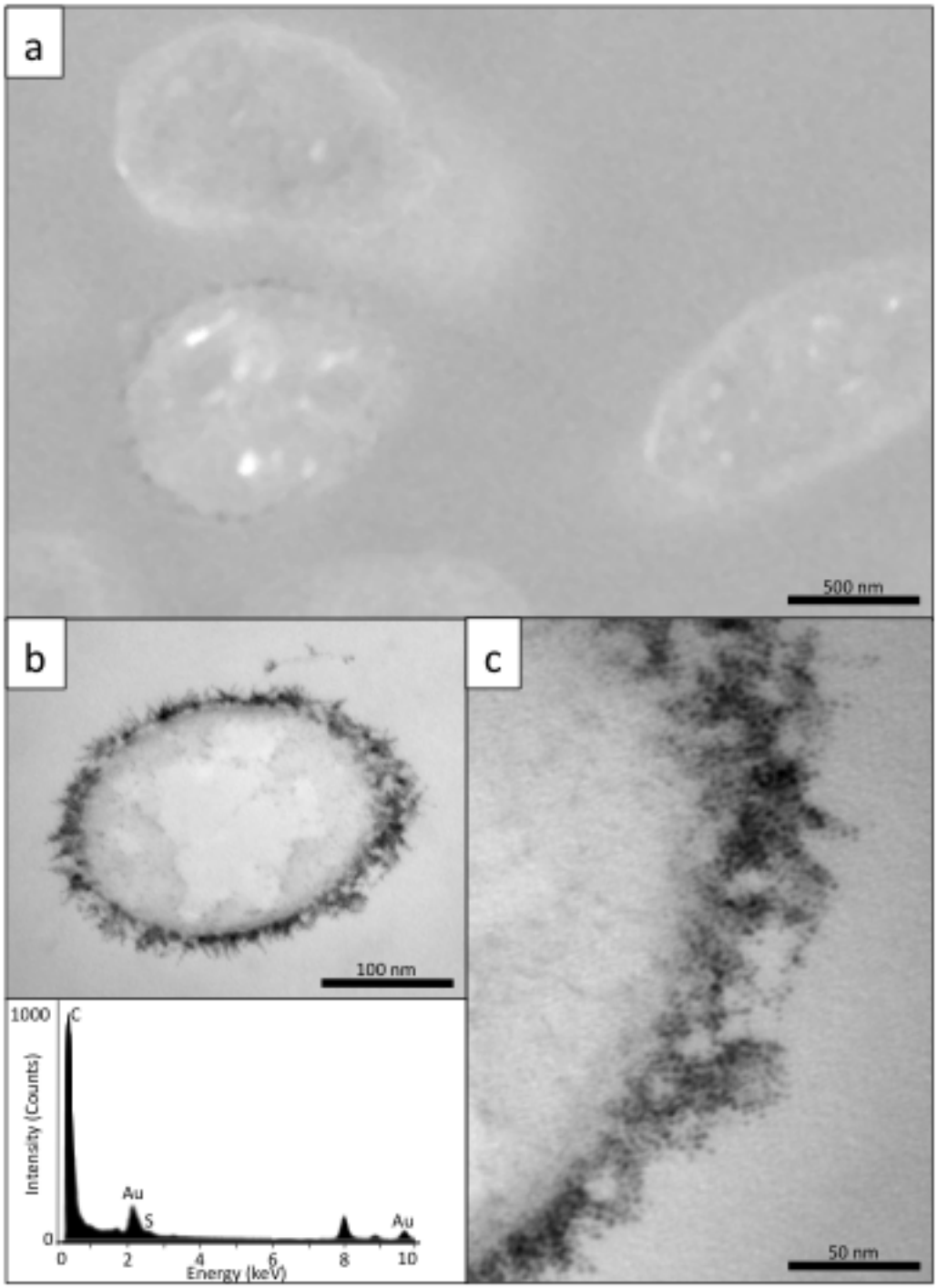


**Figure 3.5. TEM-EDS characterisation of a bacterial-gold system.** Ultra thin section TEM micrograph of a bacterial cell obtained from the fluid phase of an enriched culture (a) and bacterial cell exposed to 20 M gold for 24 hours (b). Homogeneous gold immobilisation occurred as extensive extracellular precipitation of gold-sulphide colloids. Gold-sulphide colloids were 10 nm in size and appeared to cause disruption of the cellular membrane give a frayed appearance (c).

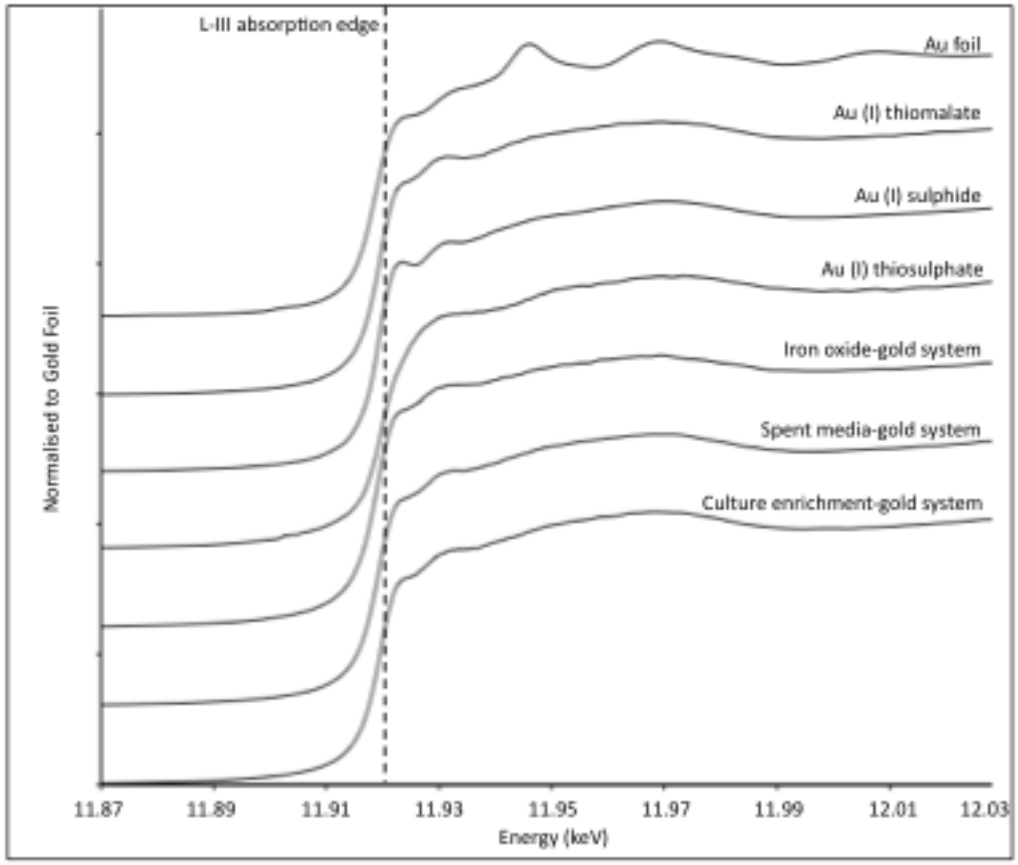


**Figure 3.6. XANES analysis of entire enrichment-, spent media-, iron oxide-gold system.** XANES spectra of the entire enrichment-, spent media-, iron oxide-gold systems and the four reference standards. The gold compounds have characteristic peaks occurring after the L-III absorption edge. Gold sulphide formed in all experimental-gold systems exposed to 20 mM gold (I) thiosulphate after 1 hour.

## 3.5 References

Alvarez-Valero, A.M., Perez-Lopez, R., Matos, J., Capitan, M.A., Nieto, J.M., Saez, R., Delgado, J., Caraballo, M., 2008. Potential environmental impact at Sao Domingos mining district (Iberian Pyrite Belt, SW Iberiam Peninsula): evidence from a chemical and mineralogical characterization. Environmental Geology, 55, 1797-1809.

Andrade, W.O., Machesky, M.L., Rose, A.W., 1991. Gold distribution and mobility in the surficial environment, Carajas region, Brazil. Journal of Geochemical Exploration, 40, 95-114.

Aylmore, M.G., Muir, D.M., 2001. Thiosulphate leaching of gold – a review. Minerals Engineering, 14, 135-174.

Benedetti, M., Boulegue, J., 1991. Mechanisms of gold transfer and deposition in a supergene environment. Geochimica et Cosmochimica Acta, 55, 1539-1547.

Blowes, D.W., Jambor, J.L., 1990. The pore-water chemistry and the mineralogy of the vadose zone of sulphide tailings, Waite Amulet, Quebec. Applied Geochemistry, 5, 327-346.

Boulegue, J., 1981. Simultaneous determination of sulphide, polysulphides and thiosulphates as an aid to ore exploration. Journal of Geochemical Exploration, 15, 21-36.

Bowell, R.J., 1992. Supergene gold mineralogy at Ashanti, Ghana: implications for the supergene behaviour of gold. Mineralogical Magazine, 56, 545-560.

Boyle, R.W., 1979. The geochemistry of gold and its deposits. Geological Survey of Canada Bulletin, 280, 1-54.

Brown, J.B., 1971. Jarosite-goethite stabilities at 25º C, 1 ATM. Mineralium Deposita, 6, 245-252.

Dold, B., Fontbote, L., 2001. Element cycling and secondary mineralogy in porphyry copper tailings as a function of climate, primary mineralogy, and mineral processing. Journal of Geochemical Exploration, 74, 3-55.

Cochran, W.G., 1950. Estimation of bacterial densities by means of the "Most Probable Number". Biometrics, 6, 105-116.

Colin, F., Sanfo, Z., Brown, E., Bourles, D., Minko, A.E., 1997. Gold: a tracer of the dynamics of tropical laterites. Geology, 25, 81-84.

Fairbrother, L., Brugger, J., Shapter, J., Laird, J.S., Southam, G., Reith, F., 2012. Supergene gold transformation: biogenic secondary and nano-particulate gold from arid Australia. Chemical Geology, 320, 17-31.

Fernandez-Remolar, D.C., Morris, R.V., Gruener, J.E., Amils, R., Knoll, A.H., 2005. The Rio Tinto Basin, Spain: mineralogy, sedimentary geobiology, and implications for interpretation of outcrop rocks at Meridiani Planum, Mars. Earth and Planetary Science Letters, 240, 149-167.

Fernandez-Remolar, D.C., Gomez, F., Prieto-Ballestros, O., Schelble, R.T., Rodriguez, N., Amils, R., 2008. Some ecological mechanisms to generate habitability in planetary subsurface areas by chemolithotrophic communities: the Rio Tinto subsurface ecosystem as a model system. Astrobiology, 8, 157-173.

Ferreira da Silva, E., Patinha, C., Reis, P. Cardoso Fonseca, E., Matos, J.X., Barrosinho, J., Santos Oliveira, J.M., 2006. Interaction of acid mine drainage with waters and sediments at the Corona stream, Lousal mine (Iberian Pyrite Belt, Southern Portugal). Environmental Geology, 50, 1-13.

Ferris, F.G., Fyfe, W.S., Beveridge, T.J., 1988. Metallic ion binding by *Bacillus subtilis* implications for the fossilisation of microorganisms. Geology, 16, 149-152.

Ferris, F.G., Hallbeck, L., Kennedy, C.B., Pedersen, K., 2004. Geochemistry of acidic Rio Tinto headwaters and role of bacteria in solid phase metal partitioning. Chemical Geology, 212, 291-300.

Freise, F.W., 1931. The transportation of gold by organic underground solutions. Economic Geology, 26, 421-431.

Freyssinet, P., Zeegers, H., Tardy, Y., 1989. Morphology and geochemistry of gold grains in lateritic profiles of southern Mali. Journal of Geochemical Exploration, 32, 17-31.

Greffie,C., Benedetti, M.F., Parron, C., Amouric, M., 1996. Gold and iron oxide association under supergene conditions: an experimental approach. Geochimica et Cosmochimic Acta, 60, 1531-1542.

Goldschmidt, V.M., 1937. The principles of distribution of chemical elements in minerals and rocks. Journal of the Chemical Society of London, 655-673.

Gonzalez-Toril, E., Gomez, F., Irazabal, N., Amils, R., Marin, I., 1999. Comparative genomic characterisation of iron oxidising bacteria isolated from the Tinto River, in: Amils, R., Ballester, A. (Eds.), Biohydrometallurgy and the Environment towards the Mining of the 21$^{st}$ century, Elsevier, Amsterdam, pp. 149-157.

Huston, D.L., Large, R.R., 1989. A chemical model for the concentration of gold in volcanogenic massive sulphide deposits. Ore Geology Reviews, 4, 171-200.

Huston, D.L., Bottrill, R.S., Creelman, R.A., Zaw, K., Ramsden, T.R., Rand, S.W., Gemmell, J.B., Jablonski, W., Sie, S.H., Large, R.R., 1992. Geologic and geochemical controls on the mineralogy and grain size of gold-bearing phases, Eastern Australian volcanic-hosted massive sulphide deposits. Economic Geology, 87, 542-563.

Hutchinson, R.W., 1990. Precious metals in massive base metal sulphide deposits. Geologische Rundschau, 79, 241-263.

Hough, R.M., Noble, R.R.P., Hitchen, G.J., Hart, R., Reddy, S.M., Saunders, M., Clode, P., Vaughan, D., Lowe, J., Gray, D.J., Anand, R.R., Butt, C.R.M., Verral, M., 2008. Naturally occurring gold nanoparticles and nonplates. Geology, 36, 571-574.

Kenney, J.P.L., Song, Z., Bunker, B.A., Fein, J.B., 2012. An experimental study of Au removal from solution by non-metabolising bacterial cells and their exudates. Geochimica et Cosmochimica Acta, 87, 51-60.

Konhauser, K.O., 1998. Diversity of bacterial iron mineralisation. Earth-Science Reviews, 43, 91-121.

Lakin, H., Curtin, G., Hubert, A., 1974. Geochemistry of gold in the weathering cycle. United States Geological Survey Bulletin, 1330, 2-29.

Large, R.R., 1990. The gold-rich seafloor massive sulphide deposits of Tasmania. Geologische Rundschau, 79, 265-278.

Leistel, J.M., Marcoux, E., Deschamps, Y., Joubert, M., 1998. Anthithetic behavour of gold in the volcanogenic massive sulphide deposits of the Iberian Pyrite Belt. Minerialium Deposita, 33, 82-97.

Lengke, M.F., Fleet, M.E., Southam, G., 2006a. Morphology of gold nanoparticles synthesized by filamentous cyanobacteria from gold(I)-thiosulfate and gold(III)-chloride complexes. Langmuir, 22, 2780-2787.

Lengke, M.F., Ravel, B., Fleet, M.E., Wanger, G., Gordon, R.A., Southam, G., 2006b. Mechanisms of gold bioaccumulation by filamentous cyanobacteria from gold (III)-chloride. Environmental Science Technology, 40, 6304-6309.

Lengke, M.F., Ravel, B., Fleet, M.E., Wanger, G., Gordon, R.A., Southam, G., 2007. Precipitation of gold by reaction of aqueous gold(III)-chloride with cyanobacteria at 25-80°C – Studied by X-ray absorption spectroscopy. Canadian Journal of Chemistry, 85, 1-9.

Levings, C.D., Varela, D.E., Mahlenbacher, N.M., Barry, K.L., Piercey, G.E., Guo, M., Harrison, P.J., 2005. Effects of an acid mine drainage effluent on photoplankton biomass and primary production at Britannia Beach, Howe Sound, British Columbia. Marine Pollution Bulletin, 50, 1585-1594.

Lopez-Archilla, A.I., Marin, I., Amils, R., 2001. Microbial community composition and ecology of an acidic aquatic environment: the Tinto Tiver, Spain. Microbial Ecology, 41, 20-35.

Machesky, M.L., Andrade, W.O., Rose, A.W., 1991. Adsorption of gold (III) chloride and gold (I) thiosulphate anions by goethite. Geochimica et Cosmochimica Acta, 55, 769-776.

Mann, A.W., 1984. Mobility of gold and silver in lateritic weathering profiles: some observations from Western Australia. Economic Geology, 79, 38-50.

McHuge, J.B., 1984. Gold in natural water: a method of determination by solvent extraction and electrothermal atomisation. Journal of Geochemical Exploration, 20, 303-310.

McHuge, J.B., 1988. Concentration of gold in natural waters. Journal of Geochemical Exploration, 30, 85-94.

Morris, T., Copeland, H., Szulczewski, G., 2002. Synthesis and characterisation of gold sulphide nanoparticles. Langmuir, 18, 535-539.

Neidhardt, F.C., Ingraham, J.L., Schaechter, M., 1990. Physiology of the bacterial cell: A molecular approach. Sinauer Associates, Sunderland. MA.

Nordstrom D.K., 1977. Thermochemical redox equilibria of ZoBell's solution. Geochimica et Cosmochimica Acta, 41, 1835-1841.

Nordstrom, D.K., Southam, G., 1997. Geomicrobiology of sulphide mineral oxidation, in: Banfield, J.F., Mealson, K.H. (Eds.), Geomicrobiology: Interactions between Microbes and Minerals. Review in Mineralogy and Geochemistry, 35, 361-390.

Nordstrom, D.K., Alpers, C.N., 1999. Negative pH, efflorescence mineralogy, and consequences for environmental restoration at the iron mountain superfund site. Proceedings of the National Academy of Science, 96, 3455-3462.

Nordstrom, D.K., 2009. Acid Rock Drainage and Climate Change. Journal of Geochemical Exploration, 100, 97-104.

Plyusnin, A.M., Pogreblnyak, Y.F., Mironov, A.G., Zhmodik, S.M., 1981. The behaviour of gold in the oxidation of gold bearing sulphides. Geochemistry International, 18, 116-123.

Preston, L.J., Shuster, J., Fernandez-Remolar, D., Banerjee, N.R., Osinski, G.R., Southam, G., 2011. The preservation and degradation of filamentous bacteria and biomolecules within iron oxide deposits at Rio Tinto, Spain. Geobiology, 9, 233-249.

Puddephatt, R., 1978. The chemistry of gold. Elsevier Publishing Company. New York. 31-87.

Ravel, B., Newville, M., 2005. Athena, Artemis, Hephaestus: Data analysis for X-ray absorption spectroscopy using IFEFFIT. Journal of Synchrotron Radiation, 12, 537-547.

Reith, F., McPhail, D.C., 2006. Effect of resident microbiota on the solubilisation of gold in soil from the Tomakin Park Gold Mine, New South Wales, Australia. Geochimica et Cosmochimica Acta, 70, 1421- 1438.

Reith, F., Rogers, S.L., McPhail, D.C., Webb, D., 2006. Biomineralisation of gold: biofilms on bacterioform gold. Science, 313, 233-236.

Reith, F., Lengke, M.F., Falconer, D., Craw, D., Southam, G., 2007. The geomicrobiology of gold. International Society of Microbial Ecology Journal, 1, 567-584.

Renders, P.J., Seward, T.M., 1989. The adsorption of thiogold (I) complexes by amorphous $As_2S_3$ and $Sb_2S_3$ at 25 and 90º C. Geochimica et Cosmochimica Acta, 53, 255-267.

Sasaki, K., Konno, H., 2000. Morphology of jarosite-group compounds precipitated from biologically and chemically oxidized Fe ions. Canadian Mineralogist, 38, 45-56.

Sasaki, K., Tsunekawa, M., Konno, H., 1995. Characterisation of argentojarosite formed from biologically oxidized Fe3+ ions. Canadian Mineralogist, 33, 1311-1319.

Schoonen, M.A.A., Fisher, N.S., Wente, M., 1992. Gold sorption onto pyrite and goethite: a radiotracter study. Geochimica et Cosmochimica Acta, 56, 1801-1814.

Silvermann, M.P., Lundgren, D.G., 1959. Studies on the chemoautotrophic iron bacterium Ferrobacillus ferrooxidans. An improved medium and a harvesting procedure for securing high cell yields. Journal of Bacteriology, 77, 642-647.

Singer, P.C., Stumm, W., 1970. Acidic mine drainage: the rate determining step. Science, 167, 1121-1123.

Song, Z., Kenney, J.P.L., Bunker, B.A., 2012. An X-ray Fine Structure study of Au adsorbed onto the non-metabolizing cells of two soil bacterial species. Geochimica et Cosmochimica Acta, 86, 103-117.

Southam, G., Beveridge, T.J., 1994. The in vitro formation of placer gold by bacteria. Geochimica et Cosmochimica Acta, 58, 4527-4530.

Southam, G., Beveridge, T.J., 1996. The occurrence of sulfur and phosphorus within bacterially derived crystalline and pseudocrystalline octahedral gold formed in vitro. Geochimica et Cosmochimica Acta, 60, 4369-4376.

Spurr, J.E., Garrey, G.H., 1908. Economic geology of the Georgetown quadrangle (together with the Empire district), Colorado, with General geology, by S.H. Ball: United States Geological Survey Professional Papers, 63, 422.

Uchida, A., Yokoyama, T., Motomura, Y., Miyazaki, A., Okaue, Y., Watanabe, K., Izawa, E., 2002. Role of iron (III) and aluminium hydroxides in concentration/reduction of Au (II) complexes. Resource Geology, 52, 223-230.

Webster, J.G., 1985. Thiosulphate in surficial geothermal waters, North Island, New Zealand. Applied Geochemistry, 2, 5-6.

Webster, J.G., Mann, A.W., 1984. The influence of climate, geomorphology and primary geology on the supergene migration of gold and silver. Journal of Geochemical Exploration, 22, 22-42.

Wilson, A.F., 1984. Origin of quartz-free gold nuggets and supergene gold found in laterites and soils-a review and some new observations. Australian Journal of Earth Science, 31, 303-316.

# Appendices to Chapter 3

## A3 The effect of iron-oxidising bacteria on the stability of the gold (III) chloride complex

In addition to the immobilisation of the gold (I) thiosulphate complex by acidophilic, iron-oxidising bacteria, it is worth considering the immobility of the gold (III) chloride complex using the same biogeochemical conditions described in Chapter 3. In near-surface environments such arid to semi-arid laterites, salinisation can increase chloride concentrations. Furthermore, chloride ions are stable under acidic, near-surface conditions and can become the dominant ligand available for auric chloride complexation thereby promoting gold solubility and subsequent mobility within groundwater systems (Mann, 1984; Webster, 1985; Benedetti and Boulegue, 1991; Marsden and House, 1992; Carey et al., 2003). Therefore, the purpose of these experiments was to provide an additional, complimentary comparison of gold (III) chloride immobilisation to the results presented in Chapter 3.

## A3.1 Material and Methods

### A3.1.1 Gold stock solutions

Calculated 20 and 40 mM gold stocks were prepared by dissolving gold (III) chloride of 99.9% purity, purchased from Alfa Aesar, in distilled, deionised water. The gold stocks were filter-sterilised using a 0.1 μm pore-size filter. These gold concentrations were used in order to be consistent with gold concentrations from Chapter 3 so that a reasonable comparison could be made between precipitates derived from gold (I) thiosulphate and gold (III) chloride reduction.

### A3.1.2 Experimental-gold systems

The process for bacterial enrichment, construction of experimental-gold systems, and arrestment of gold exposures were identical to the methods described in Chapter 3 (see section 3.1.3). However, the experimental-gold systems in this study involved the exposure of iron-oxidising bacterial enrichments and each separate component to gold (III) chloride for 24 hours. The overall gold concentration for all experimental-gold systems was 20 mM gold.

Gold (III) chloride stocks were also used as chemical controls in the same manner and purpose described in Chapter 3. Filtrates from each experimental-gold system were analysed using electron microscopy while filtered solutions were acidified with concentrated nitric acid and analysed for residual soluble gold using a Perkin-Elmer Optima 3300-DV Inductively Coupled Plasma-Atomic Emission Spectrometer (ICP-AES).

### A3.1.3 Scanning electron microscopy-energy dispersive spectroscopy

A filtrate from a fresh media-gold system was prepared for scanning electron microscopy-energy dispersive spectroscopy (SEM-EDS). The filtrate was rinsed three times with filter-sterilised distilled, deionised water, air-dried for 24 hours and mounted onto aluminium stubs with 12 mm carbon adhesive tabs. A Denton Vacuum Desk II sputter coater was used to coat the filtrates with a 5 nm thick osmium coating to reduce sample charging during SEM-EDS analysis. A LEO Ziess 1540XB field emission gun-scanning electron microscope (FEG-SEM) equipped with an Oxford Instruments' INCAx-sight energy dispersive spectrometer (EDS) operating at 10 kV accelerating voltage was used for imaging and qualitative elemental composition.

### A3.1.4 Transmission electron microscopy-energy dispersive spectroscopy

A filtrate from a bacteria-gold system was prepared for transmission electron microscopy-energy dispersive spectroscopy (TEM-EDS). The filtrate was fixed for 2 hours in $2\%_{(aq)}$ glutaraldehyde, enrobed in $2\%_{(wt/vol)}$ noble agar, dehydrated in a 25, 50, 75 and 3× $100\%_{(aq)}$ acetone series and embedded in Epon plastic. The embedded sample was cut to 70 nm ultrathin sections using a Reichert-Jung Ultracut E ultramicrotome and collected on a Formvar-carbon coated, 200-square mesh copper grids. The filtrate was then examined with a Phillips CM-10 transmission electron microscope (TEM) operating at 80 kV.

## A3.2 Results

### A3.2.1 Chemical analysis

Residual, soluble gold concentrations, from all experimental-gold systems, are listed in Table A.1. Immobilisation of gold occurred rapidly upon the addition of gold (III) chloride to the fresh media. The reaction was observed as the solution changed from transparent yellow to

clear while a brown precipitate formed in suspension then gradually settled to the bottom of the test tube. After 24 hours, the fresh media-gold system removed approx. 96% gold from solution while the bacterial- and entire enrichment-gold system removed 4% and 2% gold from solution, respectively. Spend media-, iron oxyhydroxide-gold system and chemical controls contained the same gold concentration as the initial input.

### A3.2.2 Scanning and transmission electron microscopy-energy dispersive spectroscopy

Backscatter SEM micrographs and EDS spectra of the filtrate from the fresh media-gold system indicated that the precipitates were irregular shaped, micrometre-size colloids composed of gold (Fig. A1a, b). High-resolution TEM micrographs demonstrated that iron-oxidising bacteria precipitated nanometre-size, gold colloids that occurred intracellularly and larger, crystalline, semi-octahedral gold platelets occurred on the extracellular surfaces (Fig. A1c).

## A3.3 Discussion

The spent media- and the iron oxyhydroxide-gold system had no changes in gold concentration and suggests that the iron-oxidising bacterial enrichments likely had negligible or no ferrous iron present that could have acted as a reducing agent to gold (III) chloride. Therefore, gold immobilisation in the entire enrichment-gold system was likely attributed purely to the presence of bacteria. The amount of gold immobilised in this system was half of what was immobilised in the bacterial-gold system. This difference was attributed to bacterial-gold system containing approximately double the concentration of cells (see Chapter 3, Discussion). More importantly, the bacterial-gold system reduced a similar amount of gold within 24 hours from both soluble gold (III) chloride and gold (I) thiosulphate (see Table 3.1). The precipitation of nanometre-size, colloidal gold and octahedral gold platelets was consistent with previous studies demonstrating the bacterial-mediated immobilisation of soluble auric chloride complexes (Lengke et al., 2006a,b). In this study, the fresh media-gold system immobilised the greatest amount of gold as irregular, nanometre-size gold colloids. These results support the importance of iron as an agent for destabilisation and reduction of soluble gold complexes discussed in Chapter 3. In this study,

ferrous iron from the fresh media-gold system was the agent responsible for the destabilisation and reduction of gold (III) chloride (Reaction 1). Furthermore, the articulated surface texture of colloidal gold precipitates (Fig. A1, b) were different from the smooth surfaces of the gold sulphide precipitates (Fig. 3.3a). In this study, I demonstrated that iron-oxidising bacteria directly affected the stability of gold (III) chloride by acting as a reducing agent forming nanometre-size colloidal gold. Furthermore, ferrous iron acted as an effective agent for gold (III) chloride reduction (Reaction A.1) similar to how ferric iron destabilised and reduced gold (I) thiosulphate (Chapter 3; Reaction 3.4-3.6). Soluble gold (III) chloride can be reduced by thiosulphate forming soluble gold (I) thiosulphate complexes (Puddephatt, 1978; Reaction A.2). Therefore, from a geochemical perspective, it is hard to imagine an oxidised, weathering environment containing iron-oxidising bacteria where chloride would be the dominant complexing ligand for gold mobility. Even at greater depths within lateritic profiles, suboxic conditions would promote increased concentrations of ferrous iron over ferric iron (Mann, 1984). Based on these findings, ferrous iron readily immobilises and reduces gold (III) chloride thereby hindering the mobility of soluble gold (III) chloride.

$$3\ FeSO_4 \bullet 7H_2O + AuCl_3 \rightarrow Fe_2(SO_4)_3 + FeCl_3 + Au^0 + 21\ H_2O \qquad (A.1)$$

$$AuCl_4^- + 3\ S_2O_3^{2-} + 2\ OH^- \rightarrow Au(S_2O_3)_2^{3-} + S^0 + SO_4^{2-} + 4\ Cl^- + H_2O \qquad (A.2)$$

## A3.4 Conclusion

Based on this study and Chapter 3, it can be concluded that the occurrence of gold (III) chloride represents a “snap shot” of the soluble auric complex. Gold (III) chloride is unstable and its existence as a soluble complex is finite and suggests that colloidal gold would predominantly occur in surface and near-surface weathering environments dominated by oxidised, acidic conditions and in the presence of bacteria.

**Table A.1** Residual soluble gold from each experimental system after 24 hours of exposure.

| **Gold immobilisation from experimental-gold systems exposed to 19.87 mM[a] gold** | |
|---|---|
| System | Concentration (mM) |
| *Entire enrichment - gold system* | 0.43 |
| *Bacterial - gold system* | 0.88 |
| *Fresh media - gold system* | 18.97 |

[a]same value for chemical controls, spent media- and iron oxide-gold system.

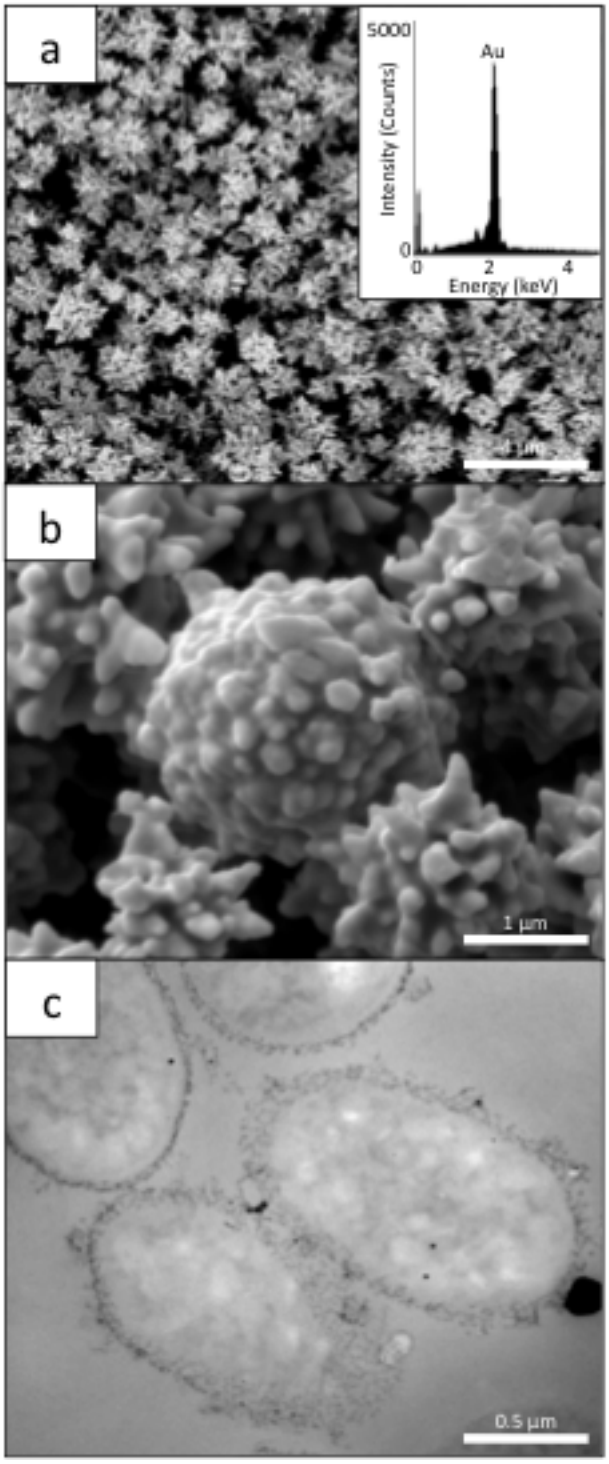


**Figure A.1. BSE-SEM characterisation of colloidal gold precipitate from a fresh media-gold system.** A low- and high-resolution backscatter SEM micrograph of the irregular-shape, colloidal gold precipitate formed in the fresh media-gold system after 24 hours of exposure (a, b). A high-resolution TEM micrograph of iron-oxidising bacteria that formed intracellular colloidal gold and extracellular pseudo-octahedral platelets from the bacterial-gold system (c).

## A3.5 References

Benedetti, M., Boulegue, J., 1991. Mechanisms of gold transfer and deposition in a supergene environment. Geochimica et Cosmochimica Acta, 55, 1539-1547.

Carey, M.L., McPhail, D.C., Taufen, P.M., 2003. Groundwater flow in playa lake environments: Impact on gold and pathfinder element distributions in groudwaters surrounding mesothermal gold deposits, St. Ives area, Eastern Goldfields, Western Australia. Geochemistry-Exploration, Environment, Analysis, 3, 57-71.

Lengke, M.F., Fleet, M.E., Southam, G., 2006a. Morphology of gold nanoparticles synthesized by filamentous cyanobacteria from gold(I)-thiosulfate and gold(III)-chloride complexes. Langmuir, 22, 2780-2787.

Lengke, M.F., Ravel, B., Fleet, M.E., Wanger, G., Gordon, R.A., Southam, G., 2006b. Mechanisms of gold bioaccumulation by filamentous cyanobacteria from gold (III)-chloride. Environmental Science and Technology, 40, 6304-6309.

Mann, A.W., 1984. Mobility of gold and silver in lateritic weathering profiles: some observations from Western Australia. Economic Geology, 79, 38-50.

Marsden, J., House, I.H., 1992. The chemistry of gold extraction. Ellis Horwood Publishing. New York. 13-58.

Puddephatt, R., 1978. The chemistry of gold. Elsevier Publishing Company. New York. 31-87.

Webster, J.G., 1985. Thiosulphate in surficial geothermal waters, North Island, New Zealand. Applied Geochemistry, 2, 5-6.

# Chapter 4

## 4 Bacteria contribute to gold grain structure and chemistry: evidence from *in situ* surface biofilms and casts

The formation of gold nuggets and grains is considered to be a dynamic process from a geochemical perspective and has been a topic of scientific debate for more than a century. Liversidge (1893) was the first to conclude that nuggets were derived from primary sources although soluble gold in groundwater systems could precipitate under surface conditions. Freise (1931) expanded on this model by suggesting that organic compounds can contribute to the formation of secondary gold. More recently, several biogeochemical studies (see below) have focused on the microbial effects on gold mobility, improving our understanding of the relationship between the biosphere and the physicochemical cycling of gold in near-surface environments.

Although gold grain sizes are not necessarily indicative of mechanical transport of gold from a primary source, grains are differentiated from nuggets by having a length less than 500 μm or a mass less than 1 g (Mann, 1984; Webster and Mann, 1984; Wilson, 1984; Hough et al., 2009). Gold grains generally exhibit increased physical alteration of their exterior surfaces, including rounded and flattened morphologies, attributed to increased flow rate and bed load within alluvial systems. Furthermore, secondary gold structures, including colloidal particles, crystalline gold and bacteriomorphic structures, are common on gold grain surfaces but are also not necessarily indicative of transport distance (Yeend, 1975; Giusti, 1986; Watterson, 1992). Previous studies have provided detailed analysis of the morphological characteristics (see Hallbauer and Utter, 1977) and the chemical composition (see Desborough, 1970; Hallbauer and Utter, 1977; Antweiler and Campbell, 1977, 1982; Giusti and Smith, 1984; Theodore et al., 1987; Mosier et al., 1989) of gold grains and how these characteristics are correlated with distances that gold was physically transported from its original source. Grant et al. (1991) demonstrated that these combined analyses had practical application to determine if grains were derived from primary or secondary sources. Variation in gold grain core chemistry is indicative of gold sources, e.g., epithermal Au-rich or Cu-rich porphyry deposits, and variations in gold grain rim chemistry is indicative of dynamic environmental geochemistry, e.g., lateritic weathering profiles (Fisher, 1945; Desborough,

1970; Giusti and Smith, 1984; Mann, 1984; Freyssinet et al., 1989; Grant et al., 1991; Townley et al., 2003; Hough et al. 2009; Larizzatti et al., 2008). Gold enrichment of grain rims is generally attributed to silver leaching (Mann, 1984; Groen et al., 1990). However, Giusti (1986) indicated that secondary gold precipitation is also possible. Studies of gold grains by Youngson and Craw (1993) identified surface crevices filled with clays and fine-grained gold suggesting "growth" of the secondary gold on grain surfaces.

The cycling of gold in the near Earth surface environment begins with primary mineralisation leading to dispersion of gold grains and soluble gold complexes, i.e., gold (III) chloride and gold (I) thiosulphate, and subsequent secondary near-surface re-concentration. Studies have indicated that Bacteria and Archaea are involved in the biogeochemical precipitation of gold (Southam and Beveridge, 1994, 1996; Southam and Saunders, 2005; Lengke and Southam, 2006, 2007; Reith and McPhail, 2006; Lengke et al., 2006a, b, 2007; Reith et al., 2006, 2007, 2009, 2011; Kenney et al., 2012).

It is reasonable that the biogeochemical interactions contributing to the immobilisation of soluble gold under a range of surface and near-surface conditions leads to enrichment of gold on the surfaces of grains and nuggets. However, the natural occurrence of bacteria on the surface of gold grains derived from a fluvial environment has not been documented. Therefore, this study integrated the analysis of natural materials and laboratory experiments to demonstrate a direct link between biogenic and secondary gold formation on gold grain surfaces within a tropical placer environment.

## 4.1 Materials and Methods

### 4.1.1 Sample acquisition and processing

A sample containing 42 g of panned heavy mineral concentrate, i.e., 0.125 mm < 0.25 mm black sand, in local river water and possessing gold grains was obtained from an open pit gravel extraction facility located along the Saldana River approximately 6 km east of Saldana, Tolima, Republic of Colombia (3° 56' 26.07" N, 74° 58' 10.09" W). Twenty-five gold grains were removed from the sample of black sand using a sterile Pasteur pipette and forceps. Twenty-four of these grains were immediately fixed with $2\%_{(aq)}$ glutaraldehyde, dehydrated in a sequential series of $25\%_{(aq)}$, $50\%_{(aq)}$, $75\%_{(aq)}$ and $3 \times 100\%$ ethanol and dried

using a Tousimis Research Corporation Samdri-PVT-3B critical point drier. All grains were coated with an osmium deposition of 3 nm using Denton Vacuum Desk II sputter coater to reduce charging effects during scanning electron microscopy.

### 4.1.2 Gold grain surface characterisation

Twelve grains were placed on Electron Microscopy Sciences aluminium stubs with 12 mm carbon adhesive tabs. Grain morphology and surface textures were characterised using a LEO (Ziess) 1540XB Field Emission Gun-Scanning Electron Microscope (FEG-SEM) equipped with a Focused Ion Beam (FIB) and an Oxford Instruments' INCAx-sight Energy Dispersive Spectrometer (EDS). An accelerating voltage of 3 or 10 kV was used for surface imaging and qualitative elemental composition, respectively. The long axis, perpendicular short axis and thickness of each grain were measured.

### 4.1.3 Gold grain cross-sections

Eleven grains were embedded in Epon plastic and sectioned by polishing to approximately half thickness for characterisation of cross-sections using Backscatter Electron (BSE) scanning electron microscopy. One gold grain, previously used for surface characterization (see section 4.1.2), was partially sectioned using the FIB to obtain a 10 μm long and 5 μm deep trough, cross-section from the grain surface and analysed using the same FEG-SEM.

### 4.1.4 Synchrotron-based spectroscopy and elemental mapping

One additional grain, from a separate Epon plastic embedding was cut to approximately half the thickness and fine polished using the FIB to obtain a surface topography less than 10 nm. Prior to synchrotron-based elemental mapping, the grain was imaged using the FEG-SEM. Maps of gold, silver and copper distributions were obtained from the Insertion Device beamline of the Pacific Northwest Consortium/X-ray Science Division (PNC-XSD) Sector 20 at the Advanced Photon Source, Argonne National Laboratory, Illinois, USA. Elemental maps were analysed using National Instruments$^{TM}$ LabVIEW$^{TH}$ 2-D Scan Plot v. 4. Gold, silver and copper detection was confirmed by X-ray emission spectra analysed using National Instruments$^{TM}$ LabVIEW$^{TH}$ 1-D Scan Plot v. 4 and compared to values from Thompson et al. (2009).

### 4.1.5 Bacterial culturing

An enrichment of naturally occurring bacteria was cultured by placing a recovered gold grain into 5 mL of Difco™ R2B general-purpose bacterial growth medium. The bacterial enrichment was incubated at room temperature (RT, approx. 22˚C) for two weeks in a Fisherbrand® 13 × 100 mm borosilicate glass tube with a sterile, plastic push cap. The enrichment was then streak-plated onto Difco™ R2A plates and incubated at RT for an additional three weeks to determine whether or not a pure or dominant bacterial enrichment was present in the test tube.

### 4.1.6 Bacterial phylogeny determination

The bacterial isolate was identified using 16*S* ribosomal DNA sequencing. For this identification, a single colony representing the dominant phenotype, grown on R2A (described above), was suspended in 1 mL of distilled, deionised water. This suspension was diluted by adding 1 μL of bacterial suspension into a solution containing 43 μL of distilled, deionised water and 3 μL each of canonical 16*S* sequencing primers 27f (5'-GAGTTTGATCCTGGCTCAG-3') and 1525r (5'- AGAAAGGAGGTGATCCAGCC-3'). Agarose gel electrophoresis verified the production of 1.5 kb bands from this Polymerase Chain Reaction (PCR) reaction, which was subsequently purified using Qiagen QIAquick PCR Purification kit and sent for nucleotide sequencing using the 27f and 1525r primers to McMaster Institute for Molecular Biology and Biotechnology, Ontario, Canada. The identity of the bacterial isolate was assessed by running the 16*S* rDNA sequence through Basic Local Alignment Search Tool (BLAST).

### 4.1.7 Bacterial-gold experiments

Twenty bacterial colonies from the pure bacterial enrichment, grown on R2A plates, were pooled in 20 mL of filter sterilised, i.e., 0.1 μm pore-size filter, deionised water to obtain a population of approximately $10^9$ bacteria/mL using a Petroff-Hauser counting chamber. One mL aliquots of this suspension were centrifuged for 1 min. at 12,000 *g*, forming a bacterial pellet and the supernatant was discarded. A 5.5 mM aqueous, filter sterilised, gold stock solution, i.e., Alfa Aesar, $HAuCl_4 \cdot 3H_2O$, was added to each bacterial pellet, forming replicate bacterial-gold systems that were mixed by vortex to disperse bacteria within the gold

solution. Triplicate bacterial-gold systems were exposed to gold for 1, 3, 6, 12 and 24 hours at RT. All bacterial-gold system were wrapped in aluminium foil to prevent photocatalytic effects. After exposure, each bacterial-gold system was passed through a 0.1 μm pore-size filter to arrest the immobilisation of gold by removing the bacteria. The filtered solution was acidified using concentrated (71%) nitric acid and analysed for soluble gold using a Perkin-Elmer Optima 3300-DV Inductively Coupled Plasma-Atomic Emission Spectrometer (ICP-AES).

Two filtrate samples from bacterial-gold systems exposed to 5.5 mM gold for 24 hours were washed three times with filter sterilised, deionised water, then centrifuged to discard the supernatant. After the final wash, one sample was collected on a new filter and prepared for SEM-EDS analysis using the same method described for gold grain surface characterisation (4.1.2). The second sample was centrifuged and the final supernatant was discarded. The remaining pellet was then fixed by adding 1 mL of $2\%_{(aq)}$ glutaraldehyde to the Eppendorf tube, homogenised by vortex and incubated at RT for 2 hour. After fixation, the bacterial suspension was re-centrifuged and the pellet was enrobed in $2\%_{(wt/vol)}$ noble agar, dehydrated using a $25\%_{(aq)}$, $50\%_{(aq)}$, $75\%_{(aq)}$ and $3 \times 100\%$ acetone series and embedded in Epon plastic and cured at 60°C for 48 hr. The embedded bacteria were trimmed and cut into 70 nm ultrathin sections using a Reichert-Jung Ultracut E ultramicrotome, placed on Electron Microscopy Sciences formvar-carbon coated 100-mesh copper grid and examined using a Phillips CM-10 Transmission Electron Microscope (TEM) operating at 80 kV.

## 4.2 Results

### 4.2.1 Gold grain surface characterisation

Three general gold grain morphologies were observed; semi-discoid ellipse, discoid ellipse, and stacked discoid ellipse grains (Fig. 4.1). The length, width and height of all grains averaged $193.5 \pm 42.1$ μm $\times$ $145.5 \pm 30.2$ μm $\times$ $23.7 \pm 3.9$ μm, respectively. The surface of semi-discoid ellipse grains had many concave crevices in comparison to the other two morphologies, which were flat with smooth, planar surfaces and crevices primarily occurring on the narrow, circumferential edge.

Detrital sedimentary material, containing carbon, oxygen, iron, sodium, aluminium, silica and sulphur, occurred within crevices and between stacked grains (Fig. 4.2a-c). Individual rod-shaped bacteria and biofilms were attached to gold and sedimentary material surfaces (Fig. 4.2a, b, d, e). The extracellular surface of some bacteria associated with the sedimentary material contained nanometre-size colloidal gold (Fig. 4.2e, f).

One gold grain was coated in iron oxyhydroxide (Fig. 4.3a). BSE-SEM imaging indicated that the iron oxide coating had varying thickness and EDS analysis confirmed that the coating also contained carbon, sodium and silicon. The thinnest coating consisted of a "patina" texture with missing angular patches revealing the gold-rich grain surface underneath (Fig. 4.3b, c). The patina texture gradually transitioned to a thicker coating consisting of clustered iron colloids ranging from approximately 200 nm to 4 μm in diameter with organic material occurring in between individual colloids (Fig. 4.3d). Clusters of bacterial casts (Fig. 4.3e, f) were observed throughout the iron oxide coating that transitioned from the patina to the colloidal texture.

### 4.2.2 Gold grain cross-sections

All polished cross-sections of the embedded grains had a solid core (see section 4.2.3) and void spaces occurring primarily within a depth of 10 μm from the outer surface (Fig. 4.4a). A possible bacterial cast in gold, similar to the iron oxide patina, was also observed at the grain surface (Fig. 4.4b, c).

The FIB-sectioned grain had nanometre-size to micrometre-size globular voids distributed within 5 μm of the grain edge. Some voids appeared empty whereas other were either completely filled or lined with carbon (Fig. 4.5b). EDS analysis confirmed the presence of carbon with voids surrounded by a gold, silver and copper matrix (Fig. 4.5c, d).

### 4.2.3 Elemental mapping of gold grain cross-section

BSE-SEM analysis of the FIB-polished gold grain revealed a solid interior with undulating banded textures (Fig. 4.6). Nanometre-size to micrometre-size bands were composed of gold, copper and silver. Band size diminished from micrometre-size near the core to

nanometre-size within 20 μm from the grain edge. Micrometre- to nanometre-size voids were distributed throughout the outer 10 μm periphery of the grains.

Analysis of X-ray emission spectra confirmed the presence of copper and silver within the grain (Fig. 4.6). Excitation energy of 11,800 eV was used to prevent oversaturation by the gold signal, allowing the detection of copper and silver. Elemental mapping demonstrated that gold was distributed throughout the grain with greater abundance at the outer surface. Greater copper and silver concentrations occurred in the core and were associated with larger bands and gradually decreased towards the edge.

### 4.2.4 Bacterial culturing and phylogeny determination

The appearance of bacterial growth, e.g., turbidity, from the gold grain inoculated in R2B liquid medium, occurred after two weeks of incubation at RT. When the enriched culture was streak-plated onto R2A plates, only one bacterial colony type appeared after three weeks incubation at RT. Phylogenetic identification determined the bacterial isolate was *Nitrobacter* sp. 263.

### 4.2.5 *Nitrobacter* sp. 263-gold experiments

The supernatant of the bacterial-gold system exposed for 24 hours appeared less yellow in comparison to the shorter time points and the initial gold stock solution. Metallic gold was observed in all bacterial-gold systems when the pellet was centrifuged. Chemical analysis of the bacterial-gold experiments indicated that the amount of gold immobilisation by *Nitrobacter* sp. 263 increased with time (Fig. 4.7a).

SEM imaging demonstrated that *Nitrobacter* sp. 263 was rod-shaped (Fig. 4.7b) and similar to naturally occurring bacteria containing gold colloids observed on the gold grain surface (see Fig. 4.2e). Interestingly, when exposed to 5.5 mM gold for 24 hours, some bacterial cells were completely mineralised and others were not. These findings were consistent with studies exposing *Ralstonia metallidurans* to gold (III) chloride performed by Reith et al., (2006). Transmission electron microscopy of the bacterial-gold system exposed to gold for 24 hours confirmed that extensive extracellular gold mineralisation occurred in approx. 0.1% of the bacterial population. Unfortunately, the structure of the cell envelope could not be

observed in any of these extensively mineralised cells. Gold was immobilised as varying sized colloids and octahedral platelets less than 100 nm by *Nitrobacter* sp. 263 (Fig. 4.7b).

## 4.3 Discussion

Grain morphologies in the Rio Saldana sediment are similar to flat and rounded grains characterised by Yeend (1975) and Giusti (1986). The discoid-elliptical appearance and stacked structure of multiple grains is likely attributed to mechanical reshaping and accumulation within the host sediment. The presence of greater crevices on semi-discoid ellipse grains (Fig. 4.1a) suggests a lesser degree of physical reshaping in comparison to the other morphologies (Fig. 4.1b, c) and could be correlated to the distance that grains had been mechanically transported from a source. Crevices enhance the accumulation of detritus, e.g., clay-size aluminosilicates or clays, and naturally occurring bacteria derived from the fluvial environment (Fig. 4.2a-c). Murr and Berry (1976) demonstrated that bacteria selectively attach to different mineral surfaces. This study was the first to demonstrate, using SEM images, the attachment of naturally occurring bacteria to the surface of gold grains. The direct attachment of individual bacteria on gold surfaces (Fig. 4.2d) and biofilms attached to sedimentary material within crevices (Fig. 4.2e) are important observations. The presence of more developed biofilms on the detrital materials suggests preferential bacterial attachment to these "non-gold" substrates. Metabolically active bacteria attached to regions subject to less physical weathering, i.e., "hiding in the crevices", would develop into biofilms with greater structural integrity.

Precipitation of iron oxide patina and colloidal textures on the grain surface can be attributed to diagenetic conditions in the river (Fig. 4.3a-d). Alternatively, precipitation could also be attributed to the oxidation of ferrous iron by chemolithotrophic, iron-oxidising bacteria (Emerson and Weiss, 2004; Emerson and Floyd, 2005), indicated by the iron-rich casts. However, gold grains placed in lithoautotrophic, modified media defined by Silverman and Lundgren (1959) did not enrich the growth of iron-oxidising bacteria. Therefore, the presence of bacterial casts and iron were likely remnants of past bacteria and iron sulphides that were weathered as the gold grain was release from the hypogene material. The primary significance of iron oxide in this study was that it acted as, and preserved, a matrix in which bacteria were either completely or partially encased. Although bacteria were not observed in

the iron oxide casts, EDS detection of carbon may represent residual material from pre-existing bacteria (Fig. 4.3e, f).

Scanning electron microscopy of grain cross-sections reveals two crystalline textures composed of gold, copper and silver: micrometre-size bands located within the grain core and nanometre-size bands occurring within 20 μm from the grain perimeter (Fig. 4.4a). The polymorphic textures and secondary enrichment of "pure" gold at the periphery of grains are consistent with observations of gold grains from Flinders Ranges, South Australian and New Zealand by Fairbrother et al. (2012) and Reith et al., (2012), respectively. The greater concentrations of copper and silver within the core suggest preferential leaching of copper and silver during biogeochemical weathering (Desborough, 1970; Desborough et al., 1970; Boyle, 1979) and contributed in part to gold enrichment around the grain perimeter. Specifically, the release of copper at the grain perimeter could directly contribute to copper-catalysed thiosulphate leaching, leading to dissolution of gold grains (Langhans et al., 1992; Aylmore and Muir, 2001). It is important to note that Rio Saldana is located approx. 100 km south east of the Middle Cauca Belt, which contains gold-rich porphyry deposits and gold-rich porphyry copper deposits (Sillitoe, 2008; Tassinari et al., 2008). The weight percent ratios of gold:copper:silver (15:6:1) from Rio Saldana grain cores correspond to Townley et al.'s (2003) compositional analysis that discriminated between different primary sources. The distal sample location, in accordance with the detection and mapping of heterogeneously distributed gold, copper and lesser silver, demonstrated that grains were originally derived from a weathered gold-rich porphyry copper source (Kesler et al., 2002; Bonev et al., 2002; Townley et al., 2003; Sillitoe, 2008; Tassinari et al., 2008; Hough et al., 2009). Therefore, physical and chemical characterisation of fluvial derived gold grains and the release of Cu and Ag can potentially be used as a means for exploration targets.

The presence of micrometre- to nanometre-size void spaces occurring along the outer 10 μm of the grain perimeter was consistent in all grain cross-sections (Figs. 4.4a, 4.5a-c) and corresponded with the porous textures observed on the grain surface (see Fig. 4.2a, arrow). The porous grain edge containing a bacterial-size void (Fig. 4.5b, c) was analogous to the bacterial casts observed in the iron oxide coating (Fig. 4.3e, f) and demonstrates that a bacterium can become entombed within the surrounding gold matrix. The occurrence of this gold-entombed bacterium may relate to the small, sub-population of bacteria that could

become completely mineralised with gold in the laboratory experiment. It is important to note that *Nitrobacter* is a genus of nitrifying bacteria commonly found in freshwater environments (Painter, 1970; Cebron and Garnier, 2005) and is known to survive under metal stressed environments (Starkenburg et al., 2008). Studies by Johnston et al. (2013) indicated that bacteria, capable of surviving in metal stressed environments, produce secondary metabolites to reduce soluble gold as a mode of protection against gold toxicity. The small percentage of the bacterial population that was completely mineralised might suggest that Nitrobacter sp. 263 may have the ability to produce secondary metabolites and survive in metal-stressed environments.

The FIB section confirmed a porous surface texture and the presence of nanometre- to micrometre-size void spaces within 5 μm from the grain surface. The horizontal distribution of carbon-filled voids was parallel to the grain surface and could be interpreted as remnants of attached biofilms that eventually became entombed within the gold matrix, analogous to the bacterial void observed in Fig. 4.5b. It is reasonable to suggest that empty voids may have also been bacterial casts but were somewhat distorted through mechanical reshaping.

Biofilms within crevices demonstrate the precipitation or adsorption of extracellular, nanometre-size gold colloids (Fig. 4.2e) and suggest that these cells were either actively immobilising gold from soluble gold complexes, e.g., derived from the environment or from the gold released from copper-catalyzed thiosulfate leaching, or that they were adsorbing colloidal gold from the environment. Both modes of microbial interaction with gold, i.e., gold grain "growth" phase, are critical for counter balancing the loss of gold through dissolution. The interpreted occurrence of *Nitrobacter* sp. 263 directly on the grain surfaces (Fig. 4.2e, f) may indicate that they are cycling gold by promoting dissolution and re-precipitation processes. The precipitation of gold colloids within detritus-filled crevices is consistent with the observations by Youngson and Craw (1993); however, in this study, secondary gold was directly associated with organics.

Gold (III) chloride is an important water-soluble gold complex found in natural systems (Puddephatt, 1978; Mann, 1984; Webster, 1985). When soluble gold was added to *Nitrobacter* sp. 263, this natural bacterial species contributed to gold biogeochemical cycling by reducing gold. Unlike previous studies involving bacterial exposures to gold (III) chloride

(Southam and Beveridge, 1994, 1996; Lengke et al., 2006ab, 2007), *Nitrobacter* sp. 263 primarily immobilised gold extracellularly as colloids and octahedral platelets less than 150 nm in size (Fig. 4.7bc) and were very different relative to bacteriomorphic gold structures found on grains from previous studies (Yeend, 1975; Hallbauer and Utter, 1977; Giusti, 1986; Watterson, 1992). Although the secondary gold structures observed in this study are larger in comparison to the colloids observed on the natural biofilm (Fig.4.2e), the increased size can be attributed to the high gold (III) chloride concentration used in the laboratory experiment. Interestingly, some bacterial cells in the *Nitrobacter*-gold experiments demonstrated gold colloid precipitation while others did not thereby highlighting the ability of these bacteria to persist in environment containing high concentrations of soluble metals. These same secondary gold structures were observed on the naturally occurring biofilms in the crevices of these gold grains. This demonstrates that a bacterium recovered from the surface of a gold grain is capable of immobilising soluble gold and precipitating the secondary gold structures commonly observed at the surface of gold grains. This may explain the enrichment of gold at gold grain surfaces. In Rio Saldana, geochemical weathering dissolves copper, silver and gold; however, subsequent biological immobilisation of the soluble gold produces the high purity secondary gold rims.

## 4.4 Conclusion

The biogeochemical cycling of gold is a dynamic process in near-surface environments and therefore requires a multi-analytical approach to "fingerprint" gold occurrences. In this study, I characterised the structure and chemical composition of gold grains using: scanning and transmission electron microscopy, FIB sectioning, synchrotron-based elemental mapping, and laboratory bacterial-gold experiments. The "journey" of gold grains from Rio Saldana originated from gold-rich porphyry copper sources. Although physical weathering of the primary gold source leads to the distribution of grains within the fluvial system, bacteria contributed to secondary gold enrichment on gold grain surfaces. This multi-analytical approach not only highlights a potential method for discovering economically significant gold sources but also provides an additional perspective on secondary gold enrichment within placer deposits. Therefore, these results contributed to the understanding of the biosphere's influence on gold cycling in a tropical environment.

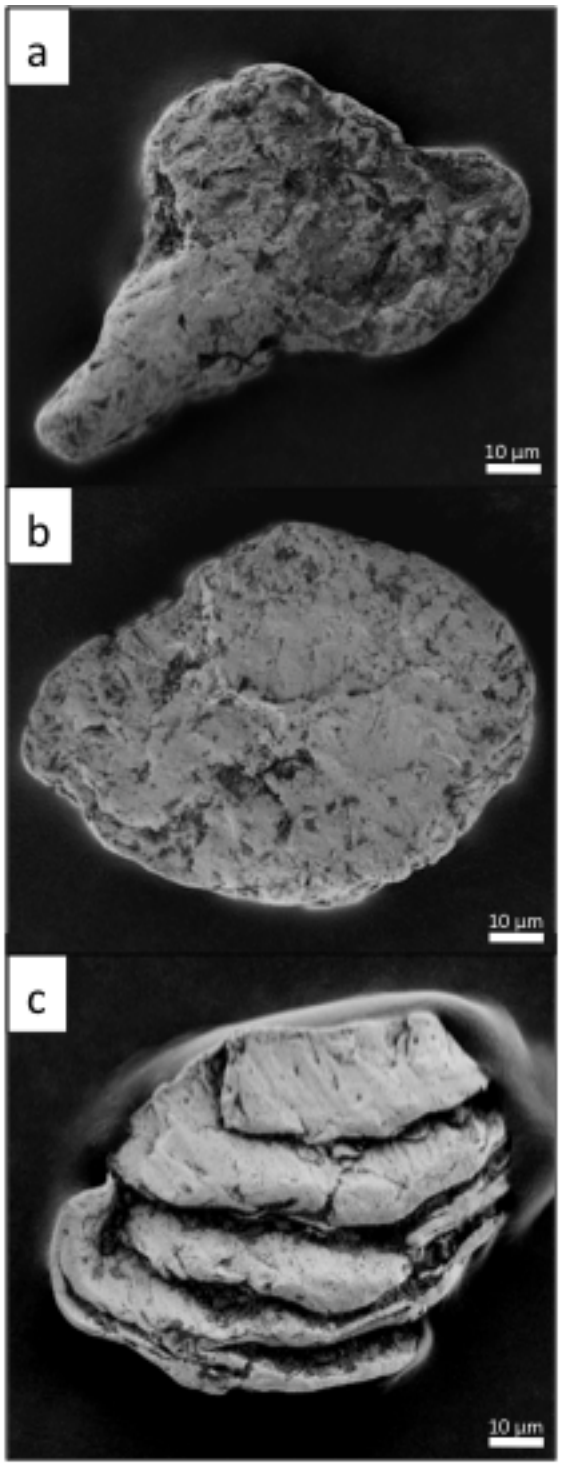


**Figure 4.1. SEM characterisation of Rio Saldana gold grains.** Low-magnification SEM micrographs of the three representative gold grain morphologies. Grains that appeared as semi-discoid ellipses had the greatest surface topography including irregular concave crevices and convex ridges (a). Discoid ellipse grains were flatter with smoother surfaces in comparison to the semi-discoid ellipse grains (b). Stacked discoid ellipses were composed of multiple grains of varying size (c).

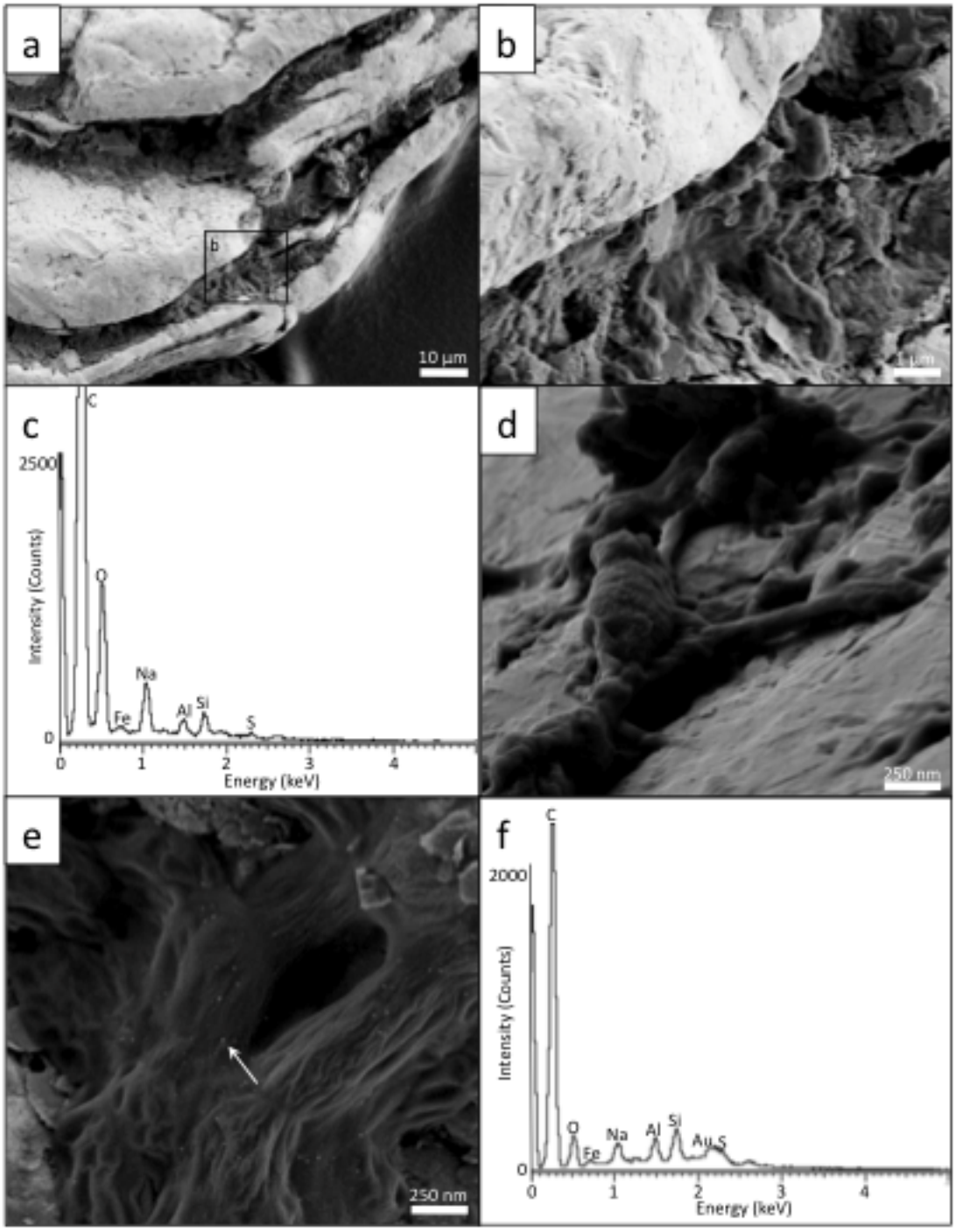


**Figure 4.2. SEM-EDS characterisation of grain surfaces.** High-resolution SEM micrographs of grain surfaces. Detrital material occurred within crevices and between stacked discoid ellipse gold grains (a, b) and was composed of C, O, Fe, Na, Al, Si and S based on EDS analysis (c). Some bacteria appeared directly attached to gold surfaces by extracellular polymeric substances (d) whereas others occurred as biofilms (b, e). Nanometre-size gold colloids (e, arrow), determined using EDS, were attached to the extracellular surface of some bacteria within these sediment-filled crevices (f).

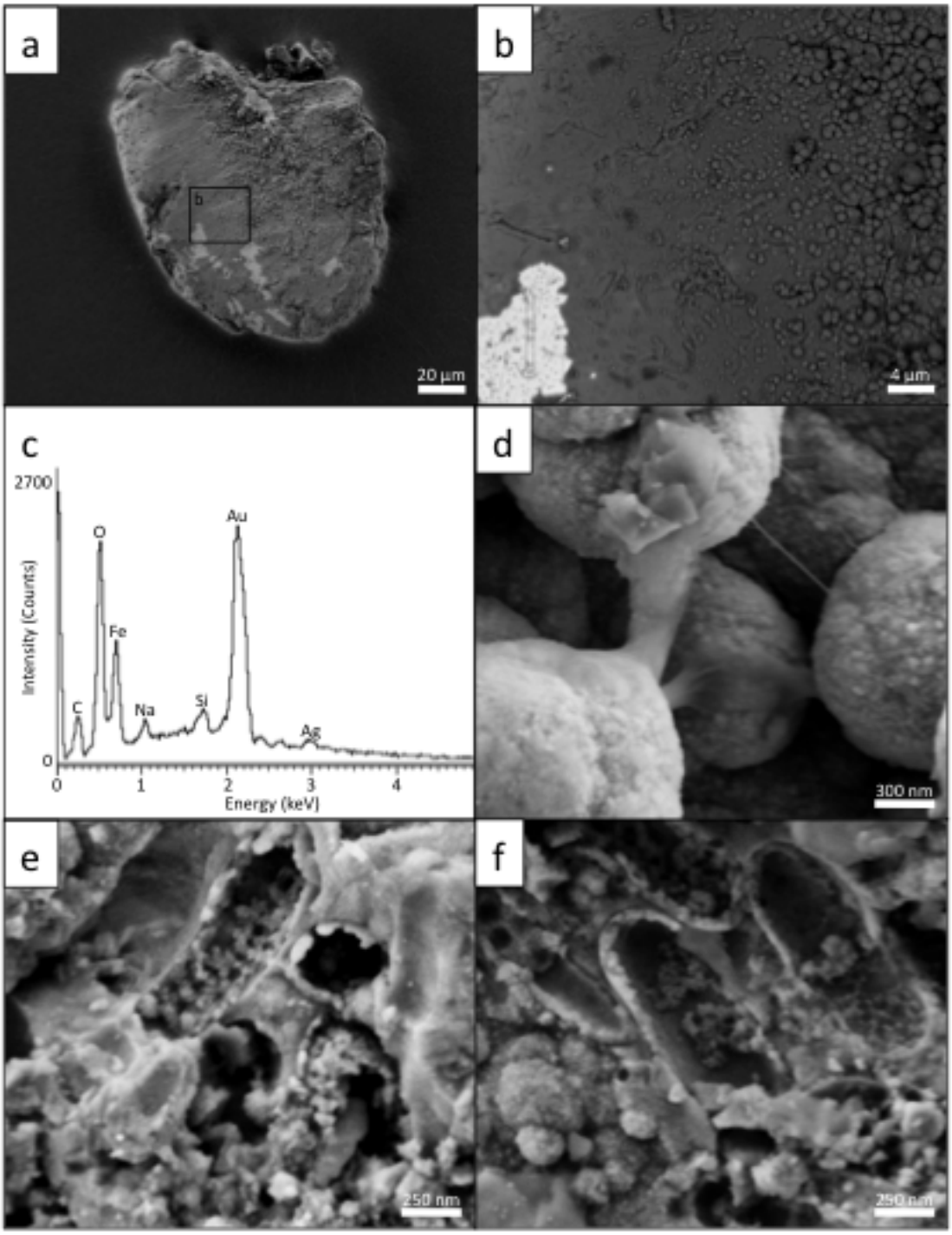


**Figure 4.3. SEM-EDS characterisation of an iron-coated gold grain.** SEM micrographs of a gold grain coated with iron oxide; parts of the "patina" appear to have broken off on the lower left side of grain allowing the gold grain to show through (a). A BSE-SEM micrograph differentiating gold from Fe and demonstrating the relative thickness of the iron oxide coating with laminate and colloidal textures (b). Detection of C, Na, Si, Cl and Si were associated with Fe, O and gold (c). A high-resolution SEM micrograph of organic material in between iron colloids (d) and clusters of bacterial casts with random orientation (e, f).

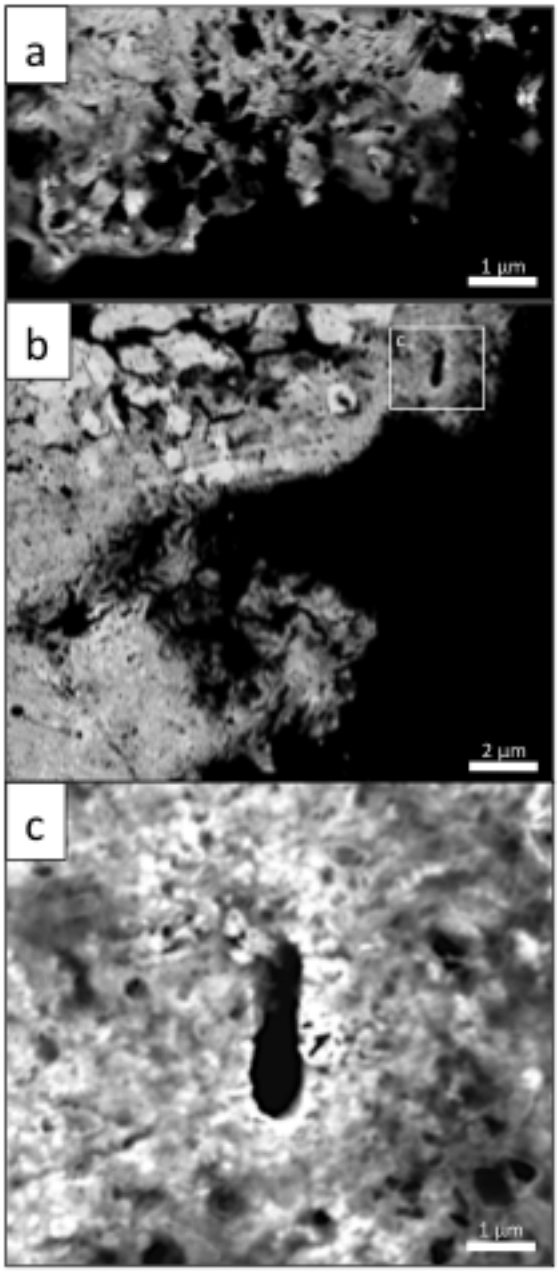


**Figure 4.4. BSE-SEM characterisation of a bacterial cast in gold.** High-resolution BSE-SEM micrograph of the outer edge of polished gold grains confirming the porous textures (a). Within the porous gold texture, a cross-section of a bacterial cast was observed (b, c).

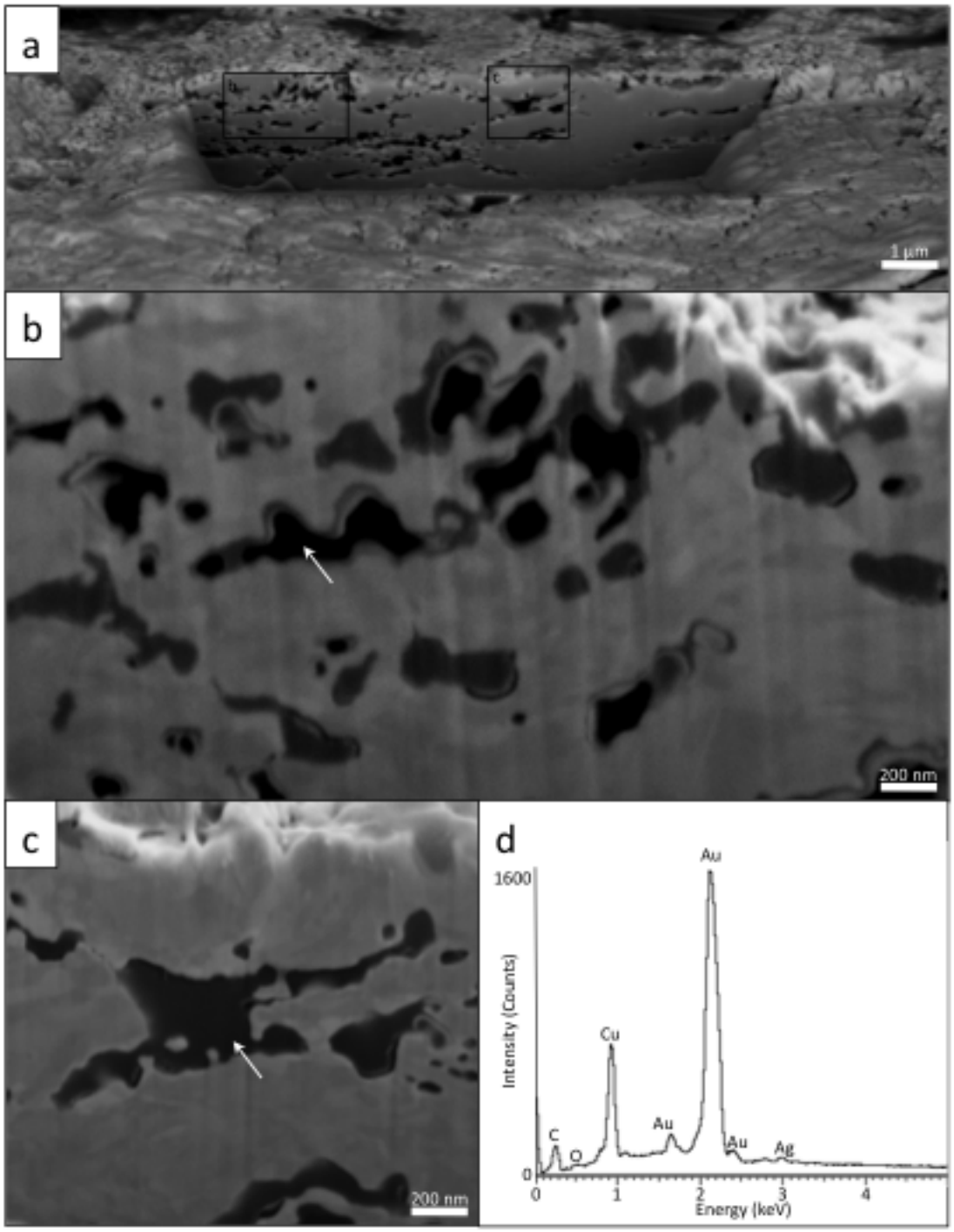


**Figure 4.5. SEM-EDS characterisation of a FIB milled gold grain surface.** High-resolution SEM micrographs of a FIB milled trough showing a 10 µm × 5 µm face that is perpendicular to the outer surface of the grain (a). Nanometre-size to micrometre-size globular voids appeared horizontally distributed and occurred mainly within the first 3 µm from the outer surface. Void spaces were either empty or contained amorphous material (b, c arrows). Energy dispersive spectroscopy indicated that amorphous material was composed of C and O and the surround gold 'matrix' contained Cu and Ag (d).

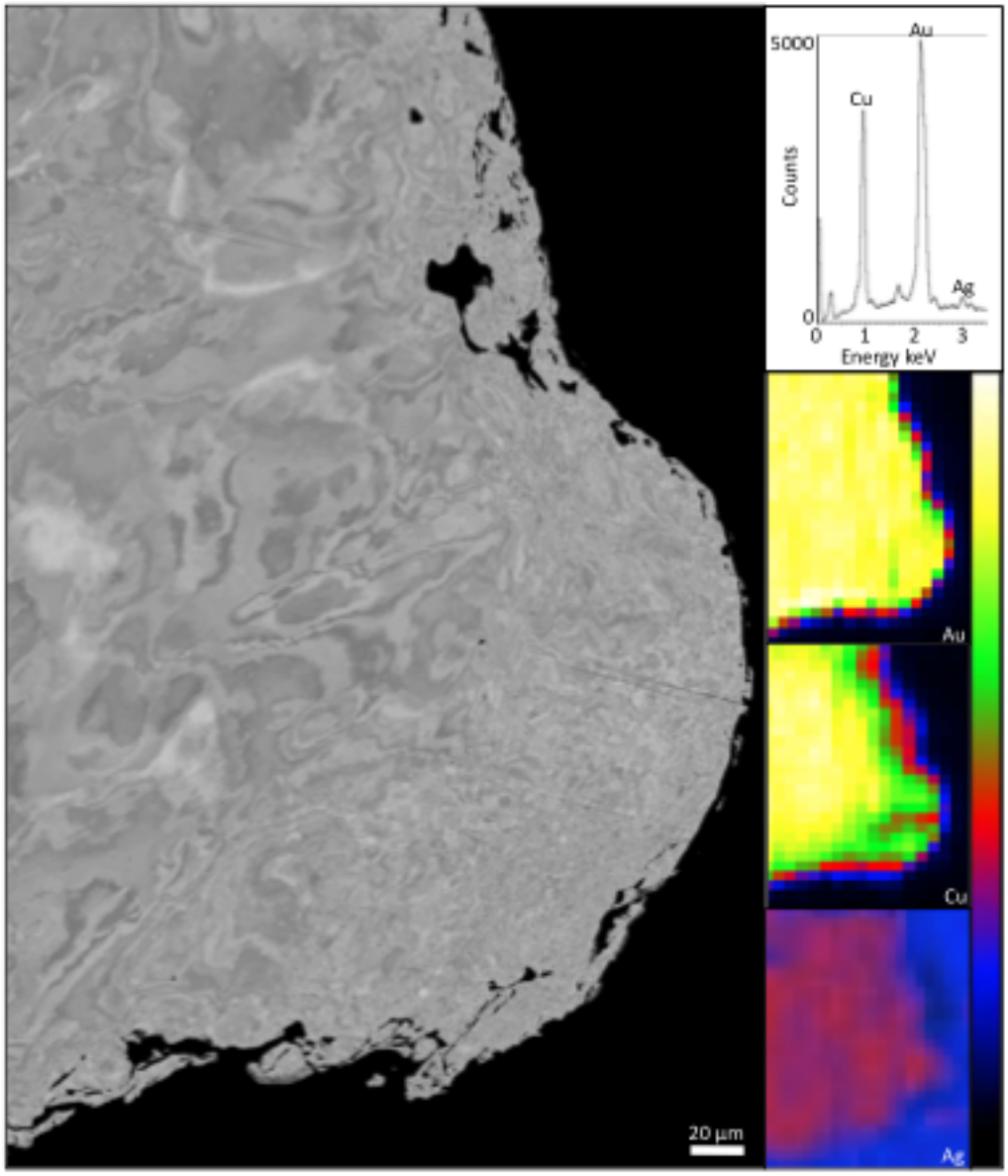


**Figure 4.6. BSE-SEM characterisation of a FIB-etched gold grain and synchrotron-generated x-ray emission spectra elemental maps.** High-resolution SEM micrograph of the FIB-etched gold grain demonstrating micrometre-size polymorphic banding texture within the grain core and nanometre-size polymorphic banding texture along the grain perimeter. A synchrotron-generated X-ray emission spectrum indicating both copper and silver associated with gold in a region containing both banding textures. Elemental mapping demonstrated that gold was enriched around the perimeter while copper was most abundant in the grain core. The scale represents a qualitative representation of each element relative to the highest detection limit (white) to the background with no detection (black). Note that no silver detection (blue) was recalibrated to allow grain identification from the background.

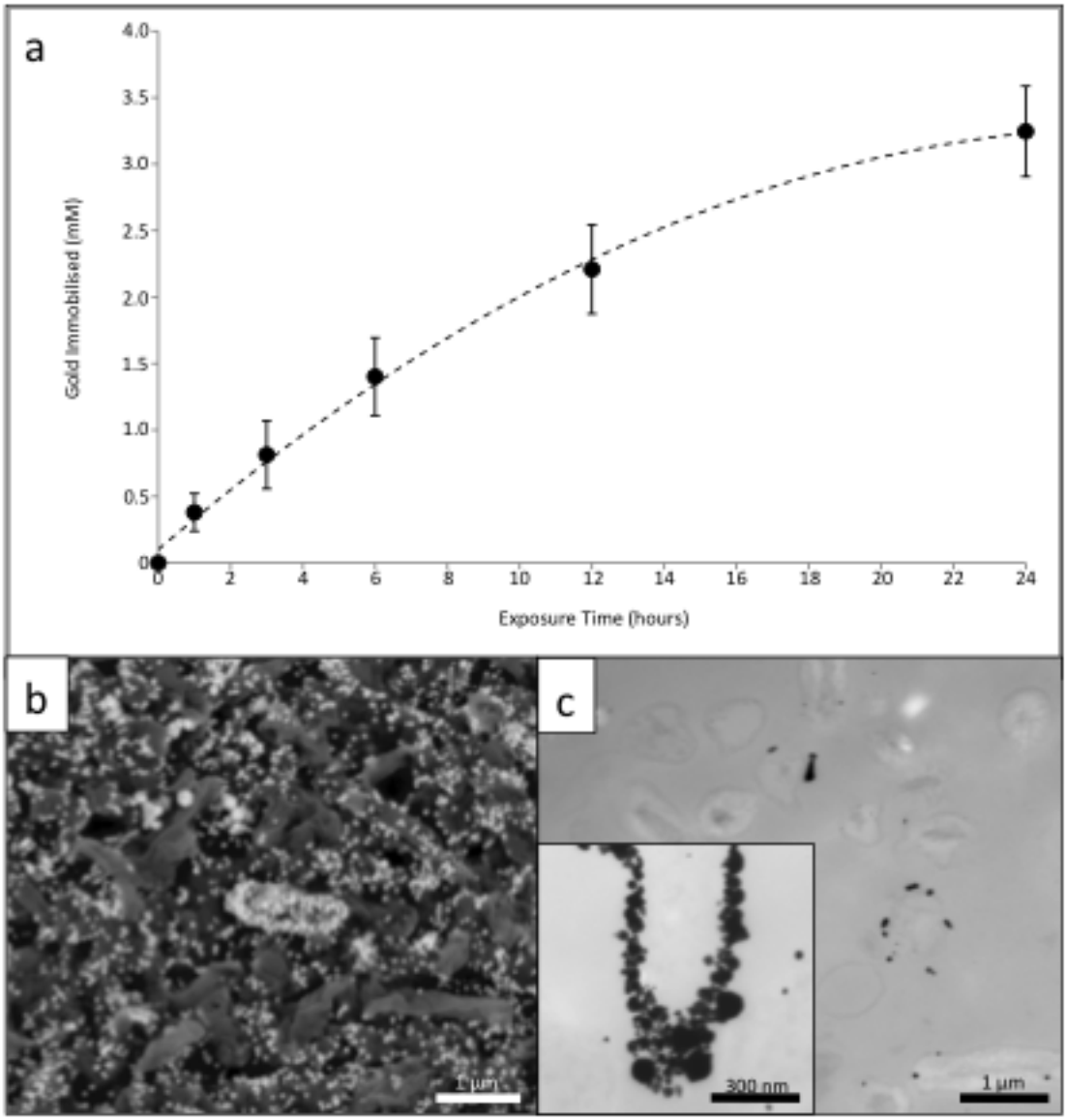


**Figure 4.7. ICP-AES and SEM characterisation of gold immobilisation by *Nitrobacter*.** Gold immobilisation versus time by *Nitrobacter* sp. 263 (a). A low-resolution SEM micrograph of *Nitrobacter* sp. 263 exposed to gold (III) chloride for 24 hours. Some bacteria appeared more extensively mineralised with gold in comparison to others (b). High-resolution TEM micrograph of the same bacterial-gold system highlighting minimally and extensively mineralised cells. Precipitation of gold colloids and octahedral platelets less than 100 nm in size was extracellularly and association with the cell envelope (c).

## 4.5 References

Antweiler, J.C., Campbell, W.L., 1977. Application of gold compositional analyses to mineral exploration in the United States. Journal of Geochemical Exploration, 8, 17-29.

Antweiler, J.C., Campbell, W.L., 1982. Gold in exploration geochemistry. In: Precious Metals in the Northern Cordillera. The Association of Exploration Geochemists, Calgary, 33-44.

Aylmore, M.G., Muir, D.M., 2001. Thiosulfate leaching of gold-a review. Minerals Engineering, 14, 135-174.

Bonev, I.K., Kerestedjian, T., Atanassova, R., Andrew, C.J., 2002. Morphogenesis and composition of native gold in the Chelopech volcanic-hosted Au-Cu epithermal deposit, Srednogorie zone, Bulgaria. Mineralium Deposita, 37, 614-629.

Boyle, R.W., 1979. The geochemistry of gold and its deposits. Geological Survey of Canada Bulletin, 280, 584.

Cebron, A., Garnier, J., 2005. Nitrobacter and Nitrospira genera as representatives of nitrite-oxidizing bacteria: Detection, quantification and growth along the lower Seine River (France). Water Research, 39, 4979-4992.

Desborough, G.A., 1970. Silver depletion indicated by microanalysis of gold from placer occurrences, western United States. Economic Geology, 65, 304-311.

Desborough, G.A., Raymond, W.H., Iagmin, P.J., 1970. Distribution of silver and copper in placer gold derived from the northeastern part of the Colorado Mineral Belt. Economic Geology, 65, 937-944.

Emerson, D., Weiss, J.V., 2004. Bacterial iron oxidation in circumneutral freshwater habitat: findings from the field and the laboratory. Geomicrobiology, 21, 405-414.

Emerson, D., Floyd, M.M., 2005. Enrichment and isolation of iron-oxidizing bacteria at neutral pH. Methods in Enzymology, 397, 112-123.

Fairbrother, L., Brugger, J., Shapter, J., Laird, J.S., Southam, G., Reith, F., 2012. Supergene gold transformation: Biogenic secondary and nano-particulate gold from arid Australia. Chemical Geology, 320, 17-31.

Fisher, N.H., 1945. The fineness of gold, with special reference to the Morobe goldfield, New Guinea. Economic Geology, 40, 449-495.

Freise, F.W., 1931. The transportation of gold by organic underground solutions. Economic Geology, 26, 421-431.

Freyssinet, P., Zeegers, H., Tardy, Y., 1989. Morphology and geochemistry of gold grains in lateritic profiles of Southern Mali. Journal of Geochemical Exploration, 32, 17-31.

Giusti, L., Smith, D.G.W., 1984. An electron microprobe study of some Alberta placer gold. Tschermaks Mineralogische und Petrographische Mitteilungen, 32, 187-202.

Giusti, L., 1986. The morphology, mineralogy, and behaviour of “fine-grained” gold from placer deposits of Alberta: Sampling and implications for exploration. Canadian Journal of Earth Science, 23, 1662-1672.

Grant, A.H., Lavin, O.P., Nichol, I., 1991. The morphology and chemistry of transported gold grains as an exploration tool. Journal of Geochemical Exploration, 40, 73-94.

Groen, J.C., Craig, J.R., Rimstidt, J.D., 1990. Gold-rich rim formation on electrum grains in placers. Canadian Mineralogist, 28, 207-228.

Hallbauer, D.K., Utter, T., 1977. Geochemical and morphological characteristics of gold particles from recent river deposits and the fossil placers of the Witwatersrand. Mineralium Deposita, 12, 293-306.

Hough, R.M., Butt, C.R.M., Fischer-Buhner, J., 2009. The crystallography, metallography and composition of gold. Elements, 5, 297-302.

Johnston, C.W., Wyatt, M.A., Li, X., Ibrahim, A., Shuster, J., Southam, G., Magarvey, N.A., 2013. Gold biomineralisation by a metallophore from gold-associated microbe. Nature Chemical Biology, 9, 241-243.

Kenney, J.P.L., Song, Z., Bunker, B.A., Fein, J.B., 2012. An experimental study of Au removal from solution by non-metabolizing bacterial cells and their exudates. Geochimica et Cosmochimica Acta, 87, 51-60.

Kesler, S.E., Chryssoulis, S.L., Simon, G., 2002. Gold in porphyry copper deposits: its abundance and fate. Ore Geology Reviews, 21, 103-124.

Langhans, J.W., Lei, K.P.V., Carnahan, T.G., 1992. Copper-catalyzed thiosulfate leaching of low-grade gold ores. Hydrometallurgy, 29, 191-203.

Larizzatti, J.H., Oliveira, S.M.B., Butt, C.R.M., 2008. Morphology and composition of gold in a lateritic profile, Fazenda Pison "Garimpo", Amazon, Brazil. Journal of South American Earth Sciences, 25, 359-376.

Lengke, M.F., Southam, G., 2006. The bioaccumulation of gold by thiosulfate-reducing bacteria cultured in the presence of gold-thiosulfate complex. Geochimica et Cosmochimica Acta, 70, 3646-3661.

Lengke, M.F., Southam, G., 2007. The role of bacteria in the accumulation of gold: Implications for placer gold formation and supergene gold enrichment. Economic Geology, 102, 109-126.

Lengke, M.F., Fleet, M.E., Southam, G., 2006a. Morphology of gold nanoparticles synthesized by filamentous cyanobacteria from gold(I)-thiosulfate and gold(III)-chloride complexes. Langmuir, 22, 2780-2787.

Lengke, M.F., Ravel, B., Fleet, M.E., Wanger, G., Gordon, R.A., Southam, G., 2006b. Mechanisms of gold bioaccumulation by filamentous cyanobacteria from gold (III)-chloride. Environmental Science and Technology, 40, 6304-6309.

Lengke, M.F., Ravel, B., Fleet, M.E., Wanger, G., Gordon, R.A., Southam, G., 2007. Precipitation of gold by reaction of aqueous gold(III)-chloride with cyanobacteria at 25-80°C – Studied by X-ray absorption spectroscopy. Canadian Journal of Chemistry, 85,1-9.

Liversidge, A., 1893. On the origin of gold nuggets. Journal and Proceedings of the Royal Society of New South Wales, 27, 303-343.

Mann, A.W., 1984. Mobility of gold and silver in lateritic weathering profiles: Some observations from Western Australia. Economic Geology, 79, 38-50.

Mosier, E.L., Cathrall, J.B., Antweiler, J.C., Tripp, R.B., 1989. Geochemistry of placer gold, Koyukuk-Chandalar mining district, Alaska. Journal of Geochemical Exploration, 31, 97-115.

Murr, L.E., Berry, V.K., 1976. Direct observations of selective attachment of bacteria on low-grade sulfide ores and other mineral surfaces. Hydrometallurgy, 2, 11-24.

Painter, H.A., 1970. A review of literature on inorganic nitrogen metabolism in microorganisms. Water Research, 4, 393-450.

Puddephatt, R., 1978. The chemistry of gold. Elsevier Publishing Company. New York. 31-87.

Reith, F., McPhail, D.C., 2006. Effect of resident microbiota on the solubilization of gold in soil from the Tomakin Park Gold Mine, New South Wales, Australia. Geochimica et Cosmochimica Acta, 70, 1421- 1438.

Reith, F., Rogers, S.L., McPhail, D.C., Webb, D., 2006. Biomineralization of gold: Biofilms on bacterioform gold. Science, 313, 233-236.

Reith, F., Lengke, M.F., Falconer, D., Craw, D., Southam, G., 2007. The geomicrobiology of gold. International Society of Microbial Ecology Journal, 1, 567-584.

Reith, F., Wakelin, S.A., Gregg, A.L., Schmidt-Mumm, A., 2009. A microbial pathway for the formation of gold-anomalous calcrete. Chemical Geology, 258, 315-326.

Reith, F., Etschmann, B., Dart, R.C., Brewe, D.L., Vogt, S., Schmidt-Mumm, A., Brugger, J., 2011. Distribution and speciation of gold in biogenic and abiogenic calcium carbonates-Implications for the formation of gold anomalous calcrete. Geochimica et Cosmochimica Acta, 75, 1942-1956.

Reith, F., Stewart, L., Wakelin, S.A., 2012. Supergene gold transformation: Secondary and nano-particulate gold from southern New Zeaand. Chemical Geology, 320-321, 32-45.

Sillitoe, R., 2008. Major gold deposits and belts of the North and South American Cordillera: distribution, tectonomagmatic settings, and metallogenic considerations. Economic Geology, 103, 663-687.

Silverman, M.P., Lundgren, D.G., 1959. Studies on the chemoautotrophic iron bacterium Ferrobacillus ferrooxidans: An improved medium and a harvesting procedure for securing high cell yields. Journal of Bacteriology, 77, 642-647.

Southam, G., Beveridge, T.J., 1994. The in vitro formation of placer gold by bacteria. Geochimica et Cosmochimica Acta, 58, 4527-4530.

Southam, G., Beveridge, T.J., 1996. The occurrence of sulfur and phosphorus within bacterially derived crystalline and pseudocrystalline octahedral gold formed in vitro. Geochimica et Cosmochimica Acta, 60, 4369-4376.

Southam, G., Saunders, J., 2005. The Geomicrobiology of ore deposits. Economic Geology, 100, 1067-1084.

Starkenburg, S.R., Larimer, F.W., Stein, L.Y., Klotz, M.G., Chain, P.S.G., Sayavedra-Soto, L.A., Poret-Peterson, A.T., Gentry, M.E., Arp, D.J., Ward, B., Bottomley, P.J., 2008. Complete genome sequence of *Nitrobacter hamburgensis* X14 and comparative genomic analysis of species within the genus *Nitrobacter*. Applied and Environmental Microbiology, 74, 2852-2863.

Tassinari, C.G.G., Pinzon, F.D., Ventura, J.B., 2008. Age and sources of gold mineralization in the Marmato mining district, NW Colombia: A Miocene-Pliocene epizonal gold deposit. Ore Geology Reviews, 33, 505-518.

Theodore, T.G., Blair, W.N., Nash, J.T., 1987. Geology and gold mineralization of the Gold Basin-Lost Basin mining districts, Mohave County, Arizona. United States Geological Survey Professional Paper, 1361, 1-167.

Thompson, A., Attwood, D., Gullikson, E., Howells, M., Kim, K., Kirz, J., Kortright, J., Lindau, I., Liu, Y., Pianetta, P., Robinson, A., Scofield, J., Underwood, J., Williams, G., 2009. Center for X-Ray Optics and Advanced Light Source. In X-Ray Data Booklet. U.S. Government Printing Office, Lawrence Berkeley National Laboratories, 15-27.

Townley, B.K., Herail, G., Maksaev, V., Palacios, C., de Parseval, P., Sepulveda, F., Orellana, R., Rivas, P., Ulloa, C., 2003. Gold grain morphology and composition as an exploration tool: Application to gold exploration in covered areas. Geochemistry Exploration, Environment, Analysis, 3, 29-38.

Watterson, J.R., 1992. Preliminary evidence for the involvement of budding bacteria in the origin of Alaskan placer gold. Geology, 20, 315-318.

Webster, J.G., 1985. Thiosulphate in surficial geothermal waters, North Island, New Zealand. Applied Geochemistry, 2, 5-6.

Webster, J.G., Mann, A.W., 1984. The influence of climate, geomorphology and primary geology on the supergene migration of gold and silver. Journal of Geochemical Exploration, 22, 22-42.

Wilson, A.F., 1984. Origin of quartz-free gold nuggets and supergene gold found in laterites and soils-a review and some new observations. Australian Journal of Earth Science, 31, 303-316.

Yeend, W., 1975. Experimental abrasion of detrital gold. United States Geological Survey Journal of Research, 3, 203-212.

Youngson, J.H., Craw, D., 1993. Gold nugget growth during tectonically induced sedimentary recycling, Otago, New Zealand. Sedimentary Geology, 84, 71-88.

# Chapter 5

# 5 The immobilisation of gold from gold (III) chloride by halophilic sulphate-reducing bacterial consortium

Relative to many other metals, gold occurs at a very low concentration in the Earth's crust. Anomalies such as economically significant ore deposits indicate that gold concentrations are unevenly distributed throughout the globe (Boyle, 1979; Cabri et al., 1989; Cathelineau et al., 1989; Marsden and House, 1992; Fleet et al., 1993; Paopongsawan and Fletcher, 1993; Fairbrother et al., 2012). The variability of gold concentrations in the lithosphere is attributed to both physical and chemical factors that control gold enrichment and transport (Frimmel, 2008). From a geochemical context, the transportation of soluble gold has been attributed to different complexing ligands that are created under different environmental conditions (Mann, 1984; Benedetti and Boulegue, 1991). Chloride anions readily form soluble, gold complexes that remain stable under acidic conditions as long as the solution contains high chloride content and a strong oxidising agent (Krauskopf, 1951; Mann, 1984). The ionisation energies of gold (I) and gold (III) are 890 $kJ \cdot mol^{-1}$ and 2942 $kJ \cdot mol^{-1}$, respectively; therefore, gold (I) is readily formed in surface environments (Puddephatt, 1978; Marsden and House, 1992; Reaction 5.1). However, since the $3^+$-oxidation state of gold is more stable at ambient temperatures, gold (I) complexes will disproportionate to gold (III) chloride and elemental gold (Puddephatt, 1978). Reaction 5.2 describes the natural geochemical process by which gold (III) chloride complexes can form under near-surface conditions that are acidic and contain high concentrations of chloride ions (Mann, 1984). Therefore, the occurrence of soluble gold must be considered dynamic since precipitation of elemental gold and formation of gold (III) chloride complexes can occur contemporaneously. It is important to note that low gold concentrations have been measured in natural saline waters (Koide et al., 1988) and in surficial, hypersaline groundwater located near mesothermal gold deposits (Carey et al., 2003).

$$2\ Au^0 + 2\ HCl + 0.5\ O_2 \rightarrow 2\ AuCl + H_2O \quad (5.1)$$

$$3\ AuCl + HCl \rightarrow 2\ Au^0 + HAuCl_4 \quad (5.2)$$

Saline and hypersaline environments are located across Earth's surface and commonly occur in hot, dry regions although arctic deserts do exist (Friedmann and Ocampo, 1976). Within

these environments, there are large variations in pH, salt concentration and ionic composition that select for a wide range of extremophiles that have existed and evolved for billions of years (Konhauser, 2007). Goldschmidt (1937) first suggested that bacteria could catalyse geochemical processes enabling increased metal accumulation within a given environment. Subsequent studies contributed to this idea by identifying the importance of bacterial cell structure as an interface between the internal cellular environment and the surrounding external milieu (Beveridge and Murray, 1980; Beveridge and Fyfe, 1985; Schultze-Lam et al., 1996; Southam, 2001) and roles bacteria have in passive mineral precipitation (Lowenstam, 1981; Daughney et al., 1998; Beveridge and Fyfe, 1985). Sulphur-reducing bacteria are an example of microorganisms capable of enriching copper in anaerobic to sub-anoxic environments surrounding ore deposits (Southam and Saunders, 2005). These chemolithotrophic bacteria obtain their metabolic energy by oxidising organic compounds and using sulphate as a terminal electron acceptor (Reaction 5.3). A by-product of their active metabolism is soluble hydrogen sulphide that readily forms insoluble iron sulphide when ferrous iron is present (Trudinger et al., 1985; Reaction 5.4).

$$2\ CH_2O + SO_4^{2-} \rightarrow H_2S + 2\ HCO_3^- \quad (5.3)$$

$$Fe^{2+} + H_2S \rightarrow FeS_{(s)} + 2\ H^+ \quad (5.4)$$

Recent research indicated that Bacteria and Archaea are involved in the biogeochemical cycling of gold; this cycle includes the solubilisation, dispersion and re-concentration of gold under near-surface conditions (Reith and McPhail, 2006; Reith et al., 2006, 2007, 2009). Many studies involving the exposure of $HAuCl_4$ solutions to a variety of different viable bacteria (Southam and Beveridge, 1994, 1996; Lengke et al., 2006ab, 2007) and non-metabolising bacteria (Kenney et al., 2012; Song et al., 2012) resulted in the formation of secondary, colloidal gold nanoparticles. However, a current unanswered question from these studies is the importance of excess chloride ions in solutions containing gold (III) chloride. The chloride ions could act as ligands that would increase gold solubility through Au-Cl complexation thereby inhibiting reduction of gold by halophilic bacteria. Therefore, it is of significant interest to determine the biogeochemical interactions that contribute to the gold reduction in saline to hypersaline fluids in anaerobic, near-surface to surface environments. Understanding these biospheric contributions to gold immobilisation has relevance because it provides information about fundamental processes that need to be incorporated into geochemical exploration programs, creating additional means of discovering buried gold

deposits and near-surface deposits containing gold. The Eastern Goldfields of Western Australia is one example of such an environment where soluble gold is transported as gold (III) chloride within groundwater systems and immobilised within calcrete (Carey et al., 2003). Studies by Lintern et al. (2009, 2011) indicated that in semiarid regions, soluble gold is derived from the leaching of underlying primary sources and transported to surficial environments. Subsequent evaporation of gold-bearing hypersaline fluids leads to the precipitation of gold within calcite (Lintern et al., 2009, 2011). Reith et al. (2009) suggested that microorganisms contribute in part to the biomineralisation of gold anomalous carbonates. Therefore, the mobility of gold in saline to hypersaline environments could be restricted by the presence of halophilic bacteria in these surface and near-surface environments.

In this study I have examined the reactivity of gold (III) chloride with halophilic, sulphate-reducing bacteria across saline to hypersaline conditions to determine how excess chloride influences the immobilisation of gold by these bacteria.

## 5.1. Materials and Methods

### 5.1.1 Gold stock solutions

A measured 50 mM gold stock solution was prepared by dissolving chloroauric acid, i.e., $HAuCl_4 \cdot 3H_2O$, purchased from Alfa Aesar, in distilled deionised water. Aliquots of the gold stock were diluted in a modified salt solution defined by Harrison et al. (1980) to obtain saline solutions containing concentrations of 5, 10, and 25 mM gold. The gold stock was also diluted in saline and hypersaline solutions to obtain 5 mM gold at three different salinities. The purpose of gold solutions containing different salt concentrations was to represent natural saline to hypersaline concentrations that matched the culturing conditions of the bacterial enrichments (see section 5.1.2). The pH values of all gold solutions were measured using Electron Microscopy Sciences colourpHast indicator strips pH 0.0-2.5. Although these gold (III) chloride concentrations do not reflect natural occurrences, increased concentrations were used in these experiments to allow: accelerated reactions in the laboratory setting, detection using scanning and transmission electron microscopy and measurement using synchrotron methods.

### 5.1.2 Bacterial enrichment and enumeration

Bacterial enrichments were obtained from a sediment sample that contained halophilic, dissimilatory sulphate-reducing bacteria collected from Basque Lake #1 (see Foster et al., 2010) located near Ashcroft, British Columbia, Canada (Fig. 5.1). Enrichments were grown in modified sulphate-reducing media (Postgate, 1984) under saline to hypersaline concentrations adapted from Harrison et al. (1980). Calculated saline concentrations contained 476 mM $MgCl_2 \cdot 6H_2O$ + CaCl while hypersaline concentrations contained 951 mM or 1428 mM $MgCl_2 \cdot 6H_2O$ + CaCl. A 1:9 molar ratio of $MgCl_2 \cdot 6H_2O$:CaCl was used for all saline solutions. Bacterial samples were incubated at room temperature (RT, approx. 22˚C) for four weeks in Fisherbrand® 13 × 100 mm borosilicate glass tubes filled with growth medium. Screw caps were used to seal the borosilicate glass tubes and allowed each individual closed system to remain anaerobic during incubation. After four weeks of incubation, pH was measured using 10 µL aliquots of the bacterial enrichment and Electron Microscopy Sciences colourpHast indicator strips pH 6.0-10.0 in order to minimize the exposure of enrichments to aerobic conditions when tubes were briefly opened. The sulphate-reducing bacterial population in a saline enrichment incubated for four weeks was determined using the Most Probable Number (MPN) statistical method described by Cochran (1950).

### 5.1.3 Bacterial experiments

Two different experiments were conducted in triplicate to examine: the effect of sulphate-reducing bacteria on the stability of gold (III) chloride in solution and whether excess chloride, acting as an available complexing ligand, would alter the effect of sulphate-reducing bacteria on the gold (III) chloride stability. Both experiments involved the same preparation before gold (III) chloride solutions were added. One mL aliquots of bacterial enrichments were transferred to 1 mL volume Eppendorf tubes. Bacterial cells and associated iron sulphide minerals from enrichments were separated from the growth media by centrifugation for 1 min. at 12,000 *g* forming a solid pellet and discarding the aqueous growth media. The pellet was then re-suspended in 1 mL deionised water using a vortex pulsed for a few seconds to rinse any residual growth media that could have been "held" within the mineralised biofilm. The washed cells and iron sulphides were re-centrifuged into

a pellet using the same method and the supernatant was discarded. The purpose of the rinse procedure was to ensure I was studying the initial reaction between soluble gold with dissimilatory sulphate-reducing bacteria upon the addition of gold (III) chloride. The rinsed pellet was finally re-suspended and vortexed in 1 mL of respective gold (III) chloride solutions forming bacterial-gold systems. Each Eppendorf tube containing a bacterial-gold system was sealed then wrapped with aluminium foil in order to prevent photocatalytic effects.

The first experiment involved the exposure of saline sulphate-reducing bacteria and associated iron sulphides to saline solutions containing different gold concentrations (5, 10, or 25 mM gold). Exposure times for each bacterial-gold system were 0.5, 1 and 2 hours. After each exposure time, the reaction was arrested by passing the entire bacterial-gold system through a 0.1 μm pore-size filter to remove cells, iron sulphides and immobilised gold from the reaction solution. The pH of the filtered solution was measured using the same method described for the bacterial enrichments. The filtered solutions were also analysed for residual soluble gold using a Perkin-Elmer Optima 3300-DV Inductively Coupled Plasma-Atomic Emission Spectrometer (ICP-AES). Filtrates from saline bacterial-gold systems exposed to 5 mM gold for 2 hours were rinsed in the same manner described above and were prepared for electron microscopy analysis (see sections 5.1.5 and 5.1.6).

The second experiment involved the exposure of saline and hypersaline sulphate-reducing bacteria and associated sulphides to 5 mM gold solutions containing the corresponding salinity. Exposure times, reaction endpoints, pH and residual soluble gold measurements for these bacterial-gold systems were processed in the same manner as the first experiment.

### 5.1.4 Chemical control

Saline solutions containing 5, 10 or 25 mM gold concentrations and 5 mM gold solutions containing the three separate salinities were also used for chemical controls. The treatments and analysis of the chemical controls were the same as the bacterial experiments; however, sulphate-reducing bacteria with associated iron sulphide minerals were not added. The purpose of these experiments was to determine whether or not elemental gold could abiotically precipitate out of saline and hypersaline solutions over time.

### 5.1.5 Scanning electron microscopy-energy dispersive spectroscopy

A filtrate from a bacterial enrichment, cultured under saline conditions for four weeks, represented a control sample for the comparable filtrate from a saline bacterial-gold system exposure to 5 mM gold for 2 hours. Both samples were fixed with $2\%_{(aq)}$ glutaraldehyde, dehydrated in a sequential $25\%_{(aq)}$, $50\%_{(aq)}$, $75\%_{(aq)}$ and $3 \times 100\%$ ethanol series, and dried using a Tousimis Research Corporation Samdri-PVT-3B critical point drier prior to being placed onto Electron Microscopy Sciences aluminium stubs using 12 mm carbon adhesive tabs. Samples were coated with a 3 nm osmium deposition using a Denton Vacuum Desk II sputter coater to reduce charging effects when examined with a LEO (Zeiss) 1540XB Field Emission Gun-Scanning Electron Microscope (FEG-SEM) operating at 3 kV. Elemental composition was determined using an Oxford Instruments' INCAx-sight Energy Dispersive Spectrometer (EDS) operating at a 10 kV accelerating voltage.

Five squares of 10 μm x 10 μm were superimposed on SEM micrographs of the control sample with approximately 2 μm depth of view. Bacterial concentration was estimated by averaging the number of cells counted within each square and converting the cubic microns to an equivalent cell-pellet volume, e.g., 1 pL. The purpose of this second cell count was to determine a more accurate, direct cell count to compare it to the results of the MPN.

### 5.1.6 Transmission electron microscopy

A second 1 mL sample from a saline bacterial-gold system exposed to 5 mM gold for 2 hours was fixed in $2\%_{(aq)}$ glutaraldehyde, centrifuged for 1 min. at 12,000 *g*, enrobed in $2\%_{(wt/vol)}$ noble agar, dehydrated in a $25\%_{(aq)}$, $50\%_{(aq)}$, $75\%_{(aq)}$ and $3 \times 100\%_{(aq)}$ ethanol series and embedded in London Resin White plastic to prevent oxidation of iron sulphides associated with the biofilm (Fortin et al., 1994). The embedded sample was ultrathin sectioned to 70 nm using a Reichert-Jung Ultracut E ultramicrotome and collected on Electron Microscopy Sciences Formvar-carbon coated 100-square mesh copper grids. Ultrathin sections were then examined using a Phillips CM-10 Transmission Electron Microscope (TEM) operating at 80 kV.

### 5.1.7 X-ray absorption near-edge spectroscopy

X-ray Absorption Near-Edge Spectroscopy (XANES) was used to determine the oxidation state of gold in all the bacterial-gold systems. Each bacterial-gold system was centrifuged to form a pellet and rinsed in deoxygenated, deionised water forming a wet paste that was sealed in an acid-resistant Teflon fluid cell, i.e., 1 cm diameter × 0.3 cm thickness, with Kapton film windows and placed in the path of the X-ray beam. Four to ten scans were collected and averaged for each sample. The analyses were conducted at Bending Magnet beamline Sector 9 at the Advanced Photon Source, Argonne National Laboratory, Illinois, USA. The Si (111) monochromator was calibrated to the Au L-111 absorption edge at 11919 eV using the first peak of the first derivative X-ray absorption near edge structure (XANES) spectrum of a gold metallic foil standard. The energy scale for each bacteria-gold system was referenced to Au L-111 absorption edge (11919 eV) of the gold foil spectrum collected in transmission mode simultaneously with the data of the bacterial-gold system.

Sodium gold thiosulphate, gold sulphide and gold foil all with 99.9% purity and purchased from Alfa Aesar, were used for reference standards. The gold thiosulphate complex was dissolved in distilled, deionised water and saline water to obtain 5 mM gold in each solution. The purpose of this experiment was to demonstrate that the presence of chloride ions did not affect the gold thiosulphate spectrum. Gold thiosulphate dissolved in saline solution represented a direct standard that was consistent with the salinity of the bacterial-gold system experiments. The XANES spectra for gold thiosulphate solutions, gold sulphide and gold foil were measured in transmission mode using an ionisation chamber filled with nitrogen gas at 1 atm. These standards represented the most probable gold complexes leading to elemental gold in the presence of sulphate-reducing bacteria. All bacterial-gold systems were collected in fluorescence mode using a Canberra solid-state germanium, multi-element detector. All spectra were monitored for potential chemical effects induced by radiation; however, none were detected.

### 5.1.8 X-ray absorption fine structure data analysis

X-ray Absorption Fine Structure (XAFS) data were processed using Athena 8.054 (Ravel and Newville, 2005). A linear regression was performed in the pre-edge, e.g., –150 to –75 eV,

and post-edge region, e.g., 150 and 300 eV, for baseline subtraction and XANES normalization.

## 5.2. Results

### 5.2.1 Bacterial enrichment and enumeration

Growth of the halophilic, sulphate-reducing bacterial enrichments occurred as mineralised, black biofilms coating the walls of the screw-capped, sealed borosilicate test tubes (Fig. 5.2a and inset). The black appearance was due to iron sulphide production. The MPN of bacterial enrichments cultured under saline conditions underestimated the population at $1.1 \times 10^4$ cells/mL. However, because the bacteria grew as a consolidated biofilm, the second cell count using SEM micrographs provided a better estimate equalling $4.5 \times 10^8$ cells/mL, which is more typical for bacterial enrichments cultured under laboratory conditions. The sulphate-reducing bacteria were comparable in size (mass) to the model bacterium, *Escherichia coli* (Neidhardt et al., 1990); therefore, each pellet in the bacterial-gold systems contained approximately 0.126 mg of cells and 0.157 mg iron sulphide.

### 5.2.2 Chemical analysis

Concentrations of immobilised soluble gold, inferred from ICP-AES analysis, and pH for both bacterial-gold experiments are summarised in Table 5.1. The initial pH of bacterial enrichments incubated for four weeks were circumneutral (pH 7.5) while all gold (III) chloride solutions were acidic (pH 1.3). After the addition of gold (III) chloride solution, all bacterial-gold systems were naturally buffered to circumneutral condition (pH 7.0) as exposure time reached 2 hours. The saline bacterial-gold system exposed to 25 mM gold was the only exception as the pH remained acidic (pH 4.0) after the 2 hour exposure.

The ICP-AES results from the first experiment indicated that saline bacterial-gold systems immobilised 98% of the 5 mM and 10 mM gold input but only 62% of the 25 mM gold input. Residual soluble gold concentrations from these systems decreased as the length of exposure time increased. More importantly, the second experiment demonstrated that increased salinities of the bacterial-gold systems had no effect on the immobilisation of 5 mM gold

from solution. The concentration of gold in the chemical controls did not change indicating that abiotic precipitation of gold in varying salinity did not occur.

### 5.2.3 Scanning electron microscopy-energy dispersive spectra analysis

The control sample of rinsed cells cultured under saline conditions had an abundant growth of cells that retained a structurally sound biofilm with extensive capsular material (Figs. 5.2 and 5.3a). Energy-dispersive spectroscopy identified carbon, oxygen, sulphur and phosphorus fluorescence peaks, which are expected elements associated with organic biofilm material. Areas of the biofilm were enriched with iron sulphides (Fig. 5.3a). Precipitation of approx. 500 μm size, calcium carbonate octahedron crystals were also observed in the control sample (Fig. 5.4) and in the cultures incubated under hypersaline conditions. The saline bacterial-gold system treated with 5 mM gold for 2 hours reduced gold (III) chloride as 100 nm gold colloids. The gold colloids appeared as a coating on the surface of the biofilm with the structural articulation of the capsular material still identifiable (Fig. 5.3b, arrow). Prominent EDS peaks of gold and carbon, e.g., bacteria and capsule, confirmed the precipitation of elemental gold on the biofilm surface.

### 5.2.4 Transmission electron microscopy analysis

The saline bacterial-gold system exposed to 5 mM gold for 2 hours and examined using TEM analysis confirmed the precipitation of approximately 10 nm colloidal gold and approximately 100 nm clusters of gold colloids at the surface of the biofilm (Fig. 5.5, arrow). The presence of 3 to 10 nm gold colloids occurred individually within the exopolymer containing iron sulphides (Fig. 5.5, circle). TEM analysis also detected the presence of extensive mineralisation of some bacterial cells that were completely encrusted in nanometre-size gold colloids (Fig. 5.6a, black arrow) along with approximately 100 nm size octahedral gold platelets (Fig. 5.6a, white arrow). Most of the cells within the biofilm did not have extracellular gold mineralisation or disruption of the cellular envelope (Fig. 5.6b, white arrow). However, bacteria closer to the biofilm-fluid interface were completely mineralised with gold colloids occurring throughout the cell envelope and the cells often appeared damaged and lysed (Fig. 5.6b, black arrow).

### 5.2.5 X-ray absorption near edge spectroscopy analysis

The XANES spectra of three relevant gold compounds are shown in Figure 5.7. Elemental gold has characteristic peaks that occur past the absorption edge whereas both the gold sulphide and gold thiosulphate standards have broad features after the white line. The XANES spectra generated from the bacterial-gold systems confirmed that elemental gold precipitated (Fig. 5.7) and that neither increased concentration of soluble gold nor salinity had an effect on the reduction of gold (III) chloride by sulphate-reducing bacteria. The positioning and broadening of the post-edge peaks suggests that the elemental gold was forming as nanometre-size gold particles smaller than the bulk foil.

## 5.3. Discussion

In surface and near-surface environments with saline to hypersaline conditions, the transportation of gold (III) chloride is facilitated by density-driven convection of different hydrological regimes possessing varying brine concentrations (Puddephatt, 1978; Webster, 1985; Benedetti and Boulegue, 1991; Carey et al., 2003). Of importance to the mobility of gold, and based on these findings, the role of the biosphere in saline to hypersaline groundwater systems is important to gold deposition. Although bacteria and gold concentrations used in this study were high, i.e., representing amplified reaction systems, the ratio of bacterial numbers to amount of gold is comparable to natural environments where sub-millimetre, secondary gold grains occur.

Growth of the halophilic, sulphate-reducing bacterial enrichments in this study formed a structurally cohesive biofilm that resulted in the low MPN value. However, SEM observations and counts of the control sample indicated an abundance of cells, 4 orders of magnitude greater than initially estimated. The resilience of this biofilm was responsible for survival of cells when temporarily exposed to oxidising conditions during the rinse procedure and to the toxic effect of the gold (Fig. 5.2 and 5.3a; Southam and Beveridge, 1994).

After four weeks of incubation, the control sample contained macroscopic, microscopic and chemical evidence of iron sulphide minerals indicating active metabolism of sulphate-reducing bacteria (Reactions 5.3 and 5.4). In saline bacterial-gold system demonstrated that iron sulphide minerals were not detected once treated with 5 mM gold. The “loss” of iron,

sulphur and phosphorus was most likely due to the strong EDS gold signal. Previous studies have demonstrated surface complexation and reductive sorption capabilities of gold complexes with solid iron sulphide substrates (Hyland and Bancroft, 1989; Enzweiler and Joekes, 1991; Schoonen et al., 1992; Moller and Kersten, 1994). The disappearance of iron sulphide within the bacterial-gold samples might also be attributed in part to the solubilisation of iron and formation and release of colloidal sulphur during the formation of colloidal gold (Reaction 5.5); although, iron sulphide minerals were observed in the 5 mM reaction system using TEM (Fig. 5.6; Fortin et al., 1994).

$$HAuCl_4 + FeS_{(s)} \rightarrow Au^0 + Fe^{3+} + S^0 + 3\ Cl^- + HCl \qquad (5.5)$$

The immobilisation of gold by biologically-mediated iron sulphide minerals exposed to gold (III) chloride suggests an indirect mode of gold reduction by sulphate-reducing bacteria. This indirect reduction is important because it can occur contemporaneously with direct bacterial immobilisation.

ICP-AES analysis of gold concentrations in the control gold solutions containing varying salinity remained unchanged indicating that soluble gold in the presence of excess chloride ligands remained in solution. On the contrary, salinity had no effect on the bacterial-gold systems with immobilised gold increasing over time. Furthermore, the amount of gold immobilised from bacterial-gold systems exposed to 5 and 10 mM gold were consistent with previous studies (Southam and Beveridge, 1994, 1996; Lengke et al., 2006a,b, 2007). The inability of the bacteria to immobilise all of the gold from the 25 mM gold solution suggests that saturation of reactive groups with gold occurred, highlighting the capacity of gold immobilisation by sulphate-reducing bacteria in this experimental model, i.e. approx. 66 μmol gold/g of cells and associated FeS. This value suggests that a relatively small number of bacteria have the capacity to produce a significant accumulation of approx. 13 mg gold.

Reduction of gold (III) chloride occurred at the biofilm-fluid interface as the biofilm retained its initial cohesive structure after exposure to gold (Fig. 5.3b). This finding is consistent with the results of Lengke and Southam (2007) who showed that bacteria within a biofilm were "protected" from the exposure of gold by cells located near the biofilm-fluid interface. Both studies demonstrated the importance of chemical gradients occurring in microenvironments surrounding sulphate-reducing bacteria during gold immobilisation. The pH buffering to circumneutral conditions, i.e., acid reaction with carbonate; see Fig. 5.4, contributed to the

survival of bacteria within the biofilm. Karthikeyan and Beveridge (2002) demonstrated that cells lyse due to toxicity at increased metal concentrations. As a result, release of intracellular organics creates additional reactive sites for metal immobilisation and contribute to buffering of the system (Fig. 5.6). Furthermore, Kenney et al. (2012) and Song et al. (2012) highlighted the importance of gold immobilisation by non-metabolizing cells. Under circumneutral pH conditions, cell wall surface reactive groups are predominantly negatively charged allowing for greater adsorption of soluble gold and resulting in subsequent gold reduction (Kenney et al., 2012). Therefore in bacterial-gold systems exposed to 5 mM and 10 mM gold, pH stabilisation by lysis of both metabolising and non-metabolising cells within the biofilm (Costerton et al., 1987) may have aided gold immobilisation. The high gold and acid concentrations in the saline bacterial-gold system exposed to 25 mM gold likely "over titrated" the buffering capacity of these reaction systems and the ability of iron sulphide minerals and organics to immobilise gold.

In previous studies, thiosulphate-reducing bacteria exposed to gold (I) thiosulphate formed intracellular, colloidal gold that subsequently transformed into octahedral gold platelets and aggregates (Lengke and Southam, 2006). In this study, however, gold (III) chloride reduction by sulphate-reducing bacteria typically occurred at the biofilm-fluid interface, forming extensive gold colloids and colloidal gold clusters on bacterial and surrounding exopolymer surfaces. The rapid formation of colloidal gold is attributed to easily oxidised, organic material donating electrons to gold (Reaction 5.6; using a fatty acid as a model compound). Although transformation to octahedral platelets was limited, "islands" of gold occurred with iron sulphide minerals (Figs. 5.5 and 5.6). These observations support the possibility that gold reduction occurred indirectly by iron sulphide minerals (Reaction 5.5) and directly by bacteria (Reaction 5.6).

$$AuCl_3 + X\text{-}CH_3COO^- + 3\ OH^- \rightarrow Au^0 + XCH_2O^- + CO_2 + 2\ H_2O + 3\ Cl^- \qquad (5.6)$$

Based on Lengke et al. (2006a), gold (I) sulphur compounds were important intermediates in the bacterial reduction of gold chloride. However, XANES analysis of these bacterial-gold systems demonstrated that these complexes did not form, or perhaps were extremely unstable transient species, during the gold transformation. Linear combination fitting of gold thiosulphate and gold sulphide required a greater than 1 eV shift in the experimental data to achieve a spectral fit. Beauchemin et al. (2002) and MacLean et al. (2011) demonstrated that

an energy shift of this size is indicative of a poor match in terms of model spectra to the experimental data. A comparison of the gold foil and the bacterial-gold spectra suggested that the elemental gold could explain the variations in the intensity of the post-edge Au peaks in the XANES spectra. Zhang and Sham (2003) demonstrated that elemental nanometre-size gold particles with size ranging from 1.6 nm to 4.0 nm had similar differences in the intensity of the XANES post-edge peaks in comparison to a gold foil (bulk gold) standard. Thus, the variations I observe in the experimental data compared to the bulk metallic gold foil are likely due to size effect of the nanometre-size gold produced in these reaction systems (see Figs. 5.5 and 5.6).

The idea of organic substances reducing and subsequently generating secondary gold concentrates was first proposed by Freise (1931). Studies on the bacterial immobilisation of gold chloride have demonstrated that bacteria ultimately transform auric chloride into octahedral gold platelets (Lengke et al., 2006a; Lengke and Southam, 2007). However, in this study, extracellular polymeric organic material primarily precipitated colloidal gold. The lack of octahedral gold in these bacterial-gold systems suggests that intracellular organo-S constituents may be integral for octahedral gold formation. Therefore, the role of bacterial and exopolymeric surfaces are important for colloidal gold precipitation and may explain the formation of colloidal gold by soil (Bergeron and Harrison, 1989).

Reith et al. (2009; 2011) identified a role for bacteria in generating metal anomalies in semi-arid environments by contributing to Ca-carbonatogenesis and the co-precipitation of gold. The formation of carbonate minerals by bacterial dissimilatory sulphate reduction (Castanier et al., 2003) and the close association between carbonates and gold (this study) provide another mechanism for producing gold-carbonate anomalies. Under anoxic, organic-rich conditions, the production of $CO_3^{2-}$ and the release of $H_2S$ favoured carbonate precipitation (Douglas and Beveridge, 1998). In natural systems, such as the Eastern Goldfields of Western Australia, where gold is mobile as chloride complexes (Carey et al., 2003) the presence of sulphate-reducing bacteria, which would naturally thrive in hypersaline groundwater, could enrich gold from solution.

## 5.4. Conclusion

In this study, I demonstrated that halophilic, sulphate-reducing bacteria could directly destabilise gold (III) chloride as precipitated 3 to 10 nm gold colloids and 100 nm colloidal clusters across a range of salinities. Evidence of microbe-mineral interaction between bacteria and soluble gold occurred at the biofilm-fluid interface. Cells occurring within the biofilm were unaffected by gold (III) chloride, indicating the importance of the biofilm structure with resilience to the toxic effects of ionic gold. Furthermore, the close association of iron sulphide minerals with bacteria also indicated the possibility of an indirect mode of gold immobilisation by these bacteria. This bacterial-gold laboratory model demonstrated the accelerated effects of biogeochemical cycling that can occur within near-surface and surface, saline to hypersaline environments containing gold. In these environments, biomineralisation of gold would continue to occur as long as non-toxic concentrations of aqueous gold (III) chloride enter the system and bacterial growth are maintained to replace any biomass that is lost to biomineralisation. This biogeochemical process could start forming large concentrations of gold that could serve as anomalous pathfinders for ore deposits and, given enough geological time, could create an economic deposit.

**Table 5.1.** The immobilisation of gold from $HAuCl_4$ solutions and changes in pH by halophilic, sulphate reducing bacteria.

| **Experiment One: Bacterial-gold systems with different gold concentrations** | | | | | | |
|---|---|---|---|---|---|---|
| **Time (hours)** | **5.08 mM Au input[a]** | | **10.05 mM Au input[a]** | | **25.03 mM Au input[a]** | |
| | **Au immobilised (mM)** | **pH** | **Au immobilised (mM)** | **pH** | **Au immobilised (mM)** | **pH** |
| 0.0 | 0 | 1.3 | 0 | 1.3 | 0 | 1.3 |
| 0.5 | 4.93 | 5.0 | 9.84 | 5.0 | 11.72 | 2.0 |
| 1.0 | 4.96 | 6.0 | 9.93 | 6.0 | 16.34 | 4.0 |
| 2.0 | 5.06 | 7.0 | 10.00 | 6.0 | 18.58 | 4.0 |
| **Experiment Two: Bacterial-gold systems with different salinities** | | | | | | |
| | **476 mM salt[b]** | | **951 mM salt[b]** | | **1428 mM salt[b]** | |
| **Time (hours)** | **Au immobilised (mM)** | **pH** | **Au immobilised (mM)** | **pH** | **Au immobilised (mM)** | **pH** |
| 0.0 | 0 | 1.3 | 0 | 1.3 | 0 | 1.3 |
| 0.5 | 4.93 | 5.0 | 5.05 | 5.0 | 4.97 | 6.0 |
| 1.0 | 4.96 | 6.0 | 5.05 | 5.0 | 4.98 | 5.0 |
| 2.0 | 5.06 | 7.0 | 5.06 | 6.0 | 4.99 | 7.0 |

[a]gold (III) chloride concentration of input and chemical controls

[b]salt = 1:9 molar ratio of $MgCl_2 \cdot 6H_2O$:CaCl

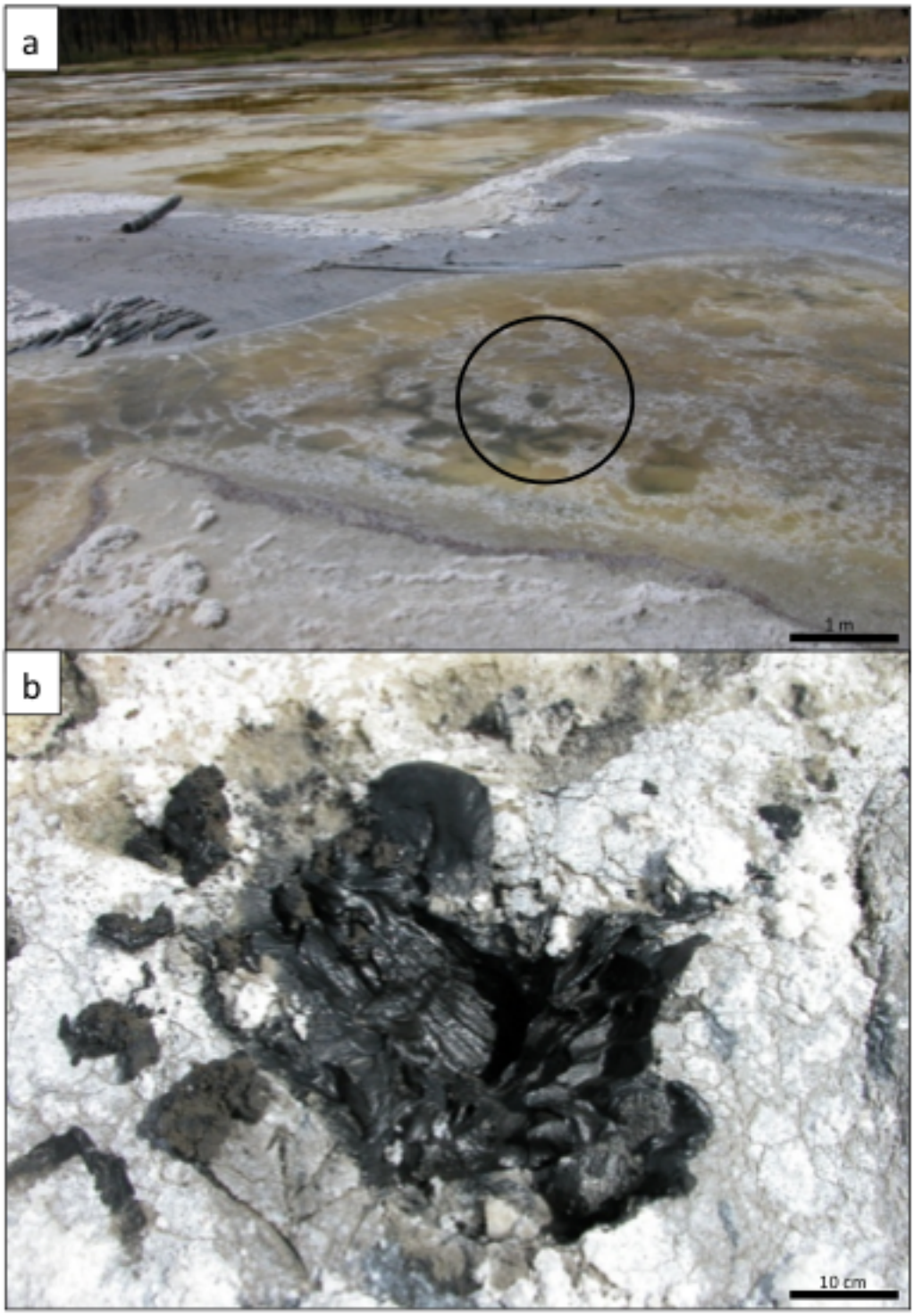


**Figure 5.1. Photograph of Basque Lake #1.** Photographs of the surface of Basque Lake #1 (a) and the occurrence of blackened sediments (a, circle; b) that served as the source material to enrich for dissimilatory sulphate-reducing bacteria used in this study.

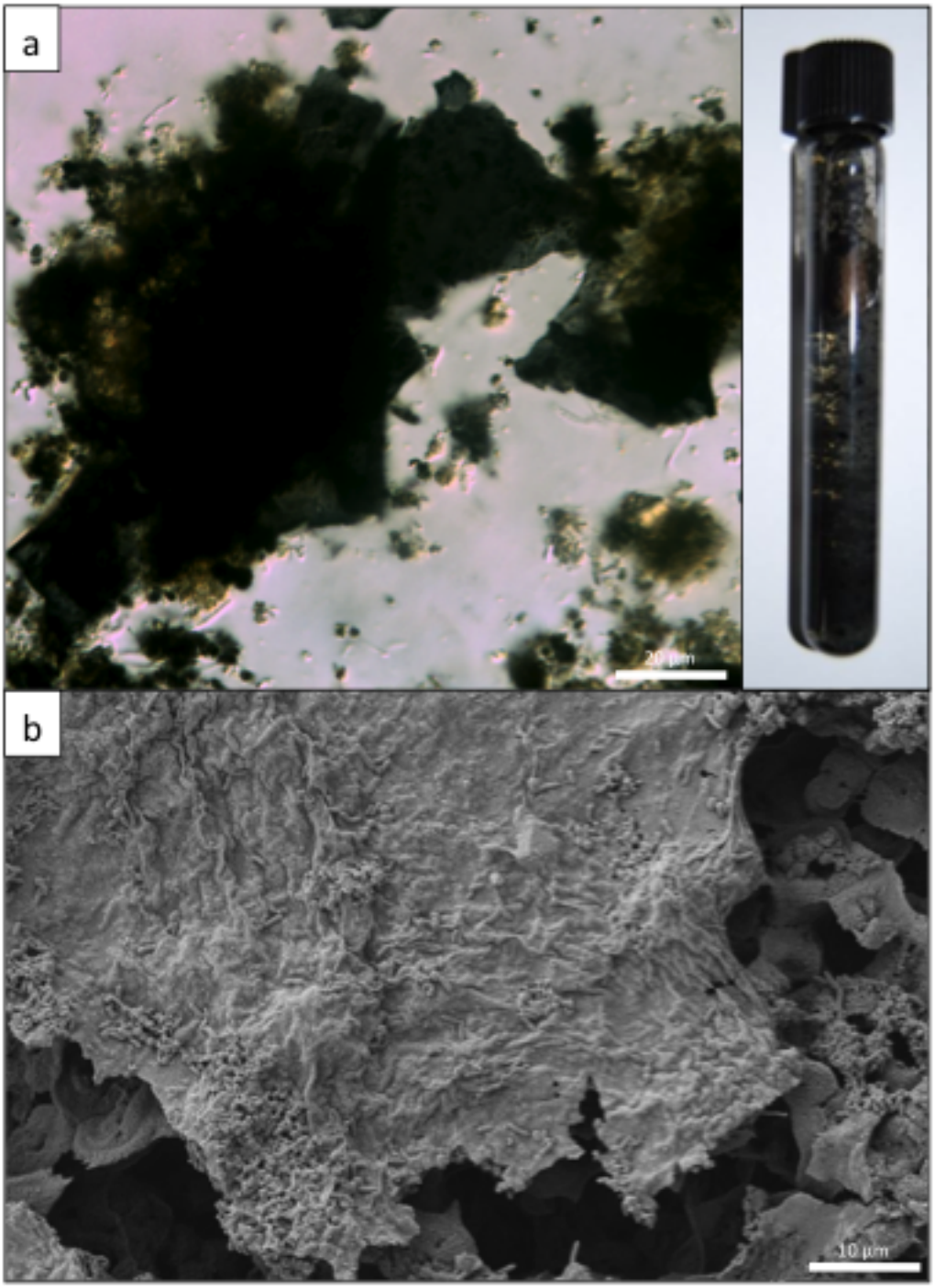


**Figure 5.2. A light micrograph and SEM characterisation of sulphur-reducing bacteria.** A phase contrast light micrograph highlighting the growth of this consortium of halophilic, sulphate-reducing bacteria (a). Inset – a representative photograph of a culture tube. Note, the biofilm on the walls of the culture tube. A low-magnification SEM micrograph of the biofilm (b).

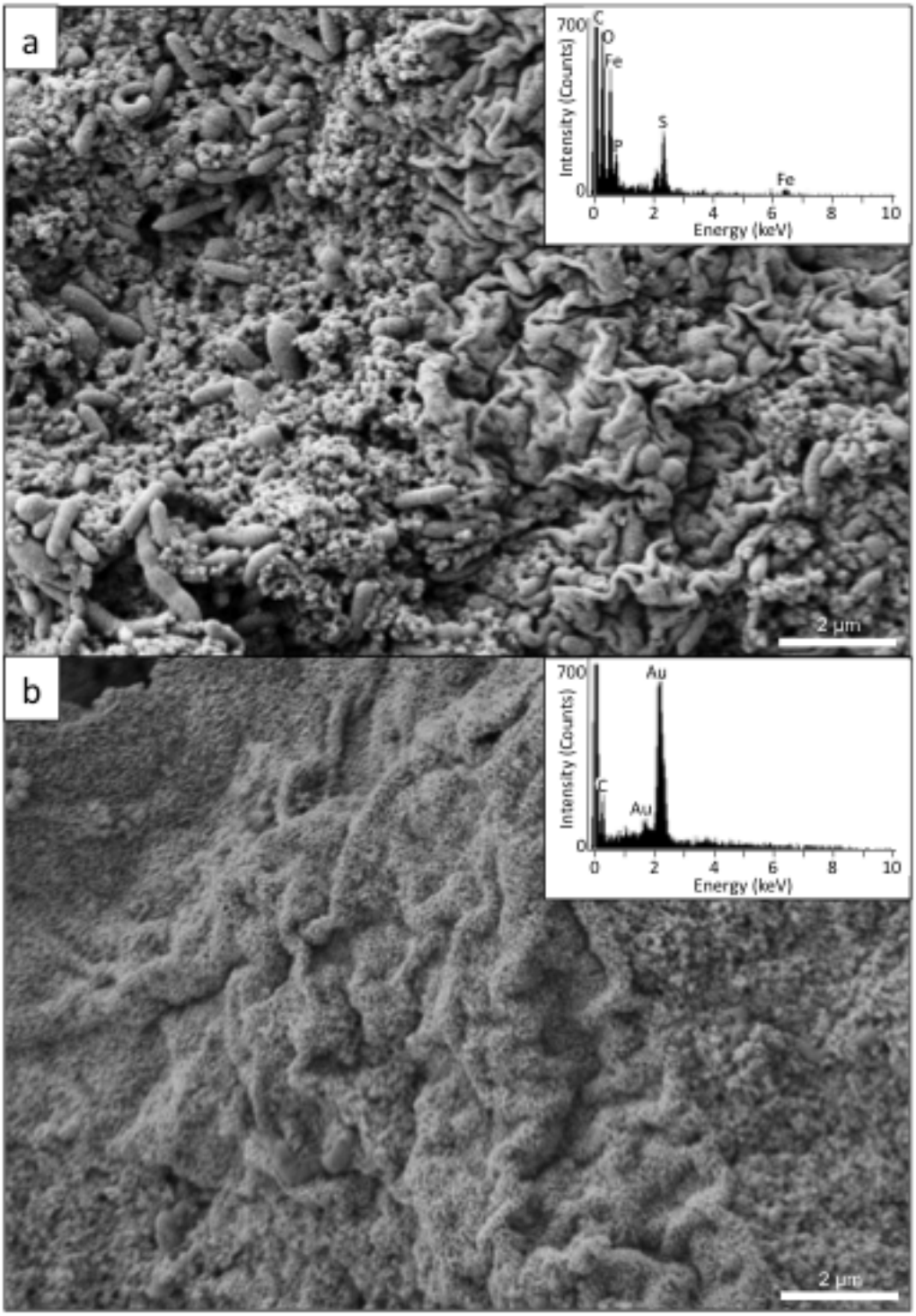


**Figure 5.3. SEM-EDS characterisation of a bacterial-gold system.** High-resolution SEM micrographs of bacteria, iron sulphide precipitates and exopolymer from a biofilm not exposed to gold (III) chloride (a). Inset – EDS analysis detected iron and sulphur. Biofilm reacted with gold (III) chloride (b). Inset – EDS analysis detected gold but iron or sulphur were no longer detected. Note the occurrence of fine-grained colloidal gold coating the entire biofilm surface preserving the original texture of the biofilm.

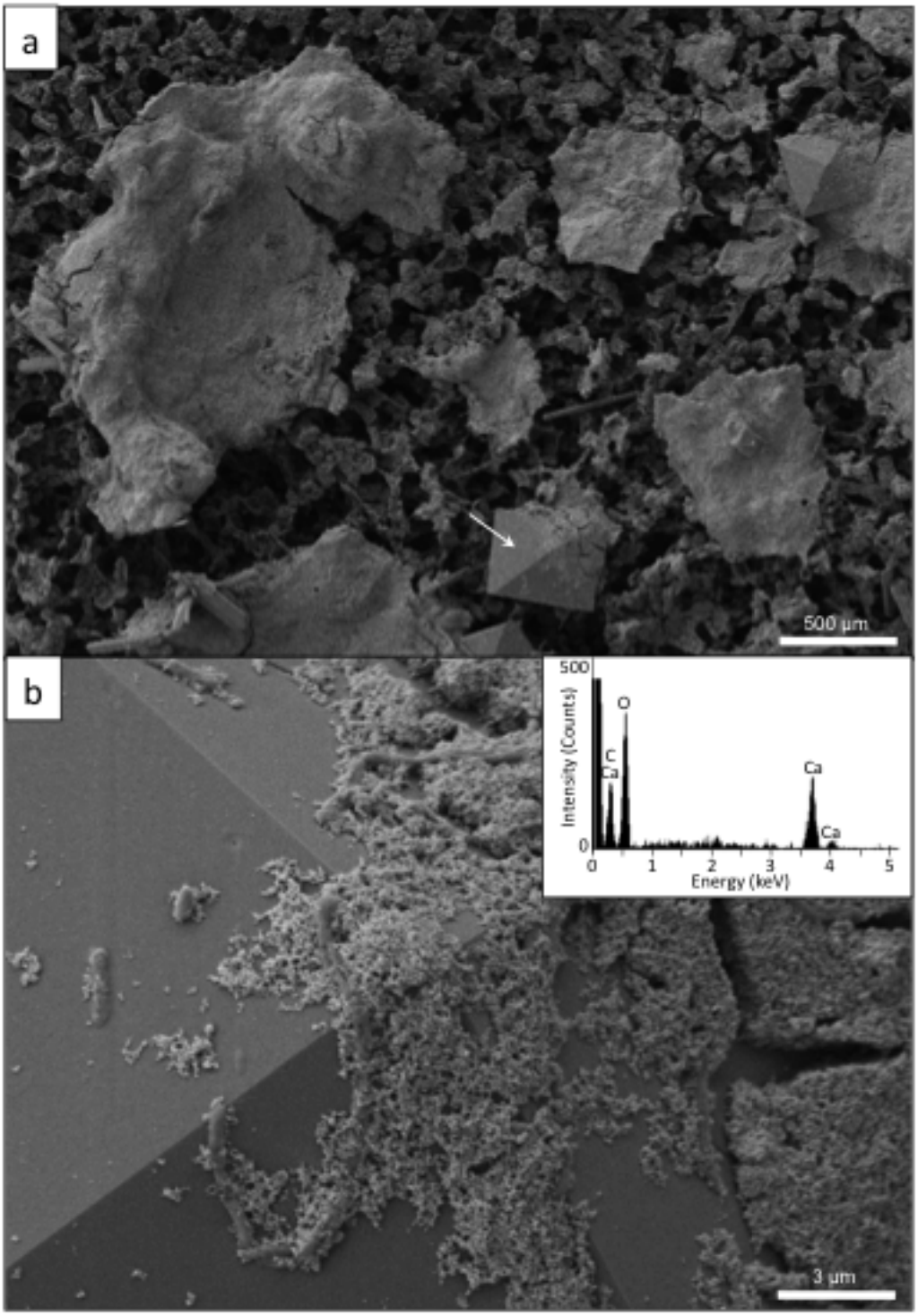


**Figure 5.4. SEM-EDS characterisation of carbonate minerals associated with sulphur-reducing bacteria.** A low-magnification SEM micrographs of octahedral calcium carbonate crystals (arrow) that precipitated in a sulphate-reducing bacterial culture incubated under saline conditions (a). At high- magnification, bacterial biofilms can be observed on the surface of the calcium carbonate (b).

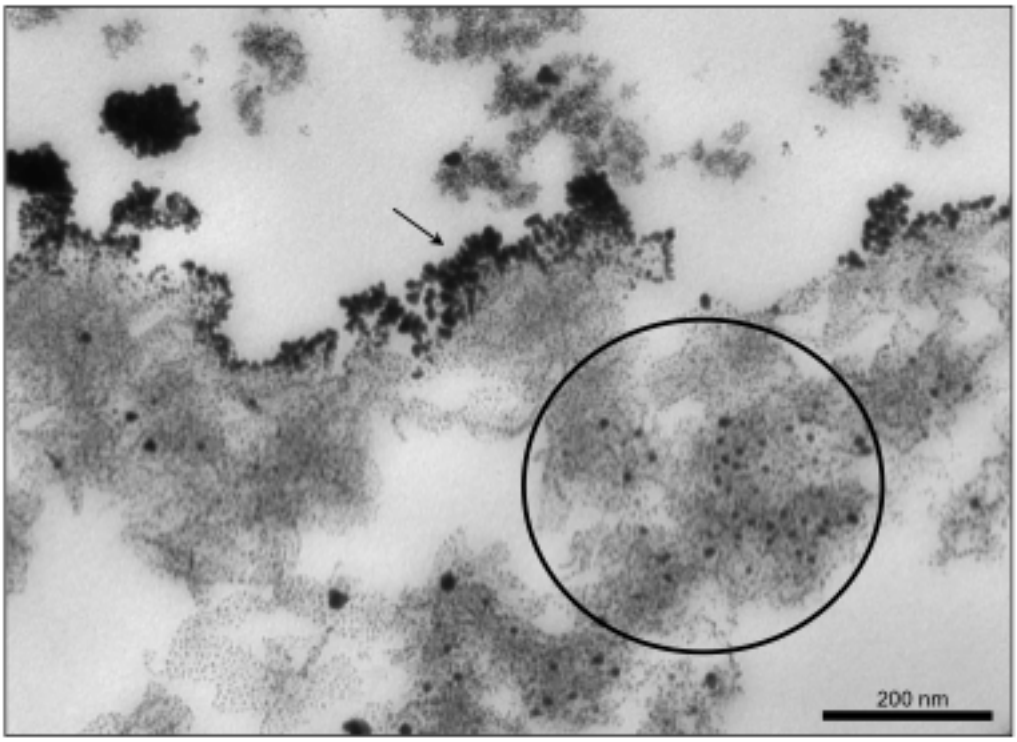


**Figure 5.5. TEM characterisation of a biofilm exposed to gold.** Ultrathin section TEM micrographs of the outer surface of the biofilm exposed to 5 mM gold. An accumulation of fine-grained, colloidal gold formed a dense coating at the biofilm-fluid interface (arrow). "Islands" of gold, 3-10 nm colloids, occurred amongst less electron dense iron sulphide minerals that were presumably adsorbed onto the bacterial exopolymer (circle).

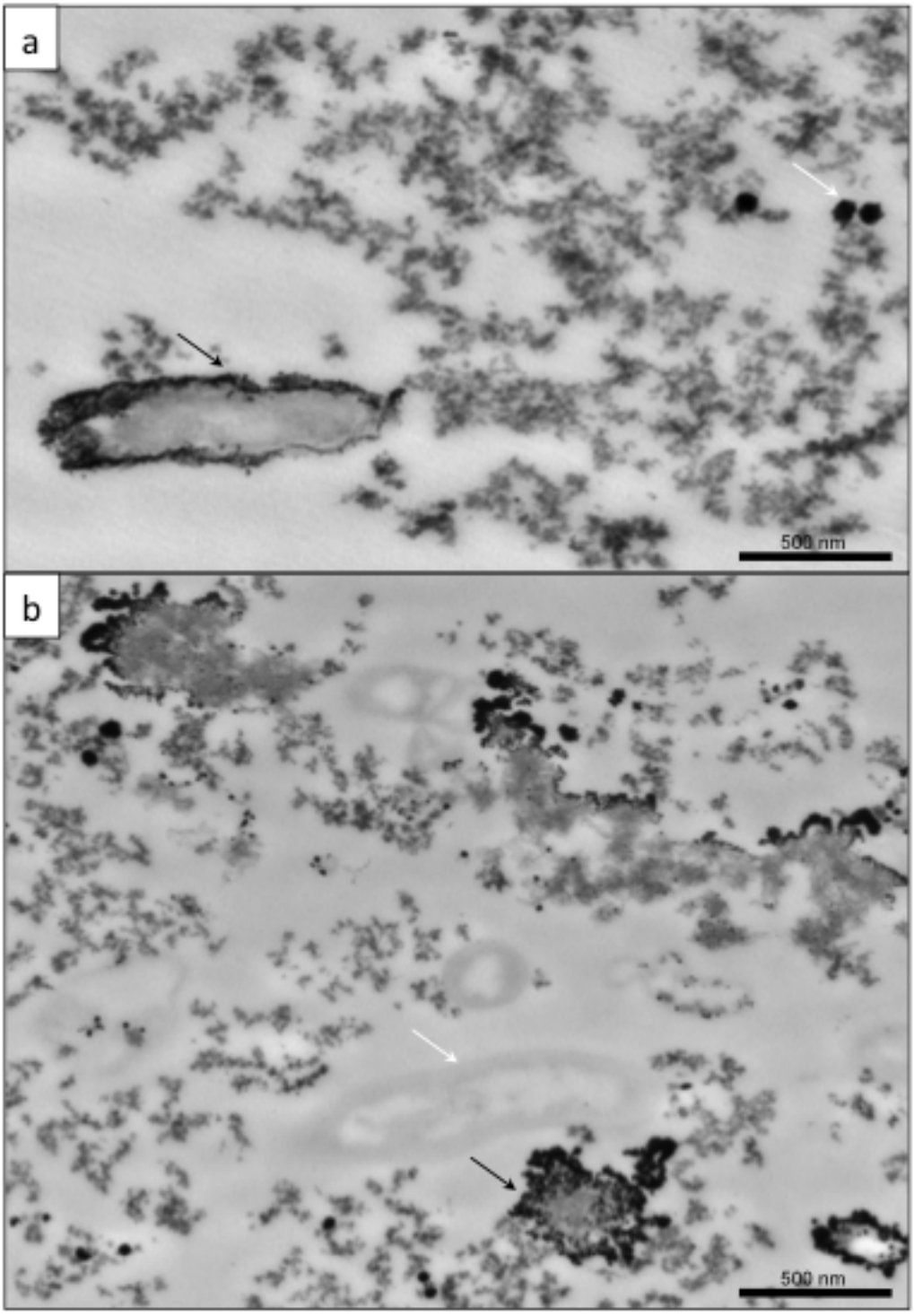


**Figure 5.6. TEM characterisation of regions within a biofilm exposed to gold.** Ultrathin section TEM micrographs of two regions from within the same biofilm exposed to gold (III) chloride. Note the heterogeneity of gold immobilisation as extensive mineralisation occurring on the bacterial surface near the periphery of the biofilm. The formation of octahedral gold (white arrow) is also associated with exopolymer material (a). Some bacteria within the biofilm did not react with gold (white arrow) while others were extensively mineralised (b, black arrow).

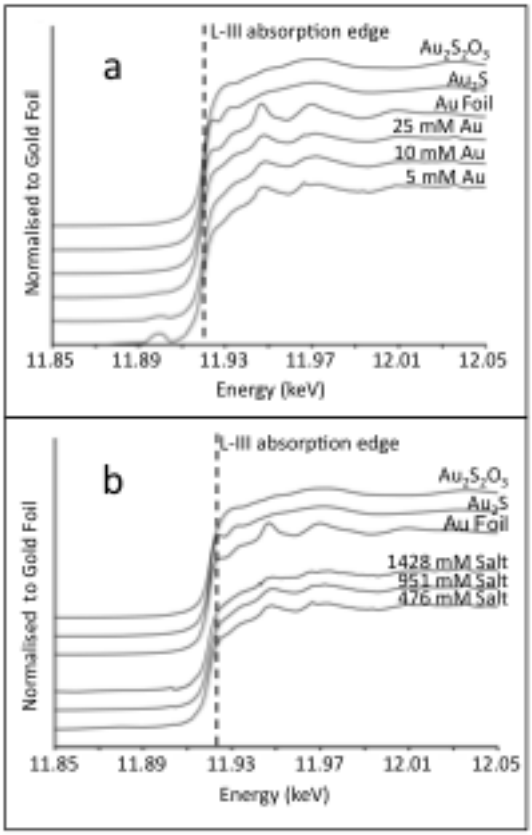


**Figure 5.7. XANES analysis of bacterial-gold systems.** XANES spectra of gold foil, gold sulphide, gold thiosulphate standards and both bacterial-gold systems. Note characteristic peaks for each compound occur after the absorption line. Elemental gold formed in all bacterial-gold systems exposed to different concentrations of gold (III) chloride input under saline conditions (a). Increased salinity had no effect on gold immobilisation in the bacterial-gold system exposed to 5 mM gold; however, variation in peak intensity did occur (b).

## 5.5. References

Beauchemin, S., Hesterberg, D., Beauchemin, M., 2002. Principal component analysis approach for modeling sulfur K-XANES spectra of humic acids. Soil Science Society of America Journal, 66, 83-91.

Benedetti, M., Boulegue, J., 1991. Mechanisms of gold transfer and deposition in a supergene environment. Geochimica et Cosmochimica Acta, 55, 1539-1547.

Bergeron, M., Harrison, Y., 1989. Le transport chimique de l'or dans les environnements de surface: formation d'un colloide et complexation organique. Canadian Journal of Earth Sciences, 26, 2327-2332.

Beveridge, T.J., Murray, R.G., 1980. Sites of metal deposition on the cell wall of Bacillus subtilis. Journal of Bacteriology, 141, 876-886.

Beveridge, T.J., Fyfe, W.S., 1985. Metal fixation by bacterial cell walls. Canadian Journal of Earth Sciences, 22, 1893-1898.

Boyle, R.W., 1979. The geochemistry of gold and its deposits. Geological Survey Canadian Bulletin, 280.

Cabri, L.J., Chryssoulis, S.L., De Villiers, J.P.R., Laflamme, J.H.G., Buseck, P.R., 1989. The nature of “invisible” gold in arsenopyrite. Canadian Mineralogist, 27, 353-362.

Carey, M.L., McPhail, D.C., Taufen, P.M., 2003. Groundwater flow in playa lake environments: Impact on gold and pathfinder element distributions in groudwaters surrounding mesothermal gold deposits, St. Ives area, Eastern Goldfields, Western Australia. Geochemistry-Exploration, Environment, Analysis, 3, 57-71.

Castanier, S., Le Metayer-Lavrel, G., Perthuisot, J., 2003. Ca-carbonates precipitation and limestone genesis-the microbiogeologist point of view. Sedimentary Geology.

Cathelineau, M., Boiron, M.C., Hollinger, P., Marion, P., Denis, M., 1989. Gold in arsenopyrites: Crystal chemistry, location and state, physical and chemical conditions of deposition. Economic Geology Monographs, 6, 328-341.

Cochran, W.G., 1950. Estimation of bacterial densities by means of the "Most Probable Number". Biometrics. 6, 105-116.

Costerton, J.W., Cheng, K.J., Geesey, G.G., Ladd, T.I., Nickel, J.C., Dasgupta, M., Marrie, T.J., 1987. Bacterial biofilms in nature and disease. Annual Reviews of Microbiology, 41, 435-464.

Daughney, C.J., Fein, J.B., Yee, N., 1998. A comparison of the thermodynamics of metal adsorption onto two common bacteria. Chemical Geology, 44, 161-176.

Douglas, S., Beveridge, T.J., 1998. Mineral formation by bacteria in natural microbial communities. FEMS Microbiology Ecology, 26, 79-88.

Enzweiler, J., Joekes, I., 1991. Adsorption of colloidal gold on colloidal iron oxides. Journal of Geochemical Exploration, 40, 133-142.

Fairbrother, L., Brugger, J., Shapter, J., Laird, J.S. Southam, G., Reith, F., 2012. Supergene gold transformation: Biogenic secondary and nano-particulate gold from arid Australia. Chemical Geology, 321, 17-31.

Fleet, M.E., Chryssoulis, S.L., MacLean, P.J., Davidson, R., Weisener, C.G., 1993. Arsenian pyrite from gold deposits: Au and As distribution investigation by SIMS and EMP, and color-staining and surface oxidation by XPS and LIMS. Canadian Mineralogist, 31, 1-17.

Fortin, D., Southam, G., Beveridge, T.J., 1994. Nickel sulphide, iron-nickel sulphide and iron sulphide precipitation by a newly isolated Desulfotomaculum species and its relation to nickel resistance. FEMS Microbiology Ecology, 14, 121-132.

Foster, I., King, P.L., Hyde, B.C., Southam, G., 2010. Characterization of halophiles in natural MgSO4 salts and laboratory enrichment samples: Astrobiological implication for Mars. Planetary and Space Science, 58, 599-615.

Freise, F.W., 1931. The transportation of gold by organic underground solutions. Economic Geology, 26, 421-431.

Friedmann, E.I., Ocampo, R., 1976. Endolithic blue-green algae in the dry valleys: Primary producers in the Antarctic desert ecosystems. Science, 193, 1247–1249.

Frimmel, H.E., 2008. Earth's continental gold endowment. Earth and Planetary Science Letters, 286, 45-55.

Goldschmidt, V.M., 1937. The principles of distribution of chemical elements in minerals and rocks. Journal of the Chemical Society, 1, 655-673.

Harrison, P.J., Waters, R.E., Taylor, F.J.R., 1980. A broad spectrum artificial seawater medium for coastal and open ocean phytoplankton. Journal of Phycology, 16, 28-35.

Hyland, M.M., Bancroft, G.M., 1989. An XPS study of gold deposition at low temperatures on sulphide minerals: Reducing agents. Geochimica et Cosmochimica Acta, 53, 367-372.

Karthikeyan, S., Beveridge, T.J., 2002. Pseudomonas aeruginosa biofilms react with and precipitate toxic soluble gold. Environmental Microbiology, 4, 667-675.

Kenny, J.P.L., Song, Z., Bunker, B.A., Fein, J.B., 2012. An experimental study of Au removal from solution by non-metabolizing bacterial cells and their exudates. Geochimica et Cosmochimica Acta, 87, 51-60.

Koide, M., Hodge, V., Goldberg, E., Bertine, K., 1988. Gold in seawater: A conservative view. Applied Geochemistry, 3, 237-241.

Konhauser, K., 2007. Introduction to geomicrobiology. Blackwell Publishing. Victoria, Australia, 1-35.

Krauskopf, K.B., 1951. The solubility of gold. Economic Geology, 46, 858-870.

Lengke, M.F., Southam, G., 2006. The bioaccumulation of gold by thiosulfate-reducing bacteria cultured in the presence of gold-thiosulfate complex. Geochimica et Cosmochimica Acta, 70, 3646-3661.

Lengke, M.F., Fleet, M.E., Southam, G., 2006a. Morphology of gold nanoparticles synthesized by filamentous cyanobacteria from gold(I)-thiosulfate and gold(III)-chloride complexes. Langmuir, 22, 2780-2787.

Lengke, M.F., Ravel, B., Fleet, M.E., Wanger, G., Gordon, R.A., Southam, G., 2006b. Mechanisms of gold bioaccumulation by filamentous cyanobacteria from gold (III)-chloride. Environmental Science and Technology, 40, 6304-6309.

Lengke, M.F., Ravel, B., Fleet, M.E., Wanger, G., Gordon, R.A., Southam, G., 2007. Precipitation of gold by reaction of aqueous gold(III)-chloride with cyanobacteria at 25-80°C – Studied by X-ray absorption spectroscopy. Canadian Journal of Chemistry, 85,1-9.

Lengke, M.F., Southam, G., 2007. The role of bacteria in the accumulation of gold: Implications for placer gold formation and supergene gold enrichment. Economic Geology, 102, 109-126.

Lintern, M.J., Hough, R.M., Ryan, C.G., Watling, J., 2009. Ionic gold in calcrete revealed by LA-ICP-MS, SXRF and XANES. Geochimica et Cosmochimica Acta, 73, 1666-1683.

Lintern, M., Sheard, M., Buller, N., 2011. The gold-in-calcrete anomaly at the ET gold prespect, Gawler Craton, South Australia. Applied Geochemistry, 26, 2027-2043.

Lowenstam, H., 1981. Minerals formed by organisms. Science, 211, 1126-1131.

MacLean, L.C.W., Beauchemin, S., Rasmussen, P.E., 2011. Application of synchrotron x-ray techniques for the determination of metal speciation in (house) dust particles. Environmental Science and Engineering, 2, 193-216.

Mann, A.W., 1984. Mobility of gold and silver in lateritic weathering profiles: Some observations from Western Australia. Economic Geology, 79, 38-50.

Marsden, J., House, I.H., 1992. The chemistry of gold extraction. Ellis Horwood Publishing. New York. 13-58.

Moller, P., Kersten, G., 1994. Electrochemical accumulation of visible gold on pyrite and arsenopyrite surfaces. Mineralium Deposita, 29, 404-413.

Neidhardt, F.C., Ingraham, J.L., Schaechter, M., 1990. Physiology of the bacterial cell: A molecular approach. Sinauer Associates, Sunderland. MA.

Paopongsawan, P., Fletcher, W.K., 1993. Distribution and dispersion of gold in point bar and pavement sediments of the Huai Hin Laep, Loei, northeastern Thailand. Journal of Geochemical Exploration, 47, 251-268.

Postgate, J.R., 1984. The sulfate-reducing bacteria. 2nd edition. Cambridge Press. 32.

Puddephatt, R., 1978. The chemistry of gold. Elsevier Publishing Company. New York. 31-87.

Ravel, B., Newville, M., 2005. Athena, Artemis, Hephaestus: Data analysis for X-ray absorption spectroscopy using IFEFFIT. Journal of Synchrotron Radiation, 12, 537-547.

Reith, F., Rogers, S.L., McPhail D.C., Webb, D., 2006. Biomineralization of gold: Biofilms on bacterioform gold. Science, 313, 233-236.

Reith, F., McPhail, D.C., 2006. Effect of resident microbiota on the solubilization of gold in soil from the Tomakin Park Gold Mine, New South Wales, Australia. Geochimica et Cosmochimica Acta, 70, 1421- 1438.

Reith, F., Lengke, M.F., Falconer, D. Craw, D., Southam, G., 2007. The geomicrobiology of gold. International Society of Microbial Ecology Journal, 1, 567-584.

Reith, F., Wakelin, S.A., Gregg, A.L., Schmidt Mumm, A., 2009. A microbial pathway for the formation of gold-anomalous calcrete. Chemical Geology, 258, 315-326.

Reith, F., Etschmann, B., Dart, R.C., Brewe, D.L., Vogt, S., Schmidt Mumm, A., Brugger, J., 2011. Distribution and speciation of gold in biogenic and abiogenic calcium carbonates-Implications for the formation of gold anomalous calcrete. Geochimica et Cosmochimica Acta, 75, 1942-1956.

Schoonen, M.A., Fisher, N.S., Wente, M., 1992. Gold sorption onto pyrite and goethite: A radiotracer study. Geochimica et Cosmochimica Acta, 56, 1801-1814.

Schultz-Lam, S., Fortin, D., Davis, B.S., Beveridge, T.J., 1996. Mineralization of bacterial surfaces. Chemical Geology, 132, 171-181.

Song, Z., Kenney, J.P.L., Fein, J.B., Bunker, B.A., 2012. An X-ray Fine Structure study of Au adsorbed onto the non-metabolizing cells of two soil bacterial species. Geochimica et Cosmochimica Acta, 86, 103-117.

Southam, G., 2001. Quantification of sulphur and phosphorus within secondary gold rims on Yukon placer gold. Geology, 26, 339-342.

Southam, G., Beveridge, T.J., 1994. The in vitro formation of placer gold by bacteria. Geochimica et Cosmochimica Acta, 58, 4527-4530.

Southam, G., Beveridge, T.J., 1996. The occurrence of sulfur and phosphorus within bacterially derived crystalline and pseudocrystalline octahedral gold formed in vitro. Geochimica et Cosmochimica Acta, 60, 4369-4376.

Southam, G., Saunders, J., 2005. The Geomicrobiology of ore deposits. Economic Geology, 100, 1067-1084.

Trudinger, P.A., Chambers, L.A., Smith, J.W., 1985. Low-temperature sulphate reduction: Biological versus abiological. Canadian Journal of Earth Sciences, 22, 1910-1918.

Webster, J.G., 1985. Thiosulphate in surficial geothermal waters, North Island, New Zealand. Applied Geochemistry, 2, 5-6.

Zhang, P., Sham, T.K., 2003. X-ray studies of the structure and electron behavior of alkanethiolate-capped gold nanoparticles: The interplay of size and surface effects. Physical Review Letters, 90, 1-4.

# Chapter 6

# 6 The *in vitro* formation of gold nuggets and other fine-particles derived from the bacterial immobilisation of soluble gold complexes.

Gold nuggets are classified as having lengths greater than 4 mm or a mass greater than 1 g (Mann, 1984; Webster and Mann, 1984; Wilson, 1984; Hough et al., 2009). Whether gold nuggets or grains are derived from a primary source or precipitated from a soluble gold complex within groundwater systems (Liversidge, 1893), their occurrence in natural system are important from an exploration perspective since the "nugget effect" poses challenges for accurate gold estimations in geochemical surveys. Gold nuggets and grains can be mechanically reshaped and altered when exposed to physical weathering conditions in fluvial environments; therefore, the size and shape of nuggets are not well correlated with transport from primary gold sources (Yeend, 1975; Giusti, 1986; Watterson, 1992; Knight et al., 1999). Physical alterations of gold nuggets and grains include smooth surface textures with round and flat morphologies that are generally attributed to flow rate and bed load within fluvial systems. Although gold grains do not have high economic significance, their morphology and surface texture are similar to gold nuggets. Therefore, many studies have used gold nugget and grain morphologies in association with chemical composition as tools for gold exploration (see Boyle, 1979; Desborough, 1970; Hallbauer and Utter, 1977; Antweiler and Campbell, 1977, 1982; Giusti and Smith, 1984; Sauerbrei et al., 1987; Mosier et al., 1989; Grant et al., 1991). However, gold grain distribution within fluvial systems is broader than that of nuggets since their dispersion is closely associated with the deposition of finer and lighter host-sediment such as suspended pebbles, sand and mud (Nesterenko and Kolpakov, 2007, 2010).

Secondary gold structures, e.g., colloids, octahedral platelets, crystalline gold and bacteriomorphic gold, occurring on the nanometre- to micrometre-scale are generally considered "invisible" from a exploration perspective yet are likely ubiquitous in natural environments (Hough et al., 2008). The significance of secondary gold structures is that they are common characteristic features found on both nugget and grain surfaces. However, secondary gold structures are not always indicative of transport since gold precipitation and

silver leaching can occur contemporaneously leading to enriched gold rims on grains (Yeend, 1975; Giusti, 1986; Watterson, 1992; Youngson and Craw, 1993; Southam, 1998; Marquez-Zavalia et al., 2004; Reith et al., 2006). Abiotic precipitation of secondary gold nanoparticles and platelets can occur in the natural environment (Hough et al., 2008); however, biological material acting as catalysts for secondary gold precipitation has been proposed (Freise, 1931). More recently, studies involving the exposure of Bacteria, Archaea and bacterially-produced metabolites to various soluble gold complexes have demonstrated the direct and indirect affects of the biosphere on the geochemical cycling of gold in surface and near-surface environments (see Southam and Beveridge, 1994, 1996; Southam and Saunders, 2005; Lengke and Southam, 2006, 2007; Reith and McPhail, 2006; Lengke et al., 2006a,b, 2007; Reith et al., 2006, 2007, 2009, 2011; Kenney et al., 2012; Johnston et al., 2013). In these studies, biogeochemical processes catalyse the immobilisation of soluble gold forming secondary gold structures.

It is reasonable to suggest that, given enough time, the accumulation of bacterial immobilised gold could lead to the growth of larger structures as gold nuggets and grains in enriched environments such as fluvial placer deposits. In this study, I document the formation of gold nuggets and grains in a laboratory model representing a fluvial system. By using an increased amount of both bacteria and gold, I "track" and characterise the occurrence of gold and the development of various structures over time using geochemical and electron microscopy analytical techniques.

## 6.1 Materials and Methods

### 6.1.1 Host-sediment - biosphere

In this experiment, bacteria-gold biofilms on quartz sand were obtained from sediment-layered columns used in a previous study by Lengke and Southam (2007). The sand was used for this study because the columns also contained sulphur-reducing bacteria (SRB) and secondary gold (see section 6.1.2). For this experiment, 100 g of sand grains ranging from 100 µm to 200 µm in diameter and possessing $2.0 \times 10^7$ sulphate-reducing bacteria/g sand was used as the initial host-sediment representing a homogeneous alluvium (see section 6.1.3).

A consortium of viable sulphur-reducing bacteria was obtained from a 3.2 km deep subsurface borehole from the Drienfontein gold mine, Witwatersrand basin, South Africa (see Moser et al., 2003). Initial bacterial enrichments were cultured and maintained as a stock (see Lengke and Southam, 2007) in the modified medium defined by Postgate (1984). For this study, "fresh" bacterial enrichments were obtained by inoculating 1 mL aliquots of SRB stock into 12 mL of the same modified medium in screw-cap borosilicate glass tubes, and incubation at room temperature (RT; approx. 22˚C) for three weeks. The population of SRB was determined using scanning electron microscopy (SEM) of a filtered culture corresponding to approx. 1 pL (50 μm × 10 μm with a depth of view approx. 2 μm). Bacterial counts from SEM micrographs estimated $4.5 \times 10^8$ cells/mL after three weeks of incubation (Fig. 6.1a) and 26 ml of this bacterial enrichment were added to the host-sediment to ensure that an active population of sulphate reducing bacteria was present (see section 6.1.3).

Iron-oxidising bacteria were sampled and cultured from fine-grained iron oxide (see Fernandez-Remolar et al., 2005 for mineralogy) collected from the Tinto River near Berrocal, Huelva, Spain (see Chapter 2). Briefly, these enrichments were obtained by inoculating 0.5 mL of the sample into 4 mL modified media defined by Silverman and Lundgren (1959) with 0.5 mL of 33.3 g/ 100 mL ferrous sulphate heptahydrate ($FeSO_4 \cdot 7H_2O$) and pH adjusted to 2.3 using 2 M sulphuric acid. Enrichments were incubated at RT for three weeks in Fisherbrand® 13 × 100 mm borosilicate glass test tubes with plastic push caps to maintain aerobic conditions. A second enrichment was used for an estimate cell count using the Most Probable Number (MPN) statistical method described by Cochran (1950). Five culture tubes, each containing approx. $1.2 \times 10^5$ bacteria/culture tube (Fig. 6.1b) were also added to the host-sediment.

The SRB's and iron-oxidising bacteria are comparable in mass to the model bacterium, *Escherichia coli* (Neidhardt et al., 1990). Therefore, the combined mass of bacteria from the SRB enrichment and from the iron-oxidising bacterial enrichments, added to the host-sediment, was approx. 13.7 mg.

A sample of filamentous cyanobacteria with associated heterotrophs was obtained from a wetland near Atlin, British Columbia, Canada and enriched as a bacterial stock (see Power et

al., 2007). For this study, fresh cyanobacterial enrichments were obtained by inoculating 10 ml of the stock culture into 90 ml modified BG-11 medium (Rippka et al., 1979) and incubating at RT in the presence of natural light for three months (Fig. 6.1c). After the three month incubation period, the cyanobacteria-dominated enrichment was stirred and agitated to evenly disperse the biofilms in solution for addition to the host-sediment (see section 6.1.2). Three 20 mL aliquot were rinsed with distilled, deionised water to remove any salts derived from the growth medium and collected on a 0.45 µm pore-size filter. The filtered aliquots were air-dried at RT for 24 hours to determine an average dry weight of organic material (approx. 500 mg/20 ml).

Pebbles, composed primarily of carbonate minerals, ranging from 8 mm to 20 mm in diameter were rinsed three times with sterile, distilled deionised water and autoclaved. Sterile pebbles (approx. 100 g) were added to the quartz sand at week fourteen to create a heterogeneous host-sediment alluvium.

### 6.1.2 Gold

Secondary gold structures were the source of gold used in this experiment. These structures were previously formed either by biotic or abiotic reduction of soluble gold (III) chloride and gold (I) thiosulphate complexes. Secondary gold associated with sand and sulphur-reducing bacteria from the columns occurred as nanometre- to micrometre-size colloids, octahedral platelets and foils that formed through biomineralisation and bioaccumulation processes (see Lengke and Southam, 2007). For my experiment, these secondary gold structures represented biotic reduction of soluble gold. Additional gold colloids formed by photochemical and iron oxidising bacterial cultures (see Chapter 2) represented abiotic and mixed biotic/abiotic processes leading to the reduction of soluble gold complexes, respectively.

### 6.1.3 Experimental system assemblage

An experimental system was constructed in a cylinder of a Chicago Electric® rotary tumbler. The experimental system was a laboratory model representing a suboxic riverbed / fluvial environment in which placer gold deposits are known to occur. A detailed quantification of each constituent is listed in Table 6.1. The initial experimental system contained approx.

100 g quartz sand and a calculated 525.78 mg gold. The SRB, iron-oxidising bacterial and cyanobacterial enrichments were added to increase the biodiversity of the experimental system, i.e. representing a simplified "natural" bacterial ecosystem, and to increase the total amounts of organic material. The total amount of organics at the beginning of the experiment was approx. 534 mg. Distilled, deionised water was filtered-sterilised using a 0.1 µm pore-size filter and added to the experimental system to give a total fluid volume of 500 mL, which was then capped. It should be noted that the conditions within the experimental system represented a suboxic environment because the cylinder still contained headspace and the cap was not airtight. The death and decomposition of cyanobacteria, due to inadequate light for photosynthesis, could provide a source of nutrients for sulphur-reducing bacterial metabolism (see Freise, 1931). In addition, iron-oxidising bacterial metabolism could be maintained through the periodic input of oxygen supporting oxidation of iron sulphides formed as a by-product of sulphur-reducing bacterial metabolism. The amount of bacteria and gold used in the experimental system represented amplified fluvial systems. Increased amounts of bacteria and gold enabled a more rapid biogeochemical gold cycling in a laboratory setting and sufficient material for sampling and analysis using scanning and transmission electron microscopy.

### 6.1.4 Running and maintenance of the experimental fluvial system

The experimental system was rotated at 60 rpm for 24 hours once a week for sixteen weeks to represent punctuated episodes of fluvial activity. Every four weeks, a 20 mL aliquot of the cyanobacterial enrichment was added to the experimental system to provide a source of nutrients to sustain sulphur-reducing bacterial metabolism. Equivalent aliquots of cyanobacterial enrichments were rinsed, dried and weighed in the same manner and purposes previously described in section 6.1.1. Details of the dry weights of cyanobacterial enrichments added to the experimental system are listed in Table 6.1. At the beginning of the fourteenth week of the experiment, approx. 100 g of pebbles was added to the experimental system, which was rotated in the same manner for an additional two weeks. The purpose for adding pebbles was to compare the effect of a heterogeneous host-sediment on gold nuggets and grains that initially formed in the sand, i.e., a homogeneous host-sediment.

### 6.1.5 Experimental system sampling

Solid constituents, i.e., sand, biofilms, clay-size particles and gold, were sampled either with sterile forceps, scoopula or pipette from the experimental system at four week intervals. At the end of sixteen weeks, the entire experimental system was panned as a "traditional" extraction method to recover gold that remained in the system. The sampled gold was weighed and recorded. All solid constituents were initially analysed using a Zeiss Lumar V12 stereo light microscope equipped with a Retiga 1300 digital camera. A triage of selected, representative samples were prepared for further analysis using either scanning or transmission electron microscopy (see sections 6.1.6 and 6.1.7). Furthermore, two 5 mL aliquots of the experimental system fluid phase were sampled at bi-week intervals and filtered twice with a 0.1 μm pore-size filter to remove any solid material. The pH was measured using a Denver Instrument Basic pH Meter with an electrode calibrated to pH 7 and 10 reference standards using potassium biphthalate buffer at RT. Uncertainties of pH measurements were ±0.04 pH units. The filtered aliquots were acidified to pH 1 with concentrated (71%) nitric acid and analysed for soluble gold using a Perkin-Elmer Optima 3300-DV Inductively Coupled Plasma-Atomic Emission Spectrometer (ICP-AES). Soluble gold concentrations were converted to equivalent masses based on the fluid volume of the reaction system, with uncertainties of ± 4.71 mg. These mass equivalents, calculated total gold mass added to the experimental system and weighed, gold nugget and grain samples were used to determine the final amount of gold at the end of the experiment.

### 6.1.6 Scanning electron microscopy-energy dispersive spectroscopy

Sulphur-reducing bacterial, iron-oxidising bacterial and cyanobacterial enrichments along with sampled gold, sand and clay-size particles were prepared for Scanning Electron Microscopy-Energy Dispersive Spectroscopy (SEM-EDS). All samples were fixed with $2\%_{(aq)}$ glutaraldehyde for 24 hours, dehydrated in sequential $25\%_{(aq)}$, $50\%_{(aq)}$, $75\%_{(aq)}$ and 3 × 100% ethanol series and dried using a Tousimis Research Corporation Samdri-PVT-3B critical point drier. Each sample was then mounted on separate aluminium stubs using Electron Microscopy Sciences 12 mm carbon adhesive tabs. A Denton Vacuum Desk II sputter coater was used to deposit a 5 nm thick osmium coating to prevent charging effects during SEM analysis. A LEO Ziess 1540XB Field Emission Gun-Scanning Electron

Microscope (FEG-SEM) equipped with an Oxford Instruments' INCAx-sight Energy Dispersive Spectrometer (EDS) operating at 3 kV and 10 kV accelerating voltage was used for imaging and qualitative elemental composition of each sample.

### 6.1.7 Transmission electron microscopy – Energy Dispersive X-ray Spectroscopy

Biofilms, sampled from the experimental system, were prepared for Transmission Electron Microscopy-Energy Dispersive Spectroscopy (TEM-EDS). The biofilms were fixed in $2\%_{(aq)}$ glutaraldehyde for 2 hours, enrobed in $2\%_{(wt/vol)}$ noble agar, dehydrated in a $25\%_{(aq)}$, $50\%_{(aq)}$, $75\%_{(aq)}$ and $3 \times 100\%$ acetone series and embedded in Epon plastic. The embedded biofilms were cut to 70 nm ultrathin sections using a Reichert-Jung Ultracut E ultramicrotome and collected on Formvar-carbon coated, 200-square mesh copper grids. A 10 µL aliquot of the experimental system fluid phase was sampled after eight weeks and prepared as a whole mount for TEM-EDS. All samples were imaged using a Phillips CM-10 Transmission Electron Microscope (TEM) operating at 80 kV. Qualitative elemental analysis was determined using a Philips 420 TEM equipped with an EDS Genesis x-ray microanalysis system operating at the same voltage.

## 6.2 Results

### 6.2.1 Aqueous geochemical analysis

Detailed aqueous geochemical results of the experimental system are found in Table 6.2. The pH of the fluid phase consistently remained circumneutral. Although the majority of calculated gold added to experimental system occurred as secondary gold, ICP-AES analysis indicated that an equivalent 49.2 mg gold (98.1 mg/L) was "dissolved" at the beginning of the experiment. ICP-AES analysis further indicated that approx. 10% gold consistently remained dissolved over the course of sixteen weeks. However, the amounts of gold in solution at four and six weeks were greater than the amount that was measured at the beginning of the experiment.

### 6.2.2 Sand grains

When the experimental system contained a homogeneous host-sediment, the quartz sand grains generally appeared smooth with nanometre-size, black particles, i.e., FeS derived from

SRB metabolism (Fortin et al., 1994), attached to the surface (Fig. 6.2a). However, after the addition of pebbles, surfaces of sand grains appeared to have greater angular-shaped crevices. Portions of the grains also had a slight metallic lustre. High-resolution SEM micrographs confirmed the presence of angular surface "fractures" and EDS spectra confirmed the presence of nanometre-size gold colloids that were aggregated and embedded in depressions on the grain surface (Fig. 6.2b, c).

### 6.2.3 Organics

After two weeks, a black biofilm coated the inside surface of the rotary tumbler and centimetre-size pieces of the same biofilm were also observed within the sand. The black appearance was attributed to the formation of iron sulphides (Fortin et al., 1994) described in section 6.2.2. Over time, the relative abundance of biofilm forming on the inner surface increased. As the biofilm grew, an increasing number of gold grains and "leaf" were found within the biofilm (Fig. 6.3a). Low-resolution TEM micrographs of the black biofilm, sampled eight weeks into the experiment, determined that nanometre- to micrometre-size gold particles were also trapped within the biofilm and some bacteria were completely mineralised (Fig. 6.3b). High-resolution TEM micrographs demonstrated that extensive gold mineralisation occurred extracellularly. Evidence of the cellular membranes was not observed although the cell structure remained intact (Fig. 6.3b). Gold particles were composed of octahedral platelets less than 80 nm and irregular-shaped colloids less than 10 nm (Fig. 6.3c). These gold particles were also associated with other an "amorphous" material composed of iron and sulphur (Fig. 6.3d). After the addition of pebbles to the experimental system, no biofilms were observed.

### 6.2.4 Electron translucent gold

After six weeks, the surface of the fluid phase had a slight metallic lustre that dissipated when the contents of the experimental system were stirred. High-resolution TEM micrographs of the whole mount sample illustrated individual, octahedral gold platelets less than 400 nm (Fig. 6.4a). Some platelets were more transparent than others and appeared as a stack (Fig. 6.4b). The whole mount sample also contained platelets and irregular-shaped gold colloids less than 5 nm in diameter. The same amorphous material previously observed on the extracellular surface of bacteria from the black biofilm was also present (Fig. 6.4c).

Analysis using EDS spectroscopy confirmed that the transparent material "floating" on the surface of the fluid phase was composed of iron and gold (Fig. 6.4d). After the addition of pebbles, the fluid phase surface no longer had a metallic lustre when the experimental system was opened.

### 6.2.5 Gold grains

Gold grains occurred primarily within the blackened, sulphidic biofilm and were first observed on the fourth week. Analysis by SEM microscopy indicated that gold grains had a long axis less than 100 µm and a perpendicular short axis less than 60 µm. Gold grains generally appeared as globular structures forming an overall semi-oval shape (Fig. 6.5a). The globular structures comprising the grains possessed various surface textures. Regions of higher topography had smooth and rounded textures and remnants of the filamentous cyanobacteria were observed (Fig. 6.5b). Regions of lower topography occurred as crevices in between the smooth and rounded areas. These crevices contained articulated micrometre-size structures including rosette-like structures, bacteriomorphic gold and euhedral crystals (Fig. 6.5c). High-resolution SEM microscopy indicated that gold also occurred as a micrometre-size, "lace-like" texture composed nanometre-size colloids. These delicate structures appeared to be attached to mineral grains composed of iron, oxygen and sulphur (Fig. 6.5d-f). Throughout the duration of the experiment, gold grains mainly occurred within the black biofilm. The relative amount of gold grains in the sand decreased over time as the size of gold leaf and nuggets "grew" (see section 6.2.6). After the addition of pebbles, the relative number of gold grains increased and grains were the only form of gold observed. However, these gold grains were smaller in comparison to the grains initially observed after four weeks. The morphology of these grains appeared more flat and discoidal in shape with a long axis less than 60 µm and a perpendicular short axis less 30 µm (Fig. 6.5g). Furthermore, planar surfaces were smooth and smaller crevices occurred primarily along the circumferential edge of the grains (Fig. 6.5h).

### 6.2.6 Gold leaf and gold nuggets

Six gold leaf samples and one nugget were first observed within the quartz sand host-sediment after four weeks. The gold leaf structures were similar in shape to the grains but were much larger, having a long axis less than 600 µm and a perpendicular short axis less

than 200 µm (Fig. 6.6a). Furthermore, textures including smooth and rounded surfaces of topographically high regions and articulated crevices were also similar to those observed on gold grains (Fig. 6.6b). Gold nuggets were cylindrical in shape with a long axis less than 4.5 mm and perpendicular short axis less than 2 mm (Fig. 6.6c). The morphology suggests that nuggets were composed of an accumulation of folded and curled gold leaf structures (Fig. 6.6d, e). The majority of the nugget surfaces were smooth and rounded and were similar to topographically higher regions on gold grains and leaf. Nanometre-size textures including bacteriomorphic gold and micrometre-size textures including globular structures and euhedral gold crystals also occurred within crevices (Fig. 6.7a). These structures were "protected" from mechanical weathering. A rod-shaped bacterium and organic material from the addition of the bacterial enrichments were found within deeper crevices. However, unlike the black biofilm they did not demonstrate extensive extracellular mineralisation. The organic material appeared as a coating on the gold surface (Fig. 6.7b). By twelve weeks, 22 gold leaf "grains" and 4 nuggets were observed within the experimental system as the relative amount of gold grains decreased. Some gold leaf and nuggets were comparable in size to those observed after four weeks although others appeared slightly larger. After the addition of pebbles, all gold leaf and gold nuggets were no longer present within the experimental system.

### 6.2.7 Flocculant

One week after the addition of carbonate pebbles, the experimental system contained an opaque, grey flocculate material that made the fluid phase appear cloudy when agitated. The flocculate was micrometre-size aggregates composed of nanometre-size particles (Fig. 6.8a, b). Elemental analysis using EDS spectroscopy indicated that the flocculant was composed of aluminium, calcium, magnesium, sodium and oxygen (Fig. 6.8c) and suggests that these particles were likely derived from the weathering of the pebbles since the hardness of the quarts sand (Hardness = 7) was greater than that of the pebbles. Gold particles with longest dimensions less than 10 µm occurred with the flocculated material. These gold particles were irregular in shape with generally smooth, flat planar surfaces and resembled the textures observed on gold grains after the addition of pebbles (Fig. 6.8d).

### 6.2.8 Experimental system gold balance

Throughout the experiment, a total of 243.65 mg of "solid" gold was sampled from the experimental system and constituted approx. 46% of the total amount of gold (525.78 mg) initially added at the beginning of the experiment. By the end of the sixteen weeks, an equivalent of 47.04 mg gold was dissolved in solution indicating that approx. 44% of the immobilised gold was unrecovered and presumably occurred as microscopic particles.

## 6.3 Discussion

The formation of gold nuggets within placer deposits has been scientifically debated and various studies have attributed it to either detrital (see Giusti and Smith, 1984; Knight et al., 1999; Hough et al., 2007) or accretionary processes (Bowles, 1988; Clough and Craw, 1989; Youngson and Craw, 1993). More recently, Reith et al. (2010) proposed an alternative model advocating a biogeochemical process in which primary gold sources, secondary gold mineralisation and aggregation processes are integrated. By applying these biogeochemical processes, the primary purpose of this study was to "grow" a gold nugget. The biogeochemical laboratory model combined organic material, host-sediments and secondary gold into an experimental system representing an amplified natural fluvial environment in which placer gold can occur.

Approximately 90% of the total gold added to the experimental system, occurred as secondary gold colloids, platelets and foils derived from biotic and abiotic reduction of soluble gold (III) chloride and gold (I) thiosulphate complexes. At the end of sixteen weeks, the experimental system contained approx. 2.5 g of organic material mainly derived from the addition of cyanobacterial enrichments. Lengke et al. (2006b) demonstrated that the exposure of filamentous cyanobacteria to soluble gold (III) chloride precipitated nanometre-size, amorphous gold (I) sulphide and octahedral gold platelets. Furthermore, other studies have demonstrated the immobilisation of soluble gold complexes as secondary gold structures by various metabolising and non-metabolising bacteria (see Reith and McPhail, 2006; Reith et al., 2006, 2007, 2009; Southam and Beveridge, 1994, 1996; Lengke et al., 2006a, 2007; Kenney et al., 2012; Song et al., 2012; Shuster et al., 2013a). Therefore, it is surprising that the abundance of organic material in the experimental system did not immediately reduce the 10% of the total gold that remained in solution. Rather, ICP-AES

analysis indicated that gold remained in solution despite the abundance of organic material and that the amount of soluble gold even increased slightly by the fourth week. Studies by Baker (1978) demonstrated that humic acids are capable of dissolving elemental gold by forming soluble complexes that could be mobilised in surface environments. Similarly, studies by Korobushkina et al. (1974, 1976) indicated that elemental gold could be solubilised under neutral to alkaline conditions by bacterially produced amino acids. In this study, the lack of sunlight for photosynthesis would have caused the death of cyanobacteria. The decomposition of cyanobacteria could have led to the release of amino acids that subsequently dissolved gold. It is also a possibility that bacteria were indirectly responsible for gold solubilisation. SRB produce hydrogen sulphide as a by-product of their active metabolism (Reaction 6.1). After the addition of SRB to the experimental system, the cylinder was closed but not completely sealed making the system suboxic. Partial oxidation of hydrogen sulphide could have occurred over time resulting in formation of thiosulphate (Reaction 6.2). It is possible that elemental gold in the experimental system was dissolved through thiosulphate leaching thereby forming soluble gold (I) thiosulphate complexes in solution (Aylmore and Muir, 2001; Reaction 6.3).

$$2\ CH_2O + SO_4^{2-} \rightarrow H_2S + 2\ HCO_3^- \quad (6.1)$$

$$4\ HS^- + 3\ O_2 \rightarrow 2\ S_2O_3^{2-} \quad (6.2)$$

$$4\ Au^0 + 8\ S_2O_3^{2-} + O_2 + 2\ H_2O \rightarrow 4\ Au(S_2O_3)_2^{3-} + 7\ OH^- \quad (6.3)$$

Growth of the biofilm over time was attributed to a continuous supply of nutrients from the decomposition of cyanobacteria. The black colour of the biofilm was identified as a nanometre-size, amorphous material composed of iron and sulphur based on the TEM-EDS analysis (Fig. 6.3a, c, d). Therefore, the biofilm was interpreted as a bacterial consortium containing SRB since these microorganisms are responsible for low temperature iron sulphide formation (Trudinger et al., 1985). As mentioned earlier, the decomposition of cyanobacteria forming amino acids led to gold solubility. However, the same organic material provided reactive groups that may have contributed to gold precipitation and also nutrients for the growth of the remaining bacterial consortium that increasingly trapped nanometre- and micrometre-size gold colloids and platelets (Fig. 6.3b) found floating in the fluid phase (Fig. 6.4). Studies have demonstrated that the negative charge of bacterial cell surfaces are capable of binding metal (Daughney et al., 1998; Beveridge and Fyfe, 1985). In

this study, the extensive gold mineralisation observed on extracellular bacterial surfaces can be attributed to either passive mineralisation of soluble complexes from solution or the accumulation of previously formed secondary gold structures. From a gold biogeochemical cycling perspective, either mode is important because gold solubility, e.g., amino acid and potentially thiosulphate leaching, was counter-balanced by gold biomineralisation. This cycling provides a plausible explanation for the relatively consistent amount of soluble gold present in this experimental system while gold grains and gold nuggets continued to grow.

In this study, the presence of the biofilm in association with a heterogeneous host-sediment was important for the formation and accumulation of gold grains. It is important to note that the majority of gold added to the experimental system occurred as nanometre- and micron-size secondary gold structures previously formed by biotic and abiotic reduction of soluble gold complexes. The accumulation and aggregation of secondary gold structures within the biofilm were subjected to episodes of punctuated fluvial activity and biogeochemical cycling in the homogeneous host-sediment, i.e., quartz sand, and led to the formation of gold grains. This overall process was described by Freise (1931) and provided a plausible explanation for the contemporaneous occurrence of gold grains associated with secondary gold trapped within the biofilm (Fig. 6.3a). The size of gold grains and the occurrence of secondary gold structures on the surface of grains, sampled from the experimental system, were analogous to those observed in previous studies (Fig. 6.5a, b; see Yeend, 1975; Hallbauer and Utter, 1977; Giusti, 1986; Watterson, 1992; McCready et al., 2003). The smooth and rounded gold surfaces of topographically high regions were attributed to the mechanical reshaping by fluvial activity within the homogeneous host-sediment. In contrast, crevices were topographically low crevices protected secondary gold structures from physical abrasion by the sand. Within these crevices a wide range of textures was observed. Hough et al. (2008) suggested that the evaporation of gold ligands results in the bulk precipitation of gold. The presence of euhedral and rosette-like gold crystals (Fig. 6.5c), in grain crevices, suggest that the formation of these “larger” structures could be attributed to abiotic seeding and nucleation processes. However, the co-occurrence of micrometre-size bacteriomorphic gold was consistent with the spheroidal, cell-like structures observed on gold grains by Reith et al. (2006). Schoonen et al. (1992) demonstrated that nanometre-size colloids, suspended in

solution, rapidly adsorb to iron- and sulphur-bearing mineral substrates such as pyrite and goethite.

In this study, mineral grains composed of iron and sulphur were associated with lacy-like gold structures within creviced regions of the gold grain (Fig. 6.5d-f). It is reasonable to suggest that these iron- and sulphur-bearing minerals were derived from the by-product of active SRB metabolism and were incorporated into crevices during the mechanical formation of gold grains within the biofilm. Furthermore, these minerals likely facilitated the adsorption of bacterially-produced, nanometre-size gold colloids resulting in the formation of the lace-like texture. The relative amount of gold grains gradually decreased over time as gold leaf and nuggets increased in size and abundance. Furthermore, the overall morphology and diversity of gold grain surface textures were consistent throughout the duration of the experiment until the addition of pebbles. The effect of a heterogeneous, host-sediment formed smaller gold grains relative to the size of grains formed in the quartz sand, i.e., a homogeneous host-sediment. The flat discoid shape and smoother planar surfaces with articulated peripheral edges were consistent with grains derived from natural environments (Fig. 6.5g, h; see Yeend, 1975; Hallbauer & Utter, 1977; Giusti, 1986; Watterson, 1992; Knight et al., 1999; Nesterenko and Kolpakov, 2007, 2010; Shuster et al., 2013b).

It is important to note that gold leaves are technically classified as grains based on their dimensions (Fig. 6.6a; Hough et al., 2009); however, gold leaf were categorised as a separate group of structures in this study because their temporal formation and location within the experimental system were more closely associated with gold nuggets than grains. The same diverse range of surface textures observed on grains was also found on gold leaf and nuggets (Fig. 6.6b, c). The difference between gold leaf and the grains was that leaves were slight larger and primarily occurred within the sand along with gold nuggets. It is a possibility that accumulated gold grains within the biofilm gradually aggregated into larger leaf structures during fluvial activity. However, as leaf size increased so did their weight thereby causing the leaf to detach from the biofilm and occur in the sand. As a result, gold nuggets likely formed in a similar manner via leaf accumulation in the sand and aggregation through sediment movement. This process highlights the importance of a biofilm for initiating the developmental accumulation of gold as nuggets. More importantly, this process provides a plausible explanation for: the occurrence of gold leaf and nuggets in the sand; the decreased

number of grains in the experimental system as the relative number and size of leaf and nuggets increased over time; and the appearance of nuggets as cylindrical structures that resembled folded and curled leaves (Fig. 6.6c, d). An interesting observation of gold nuggets was the retention of nanometre-size and micron-size gold structures, i.e., colloidal gold, octahedral gold platelets, bacteriomorphoic gold, despite the mechanical reshaping within, and by, the sand (Fig. 6.7a). The association of biofilms and bacteria attached to natural gold grain surfaces have been documented (Reith et al., 2006; Shuster et al., 2013b) while enrichment of secondary gold on natural grains has been observed (Fairbrother et al., 2012). In this study a rod-shaped bacterium along with remnants of organic material, interpreted as exopolymeric substances and potentially nanowires, were found in crevices of the nugget (Fig. 6.7b). This observation is important because the crevices provided "protection" for the bacterium from the deleterious impacts of physical weathering. The biogeochemical implications, as previously discussed for the biofilm, suggest that favourable conditions could promote bacterial growth into more structurally cohesive biofilms. The development of biofilms on the surface of gold nuggets could potentially lead to secondary gold enrichment or dissolution of gold at nugget surfaces.

In this study, sand grains appeared free of gold coatings throughout the experiment when the host-sediment was homogeneous (Fig. 6.2a). The homogeneous host-sediment contributed to gold nugget formation. However, the addition of the pebbles to sand represented a heterogeneous bed load in the experimental system that resulted in: the destruction of gold leaf and nuggets; the formation of abundant smaller grains (Fig. 6.5g, h); and an interestingly "re-coating of sand grain surfaces" with colloidal gold (Fig. 6.2b). More importantly, the physical weathering of pebbles caused the formation of clay-size flocculant material (Fig. 6.8a,b). Studies by Youngson and Craw (1993) and Hunlie et al. (1999) documented the occurrence of gold with clay particles. At the very end of the experiment only 46% of the total amount of gold added to the experimental system was recovered while 10% occurred as soluble gold in solution. The remaining 44% of unaccounted gold was attributed to the occurrence of "free" microscopic gold and flocculant material that "trapped" gold (Fig. 6.8d). However, unlike the ability of the biofilm to trap grains in a fixed location, particles derived from weathered pebbles promoted gold dispersion since conventional panning methods did not recover all gold particles. These findings are important because they indicates the extent

in which gold dispersion can occur within natural fluvial systems and potentially contribute to the over- or under-estimation of gold, e.g., nugget effect, during mineral exploration.

## 6.4 Conclusion

Abiotic and biotic processes are equally important for the formation of secondary gold structures and the growth of gold leaf and nuggets. These dynamic processes, integrated into a biogeochemical model, provide a better understanding of the accumulation of gold and the formation of gold nugget in natural environments. In this study, I constructed an experimental system that represented a fluvial environment containing amplified concentrations of gold and organics. The diverse gold occurrences, e.g., soluble gold, secondary gold structures and textures, were quantified and characterised throughout gold's "journey" to nugget formation. Gold initially occurred as soluble complexes and reduced secondary gold structures, i.e., foils, colloids, and octahedral platelets. Within the experimental system, however, the biofilm contributed to gold accumulation while movement within the host-sediment contributed to the aggregation of gold into larger structures. Characterisation of the different gold morphologies revealed that gold grains, leaf and nuggets all contained the same physical weathering textures attributed to the host-sediment and the same nanometre- and micrometre-size gold textures within creviced regions. The biosphere has a profound influence on the gold cycling in near-surface environments and therefore the processes proposed in the biogeochemical model for gold formation were applied to the experimental system in this study. The results contributed to the understanding of the biogeochemical formation of gold nuggets within a fluvial system and represented "snap shots" of gold accumulation and enrichment that can occur in placer gold deposits over geological time.

**Table 6.1.** List of constituents and respective amounts added to the experimental system.

| **Overview of experimental system constituents** | | |
|---|---|---|
| **Sediment** | | |
| **Source** | **Amount** | **Notes** |
| Sand | 100 g | see Lengke and Southam (2007) |
| Pebbles | 100 g | |
| Total sediment | 200 g | |
| **Gold** | | |
| **Source** | **Amount** | **Notes** |
| Columns | 145.78 mg | see Lengke and Southam (2007) |
| $AuCl_4$ | 180 mg | Photochemical reduction |
| $Au(S_2O_3)_2^{3-}$ | 200 mg | Reduction by $Fe^{3+}$ |
| Total gold | 525.78 mg | |
| **Bacteria** | | |
| **Source** | **Amount** | **Notes** |
| Sulphur-reducing bacteria (columns) | $2.0 \times 10^9$ bacteria | see Lengke and Southam (2007) |
| Sulphur-reducing bacterial enrichments | $1.17 \times 10^{10}$ bacteria | |
| Iron-oxidising bacterial enrichment | $6.0 \times 10^7$ bacteria | |
| **Nutrient** | | |
| **Source** | **Amount** | **Notes** |
| Cyanobacterial enrichment | 533.72 mg | added week 0 |
| Cyanobacterial enrichment | 487.48 mg | added week 4 |
| Cyanobacterial enrichment | 475.14 mg | added week 8 |
| Cyanobacterial enrichment | 475.07 mg | added week 12 |
| Cyanobacterial enrichment | 500.14 mg | added week 16 |

**Table 6.2.** A record of measured and calculated amounts of gold in association with pH and organics in the experimental system over time. Gold occurred in the solid and aqueous phase and is recorded in milligrams (mg). Total organic material is also recorded in mg.

| **Experimental system** | | | | | | | |
|---|---|---|---|---|---|---|---|
| **Week** | **pH** [a] | **Organics** | **$Au_{(s)}$ sampled** [a,b] | **$Au_{(aq)}$ sampled** [a,c] | **$Au_{(s)}$** | **$Au_{(aq)}$** [d] | **$Au_{(total)}$** |
| 0 | 5.92 | 547.42 | -- | 0.98 | 476.46 | 49.23 | 525.78 |
| 2 | 7.01 | 547.42 | -- | 1.12 | 468.93 | 55.86 | 524.79 |
| 4 | 6.91 | 1034.90 | 10.15 | 1.28 | 449.53 | 64.0 | 523.68 |
| 6 | 6.98 | 1034.90 | -- | 1.21 | 451.98 | 60.27 | 512.25 |
| 8 | 6.94 | 1510.04 | 12.13 | 1.13 | 442.41 | 56.5 | 511.04 |
| 10 | 7.05 | 1510.04 | -- | 1.04 | 445.84 | 51.94 | 497.78 |
| 12 | 6.85 | 1985.11 | 12.91 | 0.98 | 436.86 | 49.05 | 498.82 |
| 14 | 7.06 | 1985.11 | -- | 0.95 | 437.25 | 47.68 | 484.93 |
| 16 | 7.18 | 2471.50 | 208.46 | 0.94 | 228.47 | 47.04 | 483.98 |

[a] values obtained by measurement
[b] total weight of all sampled gold grains, leaf and nuggets from each sampling time
[c] ICP-AES analysis of soluble gold measured in (mg/L)
[d] mass equivalents converted to corresponding fluid volume in the experimental system

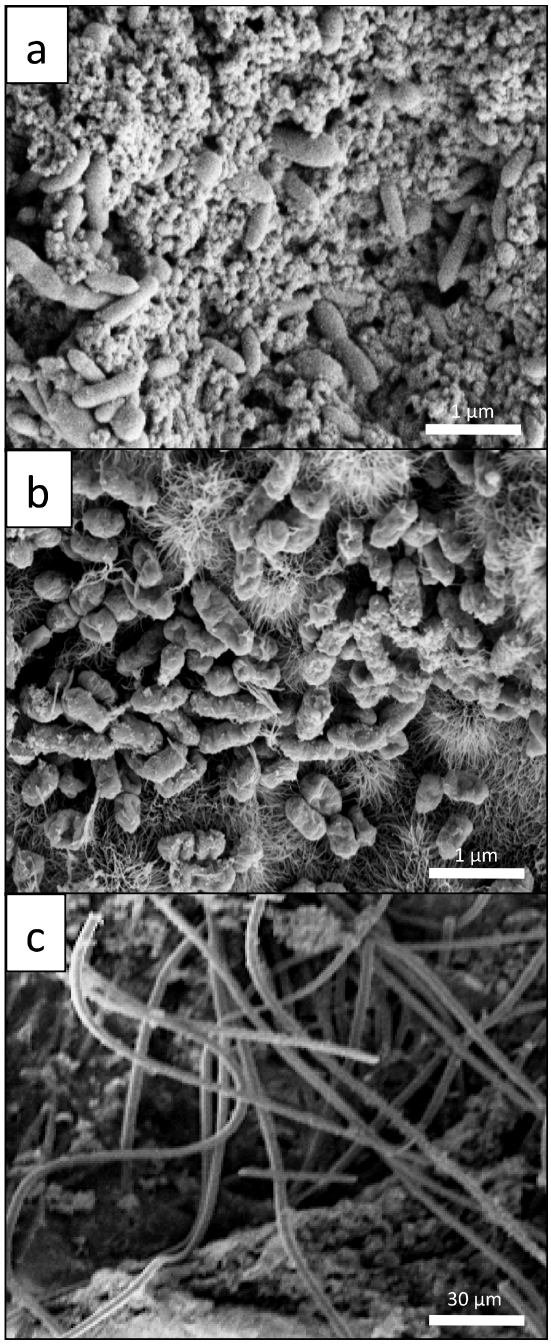


**Figure 6.1. SEM characterisation of bacterial enrichments.** High-resolution SEM micrographs of the sulphur-reducing bacterial enrichment (a), iron-oxidising bacterial enrichment (b) and cyanobacterial enrichment (c).

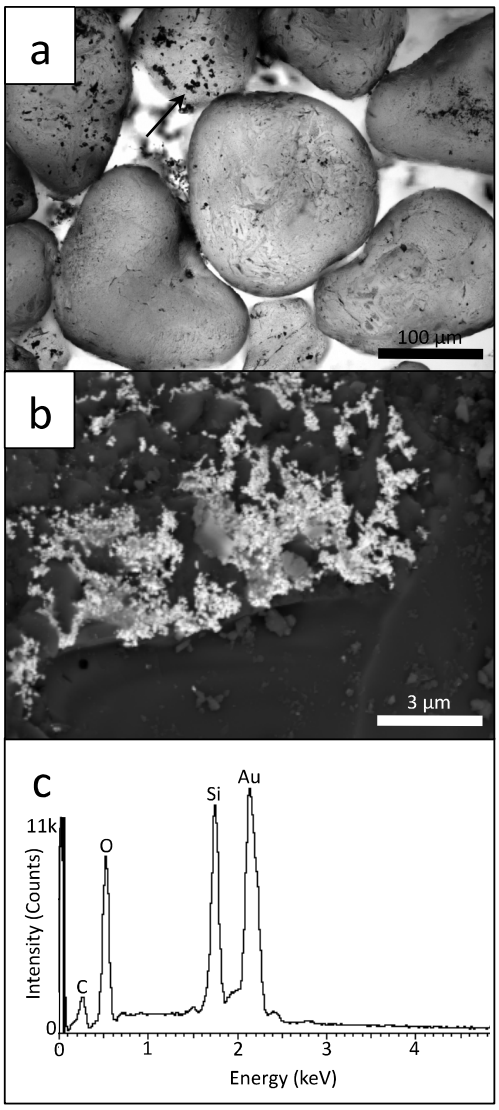


**Figure 6.2. A light micrograph and SEM-EDS characterisation of a host sediment.** A light micrograph of quartz sand grains added to the experimental system (a) with black particles attached to the surface (a, arrow). High-resolution SEM micrograph (b) and EDS spectrum (c) demonstrating the angular fracture and aggregates of nanometre-size gold colloids embedded on the sand grain surface at the end of the experiment.

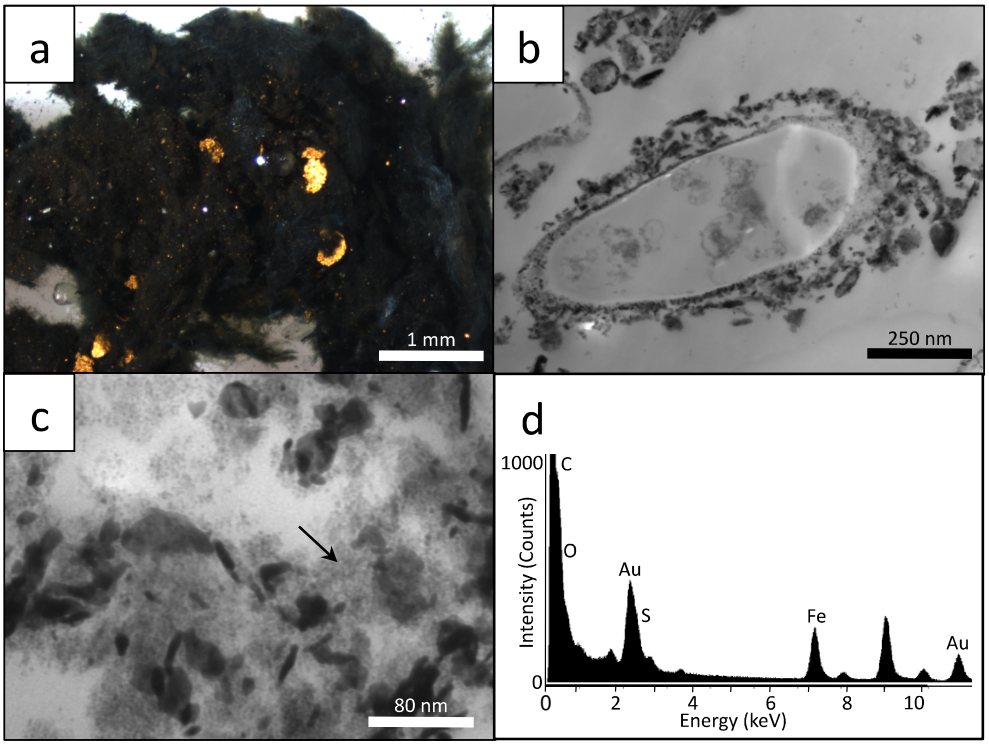


**Figure 6.3. A light micrograph and TEM-EDS characterisation of a gold-encrusted biofilm.** A light micrograph of the black biofilm, sampled after eight weeks, containing gold grain and leaf structures. These structures were less than 300 µm along the widest dimension (a). A low-resolution TEM micrograph of a gold-mineralised bacterium within the black biofilm (b). A high-resolution TEM micrograph (c) and EDS spectrum (d) demonstrated that extensive, extracellular gold mineralisation was composed of nanometre-size platelets and colloids. The associated amorphous material was composed of iron and sulphur (d, arrow). Note the unlabeled peak is Cu.

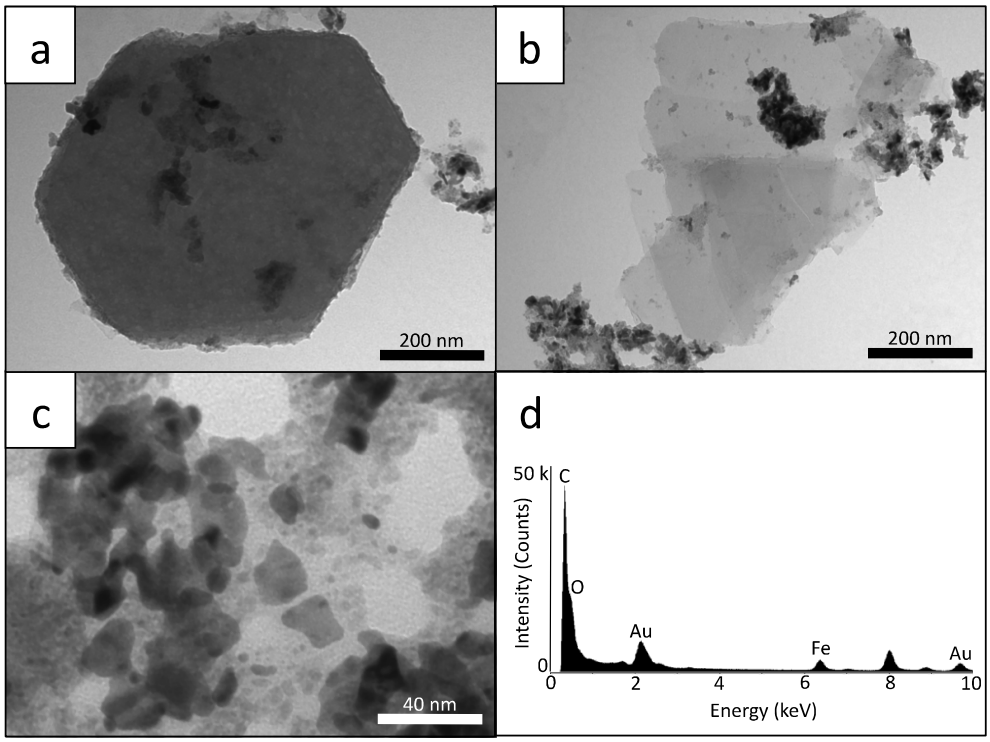


**Figure 6.4. TEM-EDS characterisation of translucent gold.** High-resolution TEM micrographs of transparent gold floating on the fluid surface sampled at eight weeks. Platelets less than 400 nm occurred individually (a). Pseudo octahedral platelets appeared more transparent and formed a layered stack (b). The floating metallic material was also composed of platelets less than 20 nm, irregular-shaped gold colloids and amorphous material containing Fe (c, d).

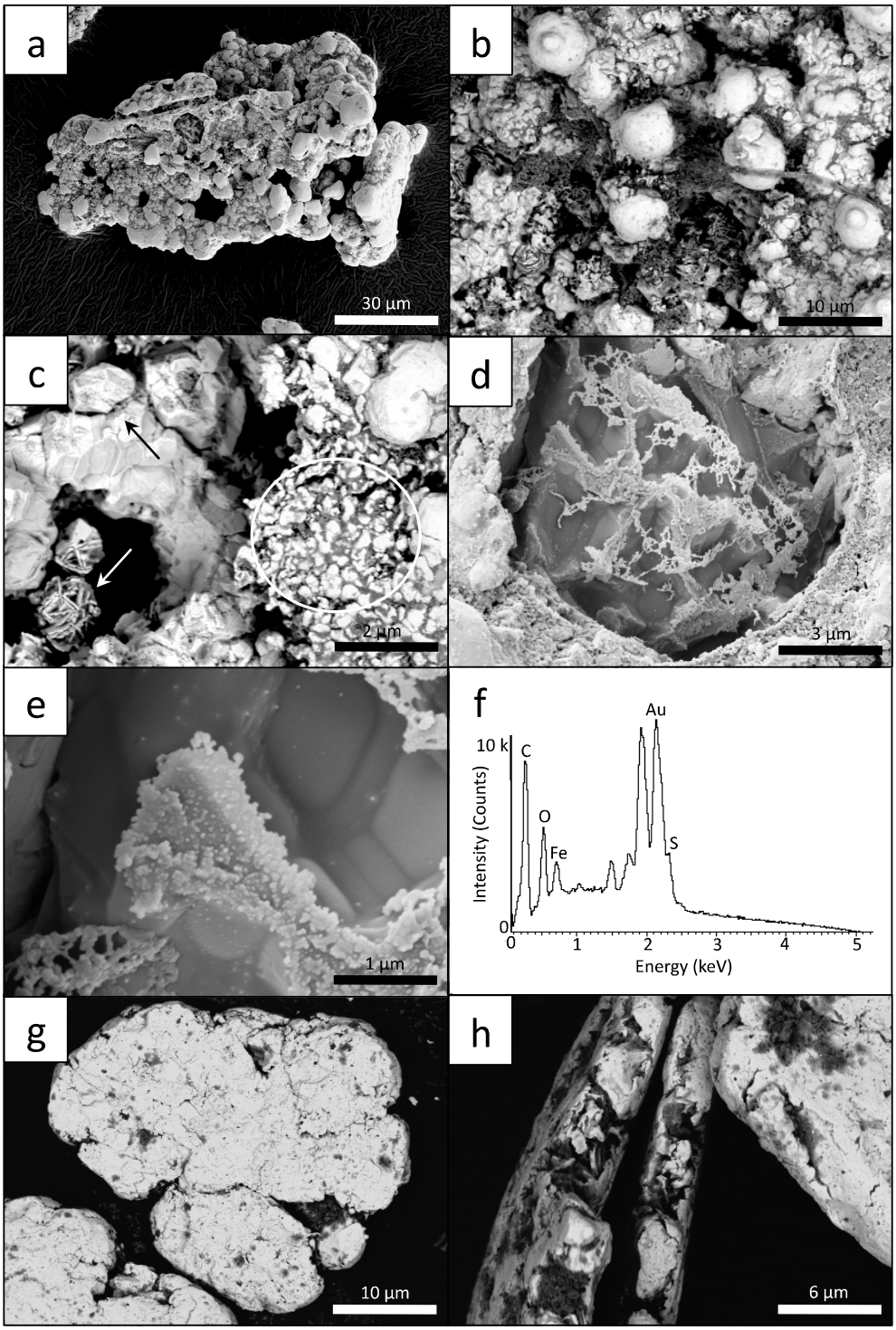


**Figure 6.5. SEM-EDS characterisation of gold grains.** A low-resolution SEM micrograph of a gold grain sampled after four weeks (a). The globular appearance of grains had smooth surface textures that were tens of microns in size with remnants of cyanobacteria (b). Creviced regions contained micrometre-size euhedral crystals (c, black arrow), bacteriomorphic gold (c, circle) and rosette-like structures (c, white arrow). High-resolution SEM micrographs of lace-like gold composed of nanometre-size gold colloids attached to a mineral grain composed of Fe, O and S (d-f). Low- (g) and high-resolution (h) SEM micrographs of small, flat and smooth gold grains after the addition of pebbles.

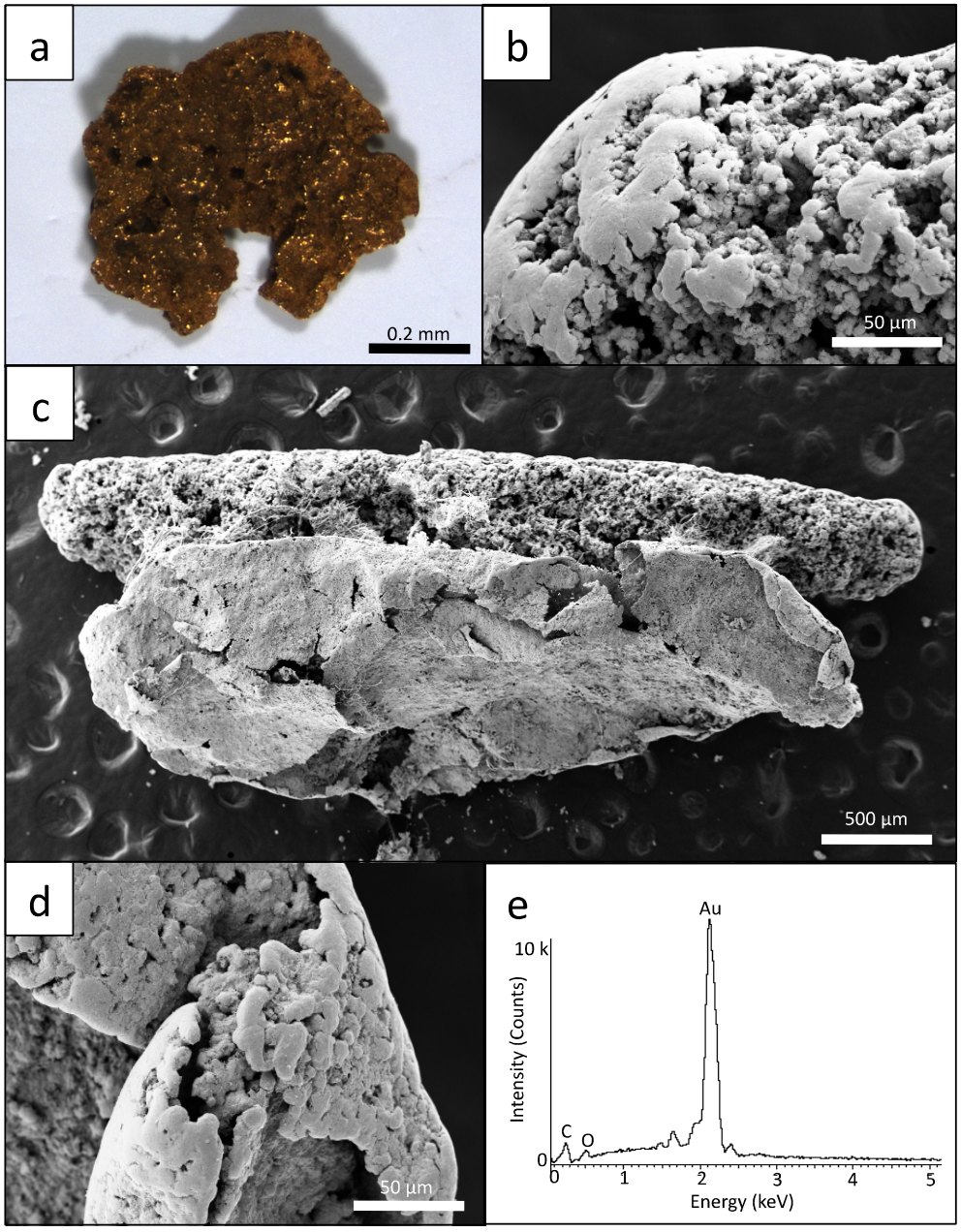


**Figure 6.6. SEM-EDS characterisation of gold leaf and nuggets.** A light micrographs of a gold leaf sampled after four weeks (a). A low-resolution SEM micrograph demonstrated the smooth and rounded textures of topographically high regions and the articulated textures of crevice that were similar to gold grains (b). A low-resolution SEM micrograph of a gold nugget sampled after eight weeks (c). The gold nugget appeared to be comprised of mechanically reshaped and accumulated leaf structures (d). EDS spectroscopy confirmed the nugget contained gold (e).

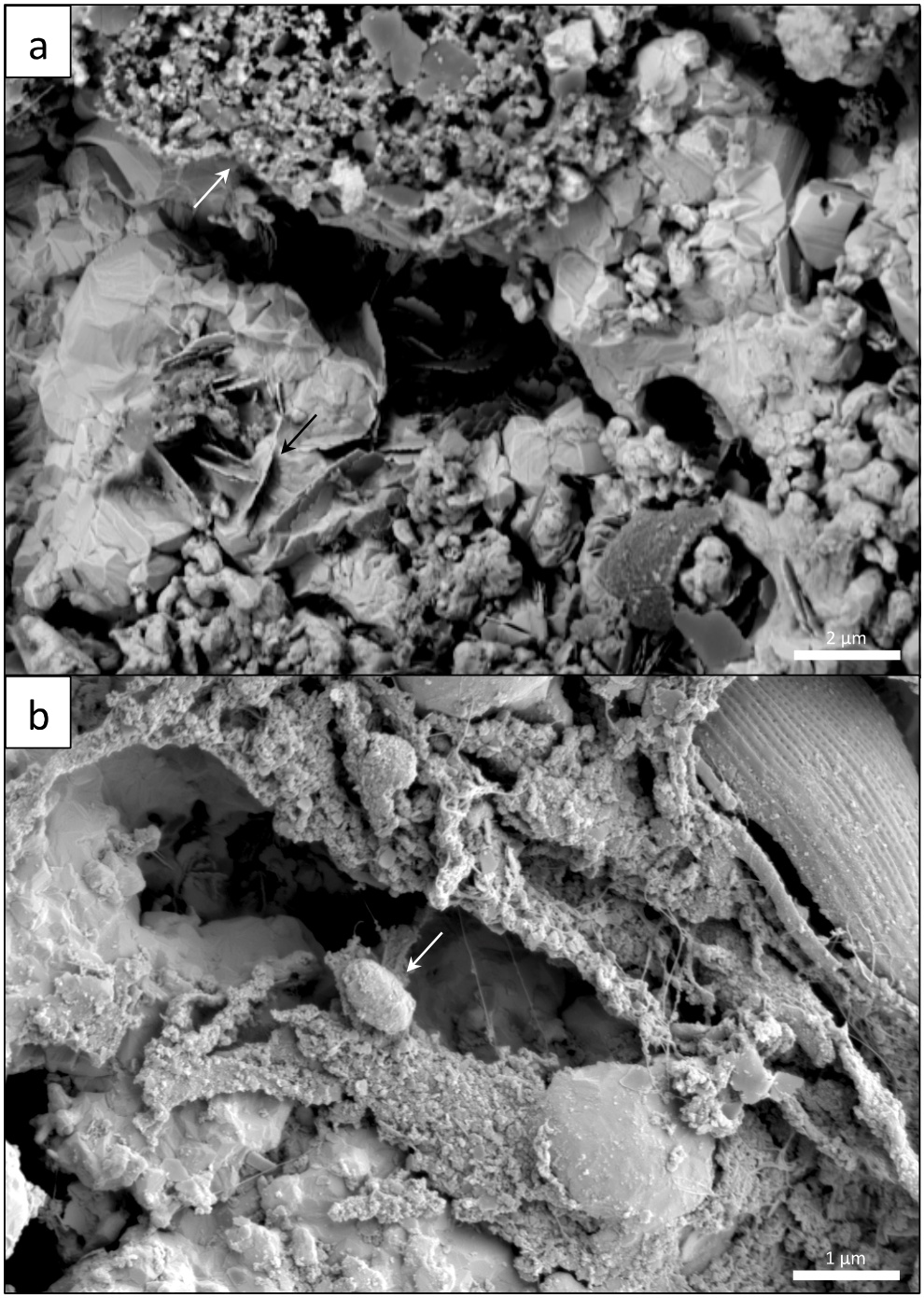


**Figure 6.7. SEM characterisation of creviced regions on a gold grain.** A high-resolution SEM micrograph of a creviced region from a gold nugget (a). Similar to gold grain and leaf crevices, bacteriomorphic gold (white arrow) and euhedral crystals were present. Micrometre-size gold platelets (black arrow) along with globular structures were observed. A high-resolution SEM micrograph demonstrating the occurrence of a rod-shaped bacterium and other organic material within a deep crevice from the gold nugget (b). The structure in the top right corner is interpreted to be a diatom likely derived from the cyanobacterial enrichment.

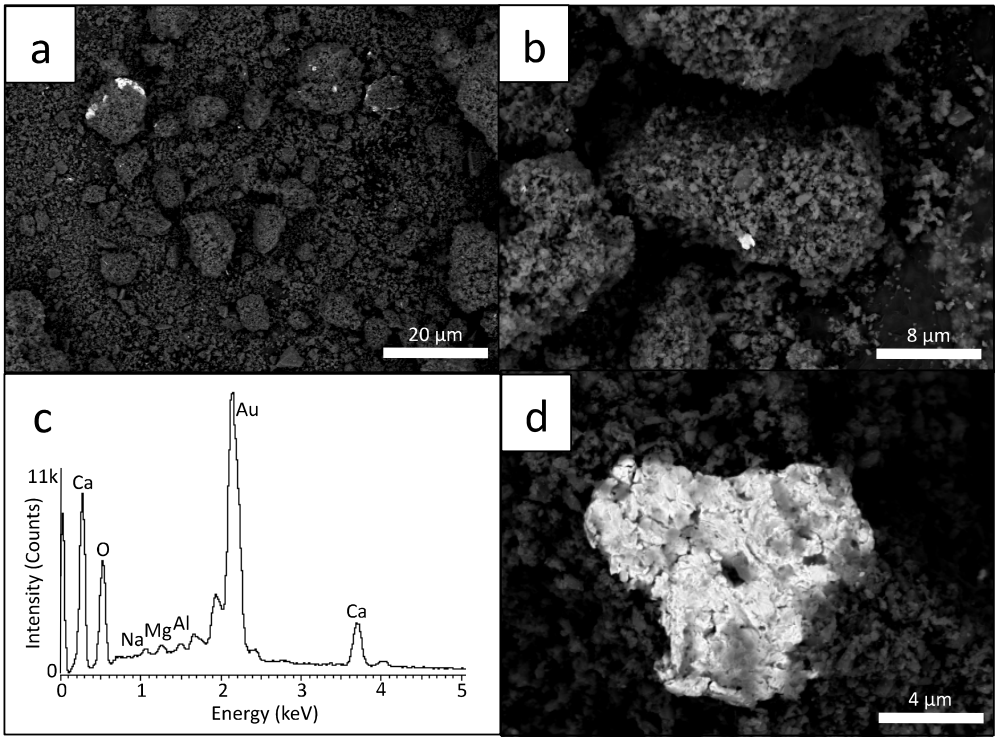


**Figure 6.8. SEM-EDS characterisation of a flocculate material and gold.** A low-resolution SEM micrographs of the flocculate material and gold sampled after fourteen weeks (a). The flocculate material was composed of particles less than 1 µm in size that formed larger aggregates (b). Flocculate particles were composed of Ca, O, Na, Mg and Al based on the EDS spectra (c). A high-resolution SEM micrograph of a gold particle "trapped" with in flocculate material (d).

## 6.5 References

Allen, M.M., 1968. Simple conditions for growth of unicellular blue-green algae on plates. Journal of Phycology 4, 1-4.

Antweiler, J.C., Campbell, W.L., 1977. Application of gold compositional analyses to mineral exploration in the United States. Journal of Geochemical Exploration, 8, 17-29.

Antweiler, J.C., Campbell, W.L., 1982. Gold in exploration geochemistry. In: Precious Metals in the Northern Cordillera. The Association of Exploration Geochemists, Calgary, 33-44.

Aylmore, M.G., Muir, D.M., 2001. Thiosulfate leaching of gold-a review. Minerals Engineering, 14, 135-174.

Baker, W.E., 1978. The role of humic acid in the transport of gold. Geochimica et Cosmochimica Acta, 42, 645-649.

Beveridge, T.J., Fyfe, W.S., 1985. Metal fixation by bacterial cell walls. Canadian Journal of Earth Science, 22, 1893-1898.

Bowles, J., 1988. Mechanical and chemical modification of alluvial gold. Bulletin and Proceeding of the Australian Institute of Mining and Metallurgy, 293, 9-11.

Boyle, R.W., 1979. The geochemistry of gold and its deposits. Geological Survey of Canada Bulletin, 280, 584.

Clough, D., Craw, D., 1989. Authigenic gold-marcasite association-evidence for nugget growth by chemical accretion in fluvial gravels, Southland, New Zealand. Economic Geology, 84, 953-958.

Cochran, W.G., 1950. Estimation of bacterial densities by means of the "Most Probable Number". Biometrics, 6, 105-116.

Daughney, C.J., Fein, J.B., Yee, N., 1998. A comparison of the thermodynamics of metal adsorption onto two common bacteria. Chemical Geology, 144, 161-176.

Desborough, G.A., 1970. Silver depletion indicated by microanalysis of gold from placer occurrences, western United States. Economic Geology, 65, 304-311.

Fairbrother, L., Brugger, J., Shapter, J., Laird, J.S., Southam, G., Reith, F., 2012. Supergene gold transformation: Biogenic secondary and nano-particulate gold from arid Australia. Chemical Geology, 320, 17-31.

Fernandez-Remolar, D.C., Morris, R.V., Gruener, J.E., Amils, R., Knoll, A.H., 2005. The Rio Tinto Basin, Spain: mineralogy, sedimentary geobiology, and implications for interpretation of outcrop rocks at Meridiani Planum, Mars. Earth and Planetary Science Letters, 240, 149-167.

Freise, F.W., 1931. The transportation of gold by organic underground solutions. Economic Geology, 26, 421-431.

Giusti, L., 1986. The morphology, mineralogy, and behaviour of “fine-grained” gold from placer deposits of Alberta: Sampling and implications for exploration. Canadian Journal of Earth Science, 23, 1662-1672.

Giusti, L., Smith, D.G.W., 1984. An electron microprobe study of some Alberta placer gold. Tschermaks Mineralogische und Petrographische Mitteilungen, 32, 187-202.

Grant, A.H., Lavin, O.P., Nichol, I., 1991. The morphology and chemistry of transported gold grains as an exploration tool. Journal of Geochemical Exploration, 40, 73-94.

Hallbauer, D.K., Utter, T., 1977. Geochemical and morphological characteristics of gold particles from recent river deposits and the fossil placers of the Witwatersrand. Mineralium Deposita, 12, 293-306.

Hough, R.M., Butt, C.R.M., Reddy, S.M., Verrall, M., 2007. Gold nuggets: supergene or hypogene? Australian Journal of Earth Sciences, 54, 959-964.

Hough, R.M., Noble, R.R.P., Hitchen, G.J., Hart, R., Reddy, S.M., Saunders, M., Clode, P., Vaughan, D., Lowe, J., Gray, D.J., Anand, R.R., Butt, C.R.M., Verrall, M., 2008. Naturally occurring gold nanoparticles and nanoplates. Geology, 36, 571-574.

Hough, R.M., Butt, C.R.M., Fischer-Buhner, J., 2009. The crystallography, metallography and composition of gold. Elements, 5, 297-302.

Hunlie, H., Qinyan, W., Jianping, C., 1999. Occurrence and distribution of invisible gold in the Shewushan supergene gold deposit, southeastern Hubei, China. The Canadian Mineralogist, 37, 1525-1531.

Johnston, C.W., Wyatt, M.A., Li, X., Ibrahim, A., Shuster, J., Southam, G., Magarvey, N.A., 2013. Gold biomineralisation by a metallophore from a gold-associated microbe. Nature Chemical Biology, advanced online publication.

Kenney, J.P.L., Song, Z., Bunker, B.A., Fein, J.B., 2012. An experimental study of Au removal from solution by non-metabolizing bacterial cells and their exudates. Geochimica et Cosmochimica Acta, 87, 51-60.

Knight, J.B., Morison, S.R., Mortensen, J.K., 1999. The relationship between placer gold particle shape, rimming and distance of fluvial transport as exemplified by gold from the Klondike District, Yukon Territory, Canada. Economic Geology, 94, 635-648.

Korobushkina, E.D., Chernyak, A.S., Mineev, G.G., 1974. Dissolution of gold by microorganisms and products of their metabolism. Mikrobiologiya, 43, 9-54.

Korobushkina, E.D., Mineev, G.G., Praded, G.P., 1976. Mechanism of the microgological process of dissolution of gold. Geokhimiya, 45, 535-538.

Lengke, M.F., Fleet, M.E., Southam, G., 2006a. Morphology of gold nanoparticles synthesized by filamentous cyanobacteria from gold(I)-thiosulfate and gold(III)-chloride complexes. Langmuir, 22, 2780-2787.

Lengke, M.F., Ravel, B., Fleet, M.E., Wanger, G., Gordon, R.A., Southam, G., 2006b. Mechanisms of gold bioaccumulation by filamentous cyanobacteria from gold (III)-chloride. Environmental Science and Technology, 40, 6304-6309.

Lengke, M.F., Ravel, B., Fleet, M.E., Wanger, G., Gordon, R.A., Southam, G., 2007. Precipitation of gold by reaction of aqueous gold(III)-chloride with cyanobacteria at 25-80°C – Studied by X-ray absorption spectroscopy. Canadian Journal of Chemistry, 85,1-9.

Lengke, M.F., Southam, G., 2006. The bioaccumulation of gold by thiosulfate-reducing bacteria cultured in the presence of gold-thiosulfate complex. Geochimica et Cosmochimica Acta, 70, 3646-3661.

Lengke, M.F., Southam, G., 2007. The role of bacteria in the accumulation of gold: Implications for placer gold formation and supergene gold enrichment. Economic Geology, 102, 109-126.

Liversidge, A., 1893. On the origin of gold nuggets. Journal and Proceedings of the Royal Society of New South Wales, 27, 303-343.

Mann, A.W., 1984. Mobility of gold and silver in lateritic weathering profiles: Some observations from Western Australia. Economic Geology, 79, 38-50.

Marquez-Zavalia, M.R., Southam, G., Craig, J.R., Galliski, M.A., 2004. Morphological and chemical study of placer gold from the San Luis Range, Argentina. The Canadian Mineralogist, 42, 169-182.

McCready, A.J., Parnell, J., Castro, L., 2003. Crystalline placer gold from the Rio Neuguen, Argentina: Implications for the gold budget in placer gold formation. Economic Geology, 98, 623-633.

Mosier, E.L., Cathrall, J.B., Antweiler, J.C., Tripp, R.B., 1989. Geochemistry of placer gold, Koyukuk-Chandalar mining district, Alaska. Journal of Geochemical Exploration, 31, 97-115.

Moser, D.P., Onstott, J.K., Fredrickson, F.K., Brockman, F.J., Balkwill, D.L., Drake, G.R., Pfiffner, S., White, D.C., Takai, K., Pratt, L.M., Fong, J., Sherwood-Lollar, B., Slater, G., Phelps, T.J., Spoelstra, N., DeFlaun, M., Southam, G., Welty, A.T., Baker, B.J., Hoek, J., 2003. Temporal shifts in the geochemistry and microbial community structure of an ultradeep mine borehole following isolaton. Geomicrobiology Journal, 20, 517-548.

Neidhardt, F.C., Ingraham, J.L. & Schaechter, M. 1990. Physiology of the bacterial cell: A molecular approach. Sinauer Associates, Sunderland. MA.

Nesterenko, G.V., Kolpakov, V.V., 2007. Fine gold particles and gold dust in alluvial autochthonous placers in southern west Siberia. Russian Geology and Geophysics, 48, 783-798.

Nesterenko, G.V., Kolpakov, V.V., 2010. Allochthonous native gold in piedmont alluvium in the southern west Siberia. Lithology and Mineral Resources, 45, 425-442.

Postgate, J.R., 1984. The sulfate-reducing bacteria. 2nd edition. Cambridge Press. 32.

Power, I.M., Wilson, S.A., Thom, J.M., Dipple, G.M., Southam, G., 2007. Biological induced mineralization of dypingite by cyanobacteria from an alkaline wetland near Atlin, British Columbia, Canada. Geochemical Transaction 8, 13.

Reith, F., McPhail, D.C., 2006. Effect of resident microbiota on the solubilization of gold in soil from the Tomakin Park Gold Mine, New South Wales, Australia. Geochimica et Cosmochimica Acta, 70, 1421- 1438.

Reith, F., Rogers, S.L., McPhail, D.C., Webb, D., 2006. Biomineralization of gold: Biofilms on bacterioform gold. Science, 313, 233-236.

Reith, F., Lengke, M.F., Falconer, D., Craw, D., Southam, G., 2007. The geomicrobiology of gold. International Society of Microbial Ecology Journal, 1, 567-584.

Reith, F., Wakelin, S.A., Gregg, A.L., Schmidt-Mumm, A., 2009. A microbial pathway for the formation of gold-anomalous calcrete. Chemical Geology, 258, 315-326.

Reith, F., Fairbrother, L., Nolze, G., Wilhelmi, O., Clode, P.L., Gregg, A., Parson, J.E., Wakelin, S.A., Pring, A., Hough, R., Southam, G., Brugger, J., 2010. Nanoparticle factories: biofilms hold the key to gold dispersion and nugget formation. Geology, 38, 843-846.

Reith, F., Etschmann, B., Dart, R.C., Brewe, D.L., Vogt, S., Schmidt-Mumm, A., Brugger, J., 2011. Distribution and speciation of gold in biogenic and abiogenic calcium carbonates-Implications for the formation of gold anomalous calcrete. Geochimica et Cosmochimica Acta, 75, 1942-1956.

Rippka, R., Deruelles, J., Waterbury, J.B., Herdman, M., Stanier, R.Y., 1979. Generic assignment, strain histories and properties of pure cultures of cyanobacteria. Journal of General Microbiology, 111, 1-61.

Sauerbrei, J.A., Pattison, E.F., Averill, S.A., 1987. Till sampling in the Casa-Berardi gold area, Quebec: a case history in orientation and discovery. Journal of Geochemical Exploration, 28, 297-314.

Schoonen, M.A.A., Fisher, N.S., Wente, M., 1992. Gold sorption onto pyrite and goethite: A radiotracer study. Geochimica et Cosmochimica Acta, 56, 1801-1814.

Shuster, J., Marsden, S., MacLean, L.C.W., Ball, J., Bolin, T., Southam, G., 2013a. The immobilisation of gold (III) chloride by a halophilic sulphate-reducing bacterial consortium. The Geological Society Special Publication, in press.

Shuster, J., Johnston, C.W., Magarvey, N.A., Gordon, R.A., Barron, K., Banerjee, N., Southam, G., 2013b. Bacteria contribute to gold nugget structure and chemistry: evidence from in situ surface biofilms and casts. Geobiology, accepted with revision.

Silverman, M.P., Lundgren, D.G., 1959. Studies on the chemoautotrophic iron bacterium Ferrobacillus ferrooxidans: An improved medium and a harvesting procedure for securing high cell yields. Journal of Bacteriology, 77, 642-647.

Song, Z., Kenney, J.P.L., Fein, J.B., Bunker, B.A., 2012. An X-ray Fine Structure study of Au adsorbed onto the non-metabolizing cells of two soil bacterial species. Geochimica et Cosmochimica Acta, 86, 103-117.

Southam, G., Beveridge, T.J., 1994. The in vitro formation of placer gold by bacteria. Geochimica et Cosmochimica Acta, 58, 4527-4530.

Southam, G., Beveridge, T.J., 1996. The occurrence of sulfur and phosphorus within bacterially derived crystalline and pseudocrystalline octahedral gold formed in vitro. Geochimica et Cosmochimica Acta, 60, 4369-4376.

Southam, G., 1998. Quantification of sulphur and phosphorus within secondary gold rims on Yukon placer gold. Geology, 26, 339-343.

Southam, G., Saunders, J., 2005. The Geomicrobiology of ore deposits. Economic Geology, 100, 1067-1084.

Trudinger, P.A., Chambers, L.A., Smith, J.W., 1985. Low-temperature sulphate reduction: Biological versus abiological. Canadian Journal of Earth Sciences, 22, 1910-1918.

Watterson, J.R., 1992. Preliminary evidence for the involvement of budding bacteria in the origin of Alaskan placer gold. Geology, 20, 315-318.

Webster, J.G., Mann, A.W., 1984. The influence of climate, geomorphology and primary geology on the supergene migration of gold and silver. Journal of Geochemical Exploration, 22, 22-42.

Wilson, A.F., 1984. Origin of quartz-free gold nuggets and supergene gold found in laterites and soils-a review and some new observations. Australian Journal of Earth Science, 31, 303-316.

Yeend, W., 1975. Experimental abrasion of detrital gold. United States Geological Survey Journal of Research, 3, 203-212.

Youngson, J.H., Craw, D., 1993. Gold nugget growth during tectonically induced sedimentary recycling, Otago, New Zealand. Sedimentary Geology, 84, 71-88.

# Chapter 7

# 7 General Summary

Bacteria and their associated biogeochemical conditions have profound effects on both soluble and elemental gold and therefore have economic importance. The effects of bacteria on gold solubilisation, immobilisation and accumulation are important for understanding how gold "travels" from a primary source and for critically evaluating secondary gold enrichment over geological time (i.e. millennia). The studies presented in this thesis were conducted using laboratory models representing natural environments to expand on previous research examining various aspects of gold biomineralisation (e.g., Southam and Beveridge, 1994, 1996; Southam and Saunders, 2005; Lengke and Southam, 2006, 2007; Reith and McPhail, 2006; Lengke et al., 2006a, b, 2007; Reith et al., 2006, 2007, 2009, 2011; Kenney et al., 2012; Song et al., 2012; Fairbrother et al., 2012; Johnston et al., 2013). Therefore, the main objective of this dissertation was to determine the microbial influence on the biogeochemical cycling of gold under surface and near-surface conditions (Fig. 7.1).

## 7.1 Gold solubility and immobilisation

Like previous studies examining bacterial-catalysed sulphide mineral dissolution (Sampson et al., 2000; Jones et al., 2003; Thurston et al., 2010), Chapter 2 involved the exposure of a gold-bearing metal sulphide to iron-oxidising bacteria. The purpose of this study was to examine the capacity for bacteria to "liberate" gold from sulphide minerals. Upon the preferential attachment of bacteria onto sulphide mineral grain boundaries, the formation of biofilms indicated positive growth. Furthermore, iron phosphate and iron potassium sulphate precipitate could have been attributed to iron oxidation by metabolically active bacteria. More importantly, secondary mineral precipitation on extracellular surfaces and the alteration to polished surfaces confirmed the dissolution of metal sulphides attributed to active iron-oxidising bacterial metabolism. Although gold was not detected in solution after the bacterial exposure, soluble silver and copper were present and suggested that gold dissolution via thiosulphate leaching could have also occurred. In addition, gold-bearing sulphide minerals occurred as weathered pits on the suspended sample and fragments of weathered sulphide minerals occurred at the bottom of the bacterial weathering system. These

observations demonstrated that acidophilic, iron-oxidising bacteria contributed to biogeochemical weathering and to physical weathering of a gold-bearing, highly-sulphidised ore. Furthermore, this study suggests that gold can readily "disappear" in weathering regimes and can be redistributed as soluble gold or fine-grain particles.

The geochemical conditions of surface and near-surface environments are the primary factors determining the type and availability of gold-complexing ligands that enable the formation and mobility of soluble gold (Mann, 1984; Webster, 1985; Benedetti and Boulegue, 1991). Experiments conducted in Chapter 3, Appendix A and Chapter 5 collectively demonstrated the immobilisation of soluble gold complexes under the biogeochemical conditions in which they would likely occur. Gold is unlikely to remain as a stable, inorganic soluble complex when bacteria are present since bacteria are ubiquitous in nature. Therefore, it would be of significant interest for exploration programs to target bacteriogenic colloidal gold.

As discussed above, the abundance of sulphide minerals under oxidised weathering conditions promote the formation and mobility of soluble gold (I) thiosulphate complexes. However, Chapter 3 highlighted the direct and indirect modes of destabilisation and reduction of gold (I) thiosulphate by iron-oxidising bacteria and the biogeochemical conditions they produce. Direct gold biomineralisation occurred extracellularly as precipitated, nanometre-size colloids and was consistent with previous studies by Lengke and Southam (2006a). More importantly, increased ferric iron concentrations attributed to bacterial metabolism was the predominant biogeochemical factor contributing to the majority of gold (I) thiosulphate destabilisation and subsequent reduction to colloidal gold sulphide. The substitution of acicular iron-oxide minerals by colloidal gold and the precipitation of gold sulphide from solution highlight the significance of ferric iron in the indirect destabilisation of gold (I) thiosulphate. In addition, the study in Appendix A demonstrated similar modes of soluble gold immobilisation using gold (III) chloride; however, ferrous iron contributed the greatest precipitation of colloidal gold. Therefore it can be inferred that the existence of either gold (I) thiosulphate or gold (III) chloride in acid rock drainage and laterite systems, where bacteria and iron exist, is finite.

When considering soluble gold mobility in the absence of thiosulphate ligands it has been accepted that gold (III) chloride complexes would exist due to the likely availability of

chloride ions (Krauskopf, 1951; Mann, 1984). Therefore, with analogous laboratory models used in Chapter 4, the destabilisation of gold (III) chloride under saline to hypersaline environmental conditions was the primary focus of Chapter 5. In this study, halophilic, sulphate-reducing bacteria directly immobilised gold (III) chloride despite increased concentrations of chloride ions that could have promoted the retention of gold solubility. Soluble gold immobilised as colloidal gold and colloidal clusters was consistent with previous studies exposing gold (III) chloride to various bacteria (see Southam and Beveridge, 1994, 1996; Lengke et al., 2006ab, 2007). Like the experiments representing oxidised weathering environments, the presence of iron in this study could have contributed to gold immobilisation. In addition, the close association of microbial-mediate carbonate and gold precipitation signified an additional mechanism of Ca-carbonatogenesis with gold co-precipitation that is observed in arid to semi-arid environments. Gold precipitation at the biofilm-fluid interface demonstrated the natural resilience of the biofilm to gold toxicity. Implications of these findings not only suggest a sustained mode of gold immobilisation but also the accumulation of secondary gold forming larger structures such as foils. Therefore, it is important to consider the potential of gold mobility as suspended secondary gold precipitates form soluble gold complexes within surface to near-surface hydrological regimes.

## 7.2 Gold accumulation

Many physical and geochemical factors are attributed to gold grain and nugget formation (Hallbauer and Utter, 1977; Giusti and Smith, 1984; Theodore et al., 1987; Mosier et al., 1989). However, since the biosphere has an influential effect on gold solubility and immobilisation, the bacterial contribution to gold accumulation is also worth considering. This aspect of gold biogeochemical cycling was addressed in Chapters 4 and 6 in which the structure and chemistry of natural and synthesized gold grains and nuggets were examined.

Colloidal, octahedral and bacteriomorphic gold occur as nanometre- to micrometre-size structures whereas gold grains are larger secondary structures ranging within hundreds of micrometres in size (Hough et al., 2009). The studies presented in Chapter 4 focused on the morphological characterisation and chemical composition of gold grains that were weathered and deposited distal from a gold-rich porphyry copper source. While grain shape and surface

texture were attributed to the mechanical reshaping within the fluvial environment, gold enriched rims were attributed in part to bacterial processes. Bacteria, containing extracellular colloidal gold, were directly and indirectly attached to grain surfaces while bacterial-size casts and carbon-filled, globular void spaces were located along the grain perimeter. Furthermore, a pure culture of *Nitrobacter* sp. 263 was obtained from a single gold grain and represented a single bacterial group derived from the natural environment that were capable of attachment to the grain surface. *Nitrobacter*-gold immobilisation experiments, analogous to those described in Chapters 3 and 5, demonstrated similar extracellular colloidal gold precipitation along with octahedral gold platelets. Collectively, the experiments in this comprehensive study demonstrated the direct link between bacterial immobilisation and their contribution to secondary gold enrichment on grains; thereby, indicating a microbial influence on the growth of gold grains.

Bacterial-catalysed gold solubility, gold immobility and gold accumulation on grains that were described in the previous chapters were the basis for the studies presented in Chapter 6. In this chapter, experiments involved the *in vitro* formation of gold nuggets to better understand the biogeochemical accumulation of secondary gold in environments where enrichment can occur, i.e., placer deposits. A system containing bacterial-catalysed secondary gold, bacterial enrichments and sediment was constructed to represent a fluvial system. Gold grain, leaf and nugget formation was attributed to the combined effect of the biofilm "trapping" gold colloids, octahedral platelets and foils and aggregation into larger structures by movement within the homogenous host-sediment. Although physically abraded to have smooth surfaces, portions of the larger gold structures still retained the delicate nanometre- to micrometre-size secondary gold textures produced by bacterial gold immobilisation. It was the addition of pebbles, creating a heterogeneous host-sediment, that led to gold leaf and nugget destruction and formation of small grains with flattened and smoother surfaces. More importantly, a fraction of gold consistently remained in solution despite the availability of organic material for potential reduction. These results indicate that bacteria contributed to gold solubility while cycling gold into various morphological structures that occurred within the solid and fluid phases of the experimental system. By the end of this experiment, approx. 46% of total amount of gold in the experimental system was recovered, which indicated that elemental gold was still mobile as microscopic particles.

## 7.3 Discussion

In light of these bacterial-gold studies, it is important to consider a greater application of gold biogeochemical cycling under surface and near-surface environmental conditions. The socioeconomic development and success of modern society is aligned with our need for natural resources including gold. However, gold has a limited supply. Most conventional resources have already been used and the discovery of new gold sources has become more difficult. Therefore, it is necessary to develop innovative strategies for exploration and exploitation to sustain development. The results presented in this thesis provide a basis for the development of novel sampling methods and strategies to expand our ability to "track" gold movement in natural systems. The refined ability to track the movement of nanophase gold would enhance the ability of exploration companies to target gold anomalies in soils and in sediments. For example, biooxidation of gold-bearing minerals leads to increased rock permeability, porosity and subsequently the "transportation" of gold as gold sulphide nanoparticles. Future experiments should be designed to determine how pH, temperature, nutrient availability, geochemistry and mineralogy promote the biooxidation of gold-bearing polymetallic sulphide minerals. Similarly, future experiments are needed to identify the exact biochemical mechanism(s) of gold-binding organic compounds that are involved in bacterially mediated secondary gold precipitation. Finally, applications of synchrotron-based methods should be evaluated for the analyses of "signature metals" to identify and differentiate gold sources within natural gold grains. Furthermore, detection of gold-binding organic compounds and trace amounts (e.g., parts per million) of gold from natural soils should be tested. Biotechnology is currently underused in industry despite the expansion of multi-disciplinary studies "fuelling" scientific advancement. Therefore, these future gold biogeochemical studies should focus on applying the fundamental understanding of nanophase gold to exploration and to biohydrometallurgical extraction processing at the industrial-scale.

## 7.4 Conclusion

It can be argued that the socioeconomical development and success of our society have been and continues to be attributed to the need of natural resources. However, these materials have limited supply and it is therefore necessary to develop innovative modes of exploitation

in order to sustain our development. Similarly, gold continues to be a valued entity that has arguably been the "axiom" for its rich and colourful history in scientific research. As modern scientific advancements expand to involve greater multi-disciplinary studies and improve current technologies, gold biotechnology harbours significant utility for application to economic exploration and methods for efficient recovery. As a model, my studies examined gold's diverse occurrence within natural systems where weathering or enrichment can occur. Improved understanding of gold biogeochemistry provides novel means for sampling techniques and strategies to expand our current ability to "track" gold mobility and reduce the problematic "nugget effect" encountered during mineral exploration. This application could reasonably enhance detection of gold anomalies in natural soils and sediment and identify additional targets of exploration. In summary, this thesis demonstrated that the continuous process of gold biogeochemical cycling under surface to near-surface environmental conditions is dynamic.

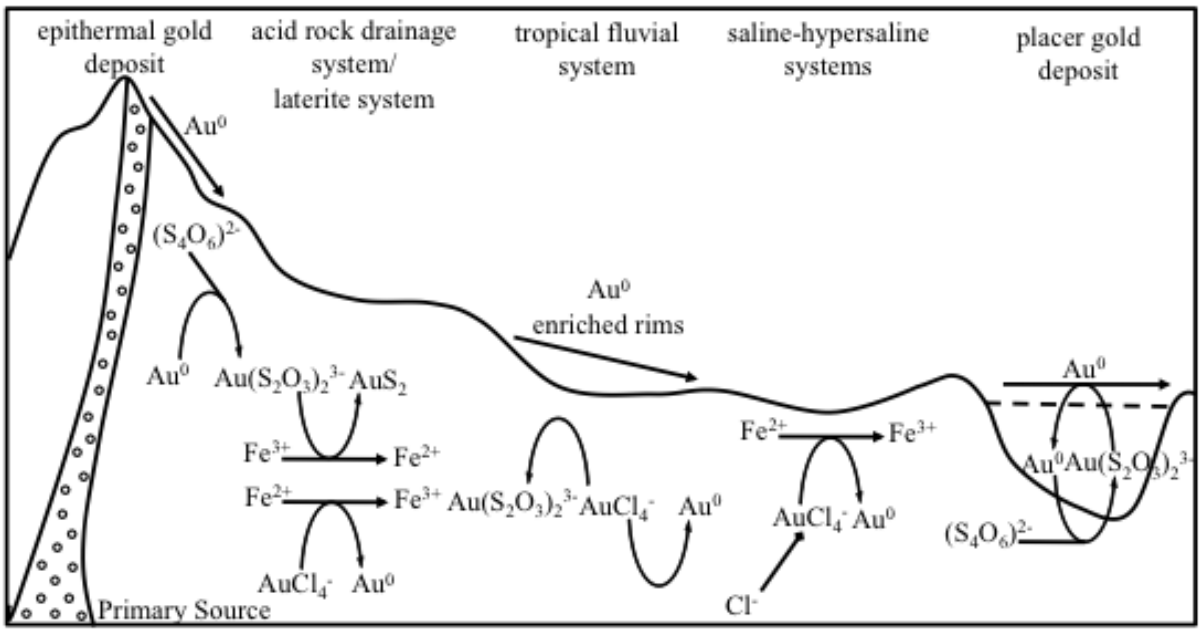


**Figure 7.1. Schematic diagram of gold biogeochemical cycling under surface and near-surface environmental conditions.** Gold is mobilised as gold grains or soluble gold (I) thiosulphate complexes through the abiotic and biotic weathering of gold-bearing, polymetallic sulphide minerals (see Chapter 2). Soluble gold (I) thiosulphate and gold (III) chloride complexes are reduced to gold sulphide and colloidal gold in the presence of bacteria and iron within weathering profiles (see Chapter 3 and Appendix). Bacteria contribute to secondary gold enrichment on the surface of gold grains from tropical fluvial environments (see Chapter 4). Bacteria and iron reduce soluble gold (III) chloride complexes to colloidal gold despite the presence of excess chloride ions under saline to hypersaline conditions (see Chapter 5). Bacteria contribute to gold accumulation forming grains and nuggets. However, bacteria also contribute to the dissolution of elemental gold resulting in the formation of soluble gold complexes in solution (see Chapter 6).

## 7.5 References

Benedetti, M., Boulegue, J., 1991. Mechanisms of gold transfer and deposition in a supergene environment. Geochimica et Cosmochimica Acta, 55, 1539-1547.

Fairbrother, L., Brugger, J., Shapter, J., Laird, J.S. Southam, G., Reith, F., 2012. Supergene gold transformation: Biogenic secondary and nano-particulate gold from arid Australia. Chemical Geology, 321, 17-31.

Giusti, L., Smith, D.G.W., 1984. An electron microprobe study of some Alberta placer gold. Tschermaks Mineralogische und Petrographische Mitteilungen, 32, 187-202.

Hallbauer, D.K., Utter, T., 1977. Geochemical and morphological characteristics of gold particles from recent river deposits and the fossil placers of the Witwatersrand. Mineralium Deposita, 12, 293-306.

Hough, R.M., Butt, C.R.M., Fischer-Buhner, J., 2009. The crystallography, metallography and composition of gold. Elements, 5, 297-302.

Johnson, D.B., Grail, B.M., Hallberg, K.B., 2013. A new direction for biomining: Extraction of metals by reductive dissolution of oxidised ores. Minerals, 3, 49-58.

Johnston, C.W., Wyatt, M.A., Li, X., Ibrahim, A., Shuster, J., Southam, G., Magarvey, N.A., 2013. Gold biomineralisation by a metallophore from a gold-associated microbe. Nature Chemical Biology, advanced online publication.

Jones, R.A., Koval, S.F., Nesbitt, H.W., 2003. Surface alteration of arsenopyrite (FeAsS) by Thiobacillus ferrooxidans. Geochimica et Cosmochimica Acta, 67, 955-965.

Kenny, J.P.L., Song, Z., Bunker, B.A., Fein, J.B., 2012. An experimental study of Au removal from solution by non-metabolizing bacterial cells and their exudates. Geochimica et Cosmochimica Acta, 87, 51-60.

Krauskopf, K.B., 1951. The solubility of gold. Economic Geology, 46, 858-870.

Lengke, M.F., Southam, G., 2006. The bioaccumulation of gold by thiosulfate-reducing bacteria cultured in the presence of gold-thiosulfate complex. Geochimica et Cosmochimica Acta, 70, 3646-3661.

Lengke, M.F., Southam, G., 2007. The role of bacteria in the accumulation of gold: Implications for placer gold formation and supergene gold enrichment. Economic Geology, 102, 109-126

Lengke, M.F., Fleet, M.E., Southam, G., 2006a. Morphology of gold nanoparticles synthesized by filamentous cyanobacteria from gold(I)-thiosulfate and gold(III)-chloride complexes. Langmuir, 22, 2780-2787.

Lengke, M.F., Ravel, B., Fleet, M.E., Wanger, G., Gordon, R.A., Southam, G., 2006b. Mechanisms of gold bioaccumulation by filamentous cyanobacteria from gold (III)-chloride. Environmental Science and Technology, 40, 6304-6309.

Lengke, M.F., Ravel, B., Fleet, M.E., Wanger, G., Gordon, R.A., Southam, G., 2007. Precipitation of gold by reaction of aqueous gold(III)-chloride with cyanobacteria at 25-80°C – Studied by X-ray absorption spectroscopy. Canadian Journal of Chemistry, 85,1-9.

Mann, A.W., 1984. Mobility of gold and silver in lateritic weathering profiles: Some observations from Western Australia. Economic Geology, 79, 38-50.

Mosier, E.L., Cathrall, J.B., Antweiler, J.C., Tripp, R.B., 1989. Geochemistry of placer gold, Koyukuk-Chandalar mining district, Alaska. Journal of Geochemical Exploration, 31, 97-115.

Rawlings, D.E., Johnson, D.B., 2007. The microbiology of biomining: Development and optimisation of mineral-oxidising microbial consortia. Microbiology, 153, 315-324.

Reith, F., McPhail, D.C., 2006. Effect of resident microbiota on the solubilization of gold in soil from the Tomakin Park Gold Mine, New South Wales, Australia. Geochimica et Cosmochimica Acta, 70, 1421- 1438.

Reith, F., Rogers, S.L., McPhail D.C., Webb, D., 2006. Biomineralization of gold: Biofilms on bacterioform gold. Science, 313, 233-236.

Reith, F., Lengke, M.F., Falconer, D. Craw, D., Southam, G., 2007. The geomicrobiology of gold. International Society of Microbial Ecology Journal, 1, 567-584.

Reith, F., Wakelin, S.A., Gregg, A.L., Schmidt Mumm, A., 2009. A microbial pathway for the formation of gold-anomalous calcrete. Chemical Geology, 258, 315-326.

Reith, F., Etschmann, B., Dart, R.C., Brewe, D.L., Vogt, S., Schmidt Mumm, A., Brugger, J., 2011. Distribution and speciation of gold in biogenic and abiogenic calcium carbonates-Implications for the formation of gold anomalous calcrete. Geochimica et Cosmochimica Acta, 75, 1942-1956.

Sampson, M.I., Phillips, C.V., Blake, R.C. II, 2000. Influence of the attachment of acidophilic bacteria during the oxidation of mineral sulphides. Mineral Engineering, 13, 373-389.

Song, Z., Kenney, J.P.L., Fein, J.B., Bunker, B.A., 2012. An X-ray Fine Structure study of Au adsorbed onto the non-metabolizing cells of two soil bacterial species. Geochimica et Cosmochimica Acta, 86, 103-117.

Southam, G., Beveridge, T.J., 1994. The in vitro formation of placer gold by bacteria. Geochimica et Cosmochimica Acta, 58, 4527-4530.

Southam, G., Beveridge, T.J., 1996. The occurrence of sulphur and phosphorus within bacterially derived crystalline and pseudocrystalline octahedral gold formed in vitro. Geochimica et Cosmochimica Acta, 60, 4369-4376.

Southam, G., Saunders, J., 2005. The Geomicrobiology of ore deposits. Economic Geology, 100, 1067-1084.

Theodore, T.G., Blair, W.N., Nash, J.T., 1987. Geology and gold mineralization of the Gold Basin-Lost Basin mining districts, Mohave County, Arizona. United States Geological Survey Professional Paper, 1361, 1-167.

Thurston, R.S., Mandernack, K.W., Shanks, W.C., 2010. Laboratory chalcopyrite oxidation by Acidithiobacillus ferrooxidans: oxygen and sulphur isotope fractionation. Chemical Geology, 269, 252-261.

Webster, J.G., 1985. Thiosulphate in surficial geothermal waters, North Island, New Zealand. Applied Geochemistry, 2, 5-6.

# Curriculum Vitae

**Name:** Jeremiah Shuster

**Post-secondary Education and Degrees:**
University of Western Ontario
London, Ontario, Canada
2003-2008 B.Sc.

**Honours and Awards:**
Western Graduate Research Scholarship
2008-2013

Queen Elizabeth II Graduate Scholarship in Science and Technology
2011

William S. Fyfe Graduate Scholarship in Natural Resources
2010

Robert Lumsden and Ruth Lumsden Award in Science
2009

**Related Work Experience**
Teaching Assistant
The University of Western Ontario
2008-2012

Research Assistant
The University of Western Ontario
2012-2013

**Publications:**

**Shuster, J.**, Johnston, C.W., Magarvey, N.A., Gordon, R., Barron, K., Banerjee, N. and Southam, G. 2013. Bacteria contribute to gold nugget structure and chemistry: evidence from in situ surface biofilms and casts. Geobiology, (accepted with revision, GB1-087-2012).

**Shuster, J.**, Izawa, M., Banerjee, N., Flemming, R., Southam, G. The occurrence of argentojarosite in the Iberian Pyrite Belt: the implication of bacteria in its formation. Economic Geology, (accepted with revision, SEG-D-11-00074).

**Shuster, J.**, Marsden, S., MacLean, M.C.W., Ball, J., Bolin, T. and Southam, G. 2013. The immobilization of gold from Au(III) chloride by a halophilic sulphate-reducing bacterial consortium. Geological Society, (in press).

Johnston, C.W., Wyatt, M.A., Li, X., Ibrahim, A., **Shuster, J.**, Southam, G. and Magarvey, N.A. 2013. Gold biomineralization by a metalophore from a gold-associated microbe. Nature Chemical Biology, 9: 241-243.

Preston, L.J., **Shuster, J.**, Fernandez-Remolar, D., Banerjee, N.R., Osinski, G.R., Southam, G. 2010. The preservation and identification of filamentous bacteria and biomolecules within iron oxide deposits at Rio Tinto, Spain. Geobiology, 9: 233-249.